NanoKaryotyping

Application of Micro- and Nanotechnologies in Cytogenetics

Kwasny, Dorota

Publication date:
2013

Document Version
Publisher's PDF, also known as Version of record

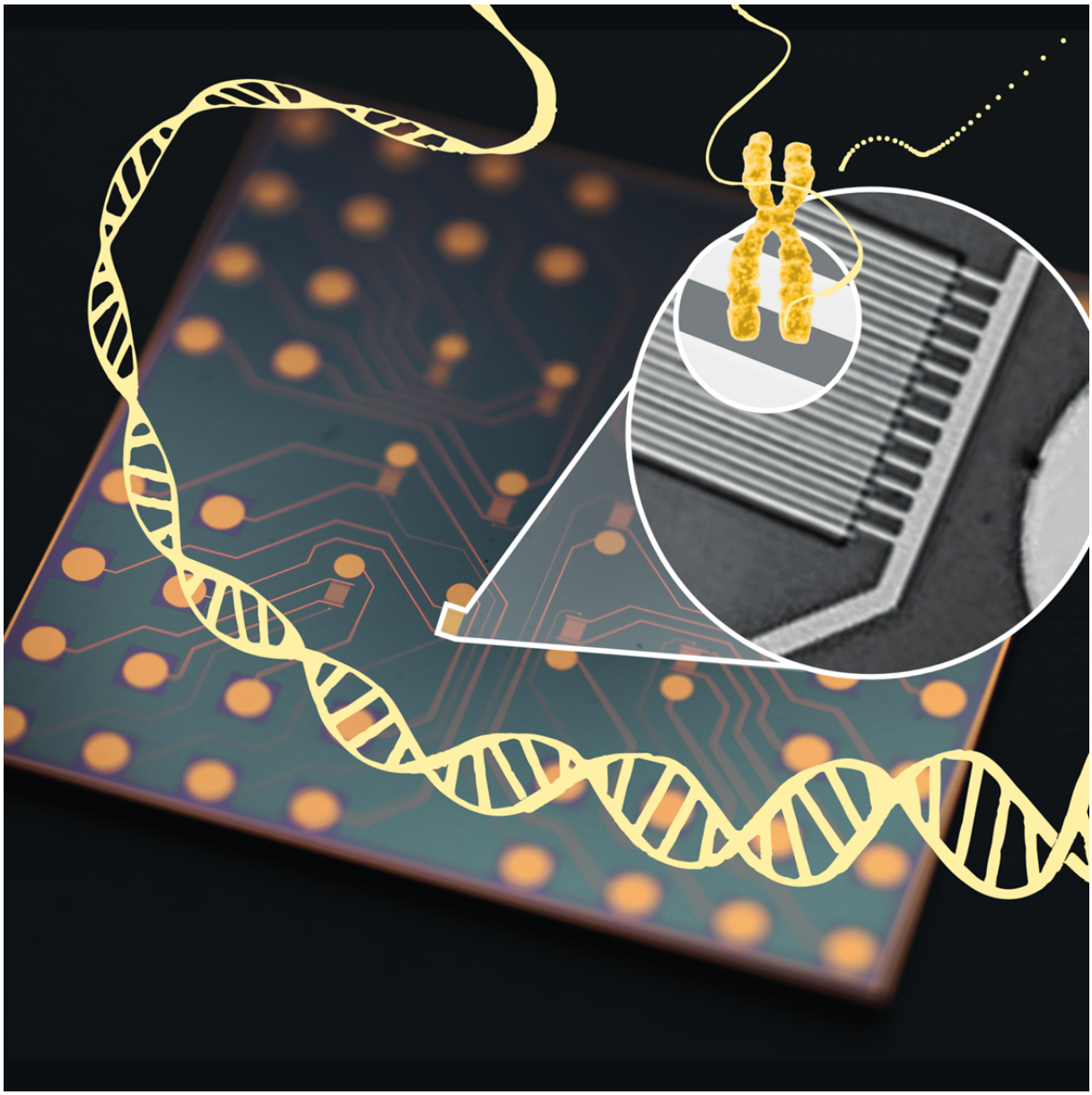

NanoKaryotyping: Application of Micro- and Nanotechnologies in Cytogenetics

Dorota Kwasny

PhD Thesis

NanoKaryotyping: Application of Micro- and Nanotechnologies in Cytogenetics

PhD Thesis

Technical University of Denmark
Department of Micro- and Nanotechnology

Author:
Dorota Kwasny

Supervisors:
Maria Dimaki
Zeynep Tümer
Winnie E. Svendsen

August 2013

DTU Nanotech
Department of Micro- and Nanotechnology

PhD Thesis

NanoKaryotyping. Application of Micro- and Nanotechnologies in Cytogenetics

Typeset using LaTeX

www.nanotech.dtu.dk/Research-mega/Forskningsgrupper/NaBIS

The front page image illustrates the chromosome translocation detection principle using electrochemical impedance spectroscopy DNA hybridisation sensor. *Image prepared by Nanna Bild.*

Dla moich rodziców

Abstract

Chromosome abnormalities, such as translocations may cause various genetic disorders and are also associated with heametological malignancies. Translocation is a rearrangement between two chromosome arms that results in two derivative chromosomes. The current detection methods such as karyotyping and FISH require a use of expensive reagents and can only be performed in specialized laboratories. This PhD project aims at developing new strategies for point-of-care detection of chromosome translocations by applying micro- and nanotechnologies to increase the sensitivity.

The project started with development of a microfluidic device for controlled chromosome spreading. The device, made in Topas®, was used to facilitate the evaporation of the fixative solution to achieve proper spreading. In the device we obtained a comparable spreading efficiency to the traditional methods but with reduced reagents volume.

To propose a new strategy for chromosome translocation detection we developed a double hybridisation assay. To detect the translocation it is necessary to determine that the two DNA sequences forming a derivative chromosome are connected, which is achieved by two subsequent hybridization steps. The first example of the translocation detection was presented on lab-on-a-disc using fluorescently labeled DNA fragments, representing the derivative chromosome. It allows for sorting of the DNA chromosomal fragments into separate compartments followed by translocation detection.

To allow for cheaper detection an electrical label-free approach has been investigated using silicon nanowires BioFETs, metallic and conductive polymer electrodes. We present here our findings regarding the DNA hybridisation sensing using these sensors. They showed an improved sensitivity and are all label-free, which makes them inexpensive candidates for a novel cytogenetic analysis as a replacement of standard techniques. The metallic electrodes as the most reliable were selected for further development of a complete device for translocation detection. We developed a setup enabling electrochemical measurements on a spinning lab-on-a-disc platform. An electrical swivel was used to provide reliable connections between the electrodes on a disc and a potentiostat. We have demonstrated the applicability of the setup to standard electrochemical techniques.

Lab-on-a-chip devices are being constantly developed to improve the analysis at a reduced cost and time. The presented devices that were developed using micro- and nanotechnologies are label-free and due to their sensitivity show a potential to be applied to chromosome translocation analysis with an improved detection efficiency.

Resumé

Abnormaliteter i kromosomerne, såsom translokationer, kan forårsage genetiske sygdomme og nogle former for kræft. En translokation opstår ved en ombytning af dele af kromosomarmene fra forskellige kromosomer, hvorved der dannes to nye afledte kromosomer. De metoder, karyotyping og FISH, der i dag benyttes til detektion af disse translokationer er afhængige af dyre kemikalier og udføres kun i specialiserede laboratorier. Målet med dette Ph.D. projekt er at udvikle nye strategier til point-of-care detektion af kromosomtranslokationer baseret på mikro- og nanoteknologier. Brugen af disse teknologier vil potentielt kunne øge følsomheden af målingerne.

I begyndelsen af dette projekt har der været fokus på udviklingen af en mikrofluid enhed designet til at assistere ved udførslen af kontrollerede kromosomspredninger. Enheden, som var fabrikeret i Topas®, var designet med fokus på faciliteringen af fordampningen af fiksativ opløsningen for at opnå en ordentlig spredning. Ved hjælp af denne enhed lykkedes det os at opnå spredninger i samme kvalitet som ved traditionelle metoder, men ved et reduceret kemikalie forbrug.

En ny strategi til kromosom translokation detektion var udviklet baseret på et dobbel hybridiserings assay. For at kunne detektere en translokation er det nødvendigt at bevise at to DNA sekvenser fra forskellige kromosomer er forbundet. Dette opnås ved hjælp af to på hindanden følgende hybridiserings skridt. Det første eksempel på et sådan detektionsprincip var baseret på flourocens markerede DNA fragmenter og realiseret på en lab-on-a-disc platform. Lab-on-a-disc platformen muliggører en sortering af kromosomfragmenterne i seperate afdelinger, hvilket følges af en detektion af translokationen.

For at reducere omkostningerne yderligere benyttes en såkaldt label-free tilgang. I dette projekt er denne tilgang undersøgt ved hjælp af både silicium nanowire BioFETs og EIS målinger med elektroder udført i enten metaller eller ledende polymerer. I denne afhandling præsenteres resultater fra alle disse tre principer. Sensitiviteten af disse tilgange kombineret med de reducerede omkostninger på baggrund af label-free princippet gør disse metoder til gode alternativer til de traditionelle cytogenetiske metoder. En komplet enhed i stand til at detektere en translokation blev udviklet på baggrund af den mest troværdige af disse metoder; EIS baseret på matal elektroder. Vi udviklede en lab-on-a-disc platform, der var i stand til at lave elektriske målinger samtidig med at denne roterede. Dette blev opnået ved hjælp af en elektrisk swivel der muliggjorde pålidelige elektriske forbindelser mellem elektroderne på discen og en potentiostat. Vi har demonstreret brugbarheden af dette setup ved at demonstrere pæne standard elektrokemiske målinger.

LOC enheder er under en konstant udvikling for at forbedre analyserne og på samme tid reducere omkostninger og tidsforbrug. Enhederne præsenteret i denne afhandling, som var baseret på mikro-og nanoteknologi, er alle label-free. På baggrund af deres høje følsomhed har de vist et stort potentiale til brug ved en forbedret og mere følsom detektion af kromosom translokationer.

Preface

This thesis is presented to fulfill criteria for obtaining a PhD degree from the Technical University of Denmark (DTU). The PhD project was conducted at DTU Nanotech, Department of Micro- and Nanotechnology, from September 2010 until August 2013 and was funded by the Danish Council for Strategic Research under project called 'NanoKaryotyping'.

The project was supervised by Associate Professor Winnie E. Svendsen, leader of the Nano Bio Integrated Systems (NaBIS) group, DTU Nanotech, and co-supervised by Zeynep Tümer, Professor in Kennedy Center and Maria Dimaki, Associate Professor in NaBIS group, DTU.

Thesis contents are based on results described within peer reviewed publications as well as unpublished material.

Kgs. Lyngby
August 2013

Dorota Kwasny

Acknowledgements

This project was realized with a great help of many wonderful people. First of all, I would like to thank Winnie Svendsen for trusting me with this project and giving me freedom to set my own research goals. I would also like to thank Zeynep Tümer for her support and sharing all her knowledge about chromosomes. They both encouraged and inspired me to work hard towards my goals.

Maria Dimaki was another supervisor who influenced me greatly over the last 3 years. She was always available to talk about any research challenges and I am especially grateful for all her help with the cleanroom fabrication processes.

Asli Silahtaroglu was introduced to me at the very beginning of my project and was involved in its initial stages. Her help and cheerful personality made it easier to get started in those first days. I would also like to acknowledge Jaime Castillo for always being professional and helping plan the publication strategy.

For the last 3 years I was a part of a wonderful working environment of NaBIS group. All present and former group members made it a special place with never ending coffee breaks and discussions over lunch. Karsten Andersen was the perfect office mate who always knew when I needed a break and was my guide through Danish culture and administration. I would like to thank Indumathi Vedarethinam and Pranjul Shah for introducing me to the world of microcytogenetics and getting me to work at 100% from the start. I thank Luigi Sasso for sharing my love for *Glee*. I want to also thank Romen Rodriguez-Trujillo and his girlfriend Maria for always being there to talk and sharing sourdough. Thanks to Casper Clausen for being his grumpy self and making me more realistic about my research. I wish to also thank Azeem for making the silicon nanowires chips. I want to acknowledge Jacob Moresco, my first supervisor at DTU for all his kind words and help with some tricky protocols. I would also like to thank the feminine part of NaBIS - Andrea, Julie, Tanya for making our workplace more girly.

I would like to thank all my students whom I supervised through all these years. Special thanks go to my master's students Line, Kasper and Sune for being the best students you can dream of.

I wish to thank Katrine for proof reading parts of this thesis and for sharing the experience of a conference in China. I would like to thank Johannes for all the work we did together, it looks like the PEDOT journey never ends. I want to also thank Kinga, Letizia, Fozia, Claudia, Agnieszka and Arto for always welcoming me in their lab and helping with all kinds of electrochemistry issues and providing me with the chips.

I would also like to acknowledge the Danchip technicians, especially Conny and

Helle for their professional help and the machine's training.

I wish to thank all my friends for their concern for my research and supporting the writing process. Last but not least I would like to thank all my loved ones for their trust, support, patience and all the care-packages with Polish treats they sent.

Publications Used in the Thesis

This thesis is based on the following papers, which are included at the end of Parts II, III and IV of the thesis.

I **Advanced microtechnologies for detection of chromosome abnormalities by fluorescent in situ hybridization**
Dorota Kwasny, Indumathi Vedarethinam, Pranjul Shah, Maria Dimaki, Asli Silahtaroglu, Zeynep Tumer, and Winnie E. Svendsen
Biomedical Microdevices, volume 14, issue 3, pp. 453-460, 2012

II **All-polymer semi-closed device for metaphase chromosome spreading**
Dorota Kwasny, Olga Mednova, Indumathi Vedarethinam, Maria Dimaki, Asli Silahtaroglu, Zeynep Tumer, Kristofer Almdal and Winnie E. Svendsen
submitted to Biomedical Microdevices

III **Centrifugally driven microfluidic system for detection of chromosomal translocation**
Anna Line Brøgger*, Dorota Kwasny*, Filippo Bosco, Zeynep Tumer, Anja Boisen and Winnie E. Svendsen
Lab on a Chip, volume 12, issue 22, pp. 4628-4634, 2012, DOI 10.1039/c2lc40554g
∗ authors contributed equally

Contents

List of Figures

List of Tables

List of Abbreviations

A	Adenine
APTES	3-aminopropyl triethoxysilane
Au	Gold
BHF	Buffered Hydrofluoric Acid
bp	base pair
C	Cytosine
CE	Counter Electrode
COC	Cyclic Olefin Copolymer
CPE	constant phase element
C-TAS	Chromosome Total Analysis System
der	derivative
DNA	deoxyribonucleic acid
EDC	1-ethyl-3-(3-dimethylaminopropyl)carbodiimide
EIS	electrochemical impedance spectroscopy
EtOH	ethanol
FET	Field Effect Transistor
FITC	fluorescein isothiocyanate
FISH	Fluorescent *In Situ* Hybridization
G	Guanine
GOD	Gluxose Oxidase
HCG	human chorionic gonadotropin
IDE	Interdigitated Electrode
µTAS	micro total analysis system
KOH	Potassium Hydroxide
LOC	Lab-on-a-chip
LSV	Linear Sweep Voltammetry
MES	2-(*N*-morpholino)ethanesulfonic acid
NGS	next generation sequencing
NHS	*N*-hydroxy succinimide
PBS	phosphate buffered saline
PC	polycarbonate
PDMS	polydimethylsiloxane
PECVD	Plasma-Enhanced Chemical Vapor Deposition
PEDOT	poly(3,4-ethylenedioxythiophene
PMMA	poly(methyl methacrylate)
POC	point-of-care
PPY	polypyrrole
RE	Reference Electrode

R_{CT}	charge transfer resistance
R_{Sol}	solution resistance
RIE	reactive ion etching
RPM	rounds per minute
SiNW	silicon nanowire
SKY	spectral karyotyping
SSC	saline sodium citrate
T	Thymine
Ti	Titanium
WCP	whole chromosome painting
WE	Working Electrode

Part I

General Overview

1. Motivation

Chromosomes have been thoroughly studied since their recognition as carriers of heredity information in late 19th century (Alberts et al., 2008). Chromosomes are susceptible to structural changes that lead to chromosome mutations that are the basis of cytogenetic research. Cytogenetics is the study of cells, with focus on the chromosome content, especially their number and structure. It is used to determine any abnormalities that might affect the individual carrying it. Some of the structural changes, especially translocations, can result in gene fusion, which plays a significant role in initiation of tumor development. Performing of such analysis is crucial for detection of cancer and its prognosis, furthermore it is used in prenatal diagnostics and genetic counselling.

Nowadays, cytogenetists use various techniques available for determining the chromosome changes, among which fluorescent *in situ* hybridisation is mostly used. The analysis provides valuable information on chromosomal breakpoints in structural changes, but it requires complex and expensive systems and expertise. Thus, its use in off-laboratory settings is still limited. To allow for widespread use of chromosome analysis micro- and nanotechnologies come into play. By miniaturizing the existing assays the analysis sensitivity can be improved and time can be reduced together with the consumables. This project was initiated to integrate the conventional cancer molecular cytogenetics with micro- and nanotechnologies. The microsystem is designed for manipulation of chromosome fragments and identification of chromosome translocations without prior knowledge of the karyotype. Application of such a microsystem for mapping of chromosomal translocation would enable faster and more accurate detection of diseases and congenital disorders.

In this introductory part of the thesis some of the basic concepts behind development of a device for chromosome analysis are described. This Part begins with a description of chromosomes, their structure in a cell nucleus and role in the cell life cycle. Afterwards, the state of the art of chromosomes aberrations detection is presented. Finally, this Part contains introduction to the field of lab-on-a-chip and point-of-care devices.

2. Chromosomes and Cell Life Cycle

The word chromosome comes from Greek *chroma* colour and *soma* body, which refers to the fact that they stain easily with various dyes. Chromosomes, as basic structures of heredity have been studied for more than a century. Cytogenetics is the research field investigating their structure. It contributes to better understanding of their organization, structural components, structural and numerical variations and the role of aberrations (Lagos and Jimenez, 2012). The foundation of human cytogenetics was laid of by the establishment of the number of human chromosomes as 46. In most of the somatic cells (other than sex cells) with a nucleus there are 22 autosomal chromosome pairs and 2 sex chromosomes, X and Y for men, and two X chromosomes for women. Chromosomes are composed of DNA coiled around histone and non-histone proteins. They are composed of a chromatid with a centromere (primary constriction) and protective ends called telomers (Gersen, 2005).

For most of the cell life the DNA in the nucleus is present as entangled strings (chromatin) (Figure 2.1A). Chromosomes are best visualized and distinguished from each other in the most condensed form just before cell division (metaphase) (Figure 2.1B). Metaphase is one of the phases of a cell life cycle. The scheme of

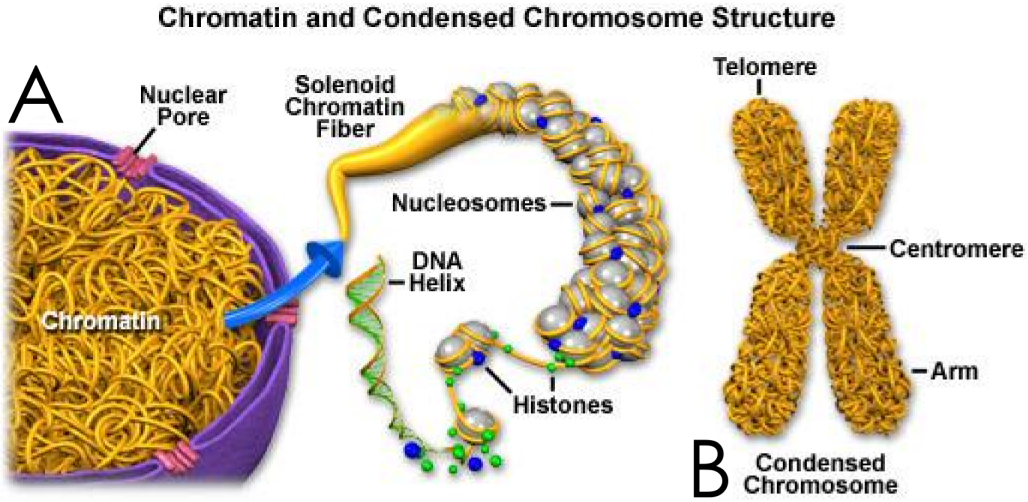

Figure 2.1: For most of the cell life DNA is present in the form chromatin (A). A DNA strand coiled around the histones forms a compact structure, which is a condensed chromosome (B). The short chromosome arm is known as p, and long as q. The chromosome ends are called telomers and a primary constriction is a centromere. *Adapted from micro.magnet.fsu.edu.*

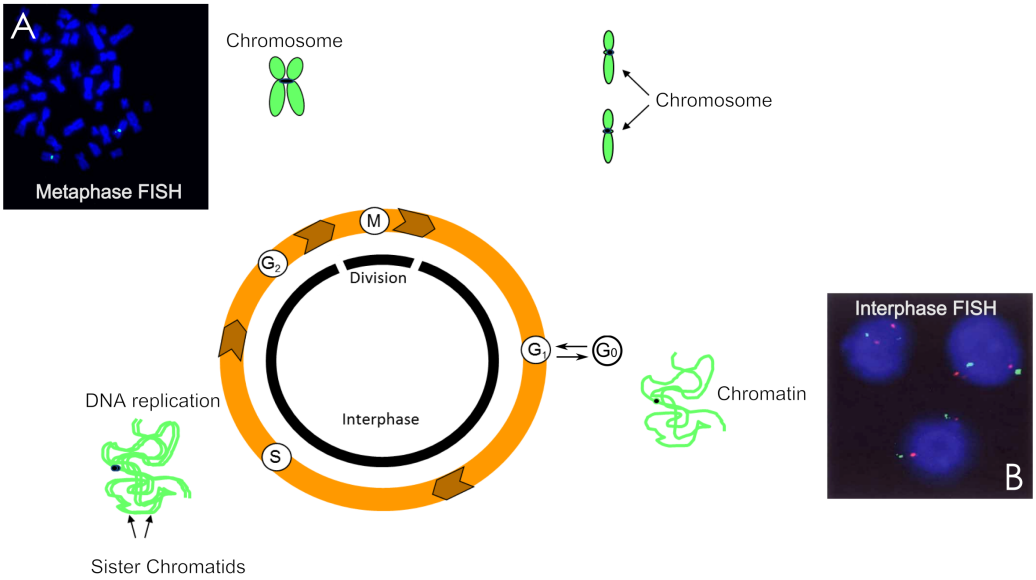

Figure 2.2: Cell Life Cycle is composed of different phases. Most cells are resting in G0 phase but once triggered to divide they go through a series of events leading to DNA replication. Afterwards the cell enters a mitosis phase, which leads to division of the cell into two daughter cells. *Courtesy of Zeynep Tumer.*

the cell life cycle is shown in Figure 2.2. Most of the cells in our body are resting in a G0 phase. When cells are triggered to divide they undergo a series of events leading to cell division and formation of daughter cells. When the process begins, the cell prepares for the division during interphase which is composed of 3 subphases G1, S and G2 in Figure 2.2. In this phase the DNA in the nucleus is present as chromatin, which is necessary for DNA replication. After the cell has prepared all the necessary proteins and doubled its DNA content it enters a mitosis (M in Figure 2.2) phase, which is relatively short lasting only 1-2 hr (Gersen, 2005). It can be divided into several subphases among which metaphase is characterized by DNA condensation into distinct chromosomes. The mitosis leads to further division of the sister chromatids into two separate nuclei and finally daughter cells. FISH can be performed on metaphase chromosomes and chromatins during interphase as shown in Figure 2.2A and B respectively. Another way that cells divide is by meiosis, which is the process required for sexual reproduction resulting in a haploid number of chromosomes (23) (Gersen, 2005). During meiosis and mitosis the chromosomes are prone to rearrangements, which alter their normal structure (Ford et al., 1959; Jacobs et al., 1959). These alterations can be either numerical characterized by an abnormal number of chromosomes such as in Down's syndrome, or structural. The structural alterations can take various forms such as deletions, duplications, etc. as shown in Figure 2.3. As the main topic of

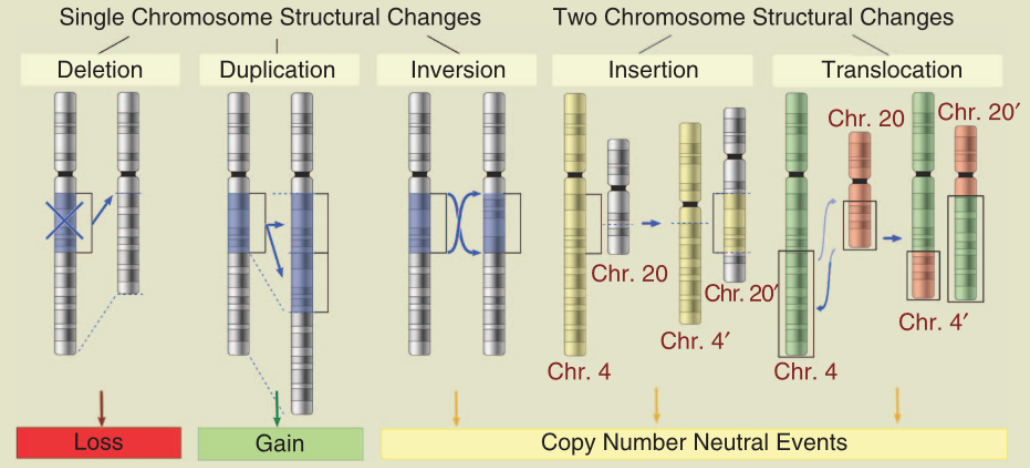

Figure 2.3: Chromosome abnormalities can involve one or more chromosomes. The changes involving a single chromosome are known as deletions, duplications or inversions. The structural rearrangements between two chromosomes result in a translocation or insertion. *Adapted from Intech Open Science.*

this thesis is on the chromosome translocations only they will be described further. Apparently balanced chromosome translocations are structural rearrangements of chromosome material involving two or more chromosomes, but a one directional inversion can sometimes be also called translocation. In this project we are mainly working with reciprocal chromosome translocations, which from now on will be referred to as translocations. During the translocation the chromosome ends are exchanged between two distinct chromosomes. After the translocation there are two derivative (der) chromosomes present, which are distinguished based on the position of the centromere.

The junction between the genetic material of distinct chromosomes in a derivative chromosome is a breakpoint. The simple structural rearrangement involves two distinct chromosomes with two visible breakpoints, in contrast to complex chromosomal rearrangements. These rearrangements may be balanced or unbalanced if associated with gain or loss of chromosomal material. The individual carrying a balanced translocation may not be affected because the entire genetic information is preserved. Unless the breakpoint is present in the middle of a gene or a regulatory sequence. The translocation illustrated in Figure 2.3 is a balanced translocation. An example of unbalanced translocations is shown in Figure 2.4. It can be present in an offspring of a person carrying a balanced translocation. During meiosis one of the derivative chromosomes is passed along to the next generation, thus part of the genetic information is lost. The mechanisms during which the structural rearrangements occur are known as homologous and non-homologous recombination, which are basic mechanisms of gene shuffling and reparation of DNA double strand breaks.

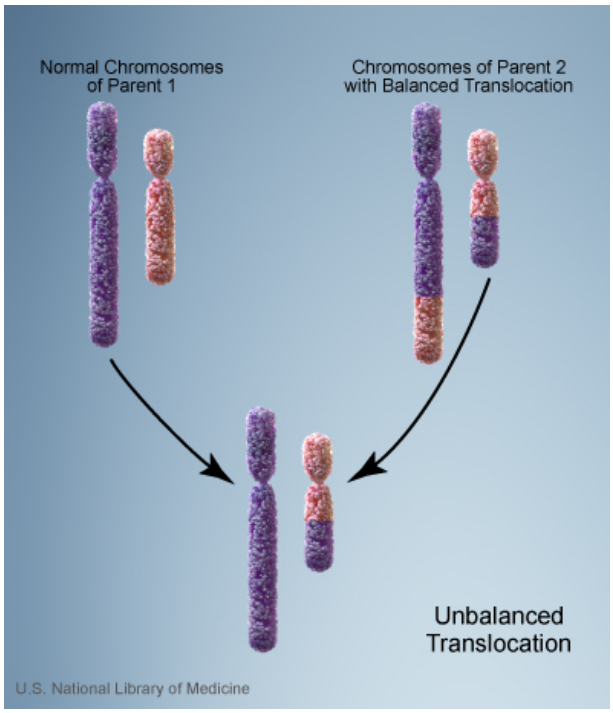

Figure 2.4: Unbalanced translocations can occur during meiosis when one of the parents is a carrier of a balanced translocation. *Adapted from Genetics Home Reference.*

3. Conventional Cytogenetic Analyses to Detect Chromosome Translocations

The first preparations of human karyotype in 1959 which identified numerical aberrations associated with Down's or Turner's syndromes, mark a breakthrough of cytogenetics (Lagos and Jimenez, 2012). Following, studies of cancer tissues revealed the presence of chromosomal translocations as cytogenetic hallmark of lymphomas and leukemias (Gu et al., 1992). For instance, a translocation between chromosome 9 and 21 leads to formation of Philadelphia chromosomes in many cases of chronic myelogenous leukemia (Rowley, 1973). Another example of a common rearrangement is a translocation between chromosome 11 and 22 found in Ewing's sarcoma (Shulman et al., 2012; Silva et al., 2012). Since their identification, the chromosome structures became routinely studied in association with various tumours to identify the aberrations associated with a specific type of cancer. The main focus of this thesis is on the structural rearrangements in the form of reciprocal chromosome translocations.

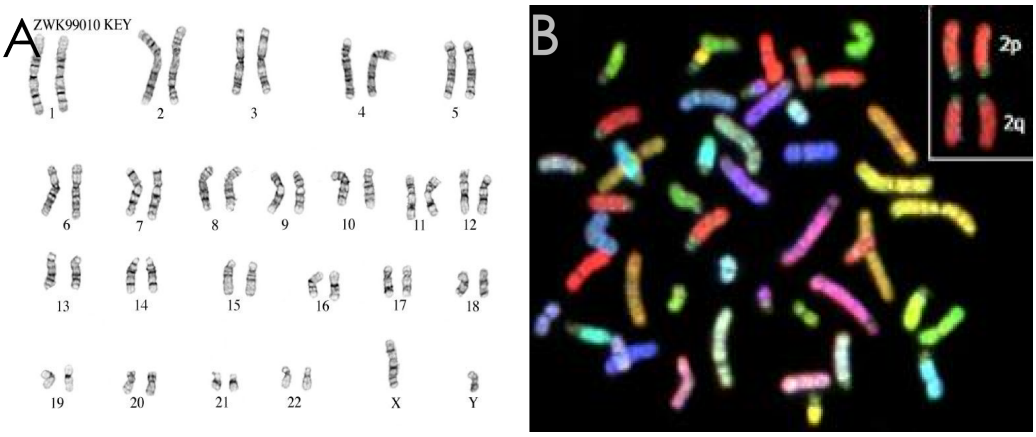

Figure 3.1: Cytogenetic Techniques that are conventionally used for detection of chromosome abnormalities - (A) Karyotyping *(from Nice Genes, nicegenes-curriculumweb.weebly.com)*, (B) Spectral Karyotyping FISH *(from Chrombios, chrombios.com)*.

Traditionally, the chromosomal aberrations were studied by classical cytogenetic techniques such as karyotyping (Figure 3.1A) (Campbell, 2005). It is based on application of a Giemsa stain that binds with high affinity to AT rich regions staining them dark. After karyotyping by banding the chromosomes are dyed with dark and light bands, which forms a pattern that is unique for each chromosome. The analysis allows visualization of the entire karyotype at once, which enables detection of complex rearrangements. Based on the analysis of the bands the abnormalities in a regular chromosome structure can be revealed. However, the resolution of this technique is limited to regions of 5-10 Mbp in size (Serakinci and Kølvraa, 2009). Thus, it has a limited capability to detect the precise location of the breakpoint.

A more recent technique is known as Fluorescent *In situ* Hybridisation (FISH) (Figure 3.1B) (Harper and Saunders, 1981; Pinkel et al., 1986). It involves use of short fluorescently labeled nucleic acid probes that can specifically hybridize to a matching sequence on the chromosome preparation (Pinkel et al., 1986). This technique requires stringent pre- and post-hybridisation washing steps to assure specificity of the signal. The analysis of the fluorescent signals on the chromosomes reveals the presence of a specific DNA sequence, and allows for determination of abnormalities. FISH allows for assessment of the structural changes at resolution down to 10-50 kbp which is higher than by karyotyping (Campbell, 2005; Nath and Johnson, 1999). It can be performed on both interphase nuclei and metaphase chromosome spreads that are fixed on a glass slide. There are many variations to the typical FISH protocol with a single or multiple fluorescent probes used. Sub-telomeric FISH probes can be used to detect the specific translocations as they bind to the chromosome ends. Whole chromosome painting (WCP) uses a pool

of probes that bind to entire chromosomes, thus it allows for individual visualization of the specific chromosomes and detection of the insertions or translocations (Ried et al., 1998). In multiplex-FISH a pool of the whole chromosome probes labeled with combinations of different fluorophores is used. The analysed images are pseudo-coloured to identify all chromosomes by their colour (Volpi and Bridger, 2008). In spectral karyotyping (SKY) 24 chromosome-specific painting probes are used in a single experiment (Figure 3.1B) (Macville et al., 1997; Volpi and Bridger, 2008). Each probe is labeled with multiple fluorophores, which results in a spectral signature individual for each chromosome (Macville et al., 1997; Volpi and Bridger, 2008). These FISH techniques are useful for analysing metaphase chromosomes but provide little information when applied on interphase nuclei (Chudoba, 2007).

The major advantage of karyotyping, metaphase SKY or multicolour FISH analysis is the visualization of the entire genome at once, which allows for detection of interchromosomal changes. However, their main drawback is resolution. Thus, these techniques may be outperformed by advances in sequencing.

4. New Technological Advances

At the beginning of the project the next generation sequencing (NGS) had not been as advanced as it is today. However, it evolved significantly during the last three years and should be mentioned here as a new way of detecting the translocations.

Sequencing of the human genome began in late 90s. by means of a sequencing method developed by Sanger and colleagues. This technique was used for sequencing of the human genome published in 2001 (Venter et al., 2001). The development of NGS has revolutionized human genomics by allowing faster and cost-effective sequencing at high resolution (Shendure, 2008; Shendure and Lieberman, 2012). The recent development of next-generation mate-pair and paired-end sequencing allowed for assessment of chromosomal aberrations at the base pair level with a precise mapping of breakpoints. Even though the advancement of sequencing technique is progressing rapidly it is still a relatively novel and expensive method. The National Institute of Health is sponsoring projects aiming at reducing the costs of genome sequencing in a long term down to $1000 (Hert et al., 2008) but the current analysis costs are much higher. Sequencing requires a vast expertise in sample preparation and amplification methods. Furthermore, the amount of data

generated from a single sequencing experiment needs to be processed by powerful computers that adds up to the total cost of the analysis. Although NGS offers great possibilities to assess the genetic changes on the genome level, sequencing is still a research method more than diagnostic tool. In many cases of the complex rearrangements karyotyping and FISH need to be performed as a primary step before sequencing. Thus, development of a simple to use microsystem for inexpensive assessment of chromosomal changes is necessary. Such a system could be used as a screening device for preliminary diagnostics, based on which the patients sample for sequencing would be selected. In this way the time and costs would be minimized.

5. Lab-on-a-Chip Systems

Lab-on-a-chip (LOC) systems exist since late 70s. In 1979 Steven Terry fabricated a gas chromatograph by using methods commonly applied in electronics. The device performed equally well as standard chromatography equipment, being three orders of magnitude smaller (Hong and Quake, 2003; Telleman, 2008). Since then miniaturized devices in the form of lab-on-a-chip or micro total analysis systems (µTAS) started appearing more frequently. These devices aim at miniaturization and automation of various biological protocols for their wide use in laboratory settings (Chin et al., 2012; Hong and Quake, 2003; Manz and Eijkel, 2001). There are many advantages associated with the use of micro devices as they allow for greater control of a reaction, minimize manual handling, are portable, and are amenable for automation and parallelization (Janasek et al., 2006; Lion et al., 2004; Manz and Eijkel, 2001). Miniaturization leads to lower consumption of reagents, which in turn may reduce the analysis cost (Hong and Quake, 2003; Lion et al., 2004). Furthermore, the reactions at microscale occur faster due to decreased diffusion length (Chin et al., 2012; Hong and Quake, 2003; Janasek et al., 2006; Manz and Eijkel, 2001). However, there are also significant drawbacks to using lab-on-a-chip devices. The technology is still relatively new and thus not thoroughly characterized (Ghallab and Badawy, 2010). Other effects such as capillary forces and surface roughness may be predominant on the microscale making the miniaturization of some processes difficult (Ghallab and Badawy, 2010). There is lack of fully integrated devices and well described protocols for the devices to be operated by researchers outside the field (Janasek et al., 2006). Moreover, the standardization of some components such as interconnections or bubble traps needs to be performed for ease of use.

LOC devices have been developed for various applications ranging from chromatography, cell based assays, detection of analytes or microreactors for chemical reactions. They integrate the microfluidic sample handling with sensors for signals detection to allow for a complete analysis of the performed protocol. The developed LOC systems presented in many scientific papers are often just chips in a lab, as they require additional peripheral equipment for their proper functioning (Hong and Quake, 2003). However, the trend is to bring the analysis closer to people, which has been present for years in the form of home pregnancy tests or blood glucose meters (Chin et al., 2012). The idea behind lab-on-a-chip development is to allow the end user to perform the test be it either at doctor's office or at home. Such devices are known as point-of-care (POC) devices. They are believed to revolutionize the way we diagnose and treat patients nowadays. Due to their low cost and portability they have a potential to be used for analyses of minute amounts of fluids in both developed and developing countries.

6. Aim of the Project

The overall aim of this PhD project is to develop microsystems for chromosome abnormalities detection, with a main focus on chromosome translocations. The microsystems combine the tools used in micro- and nanotechnology with a molecular cytogenetics methods. The purpose of **Part II** is to review the existing micro- and nanotools for detection of the chromosome abnormalities with main focus on FISH analysis.

The main goal of **Part III** is to miniaturize the standard protocols used in cytogenetics to realize a device for chromosome analysis. In this case the sample used contains fixed cells in suspension, which can be readily applied in microfluidic systems. The aim of this part of the project is to create a complete system for miniaturization and standardization of the metaphase chromosome preparation.

Another approach of detecting chromosome translocations is to use the entire human chromosomes. Their size in suspension ranges between 1-7 µm, which is ideal for their manipulation by microfluidics. However, due to the presence of histones keeping the chromosome structure together, they tend to bind to any surface, clogging the devices. To allow for multiplexing of the chromosome translocation detection we decided to use the DNA sequences representing the translocation instead. The aim of **Part IV** is to apply short DNA sequences for development

of the lab-on-a-disc platform with a fluorescent detection of chromosome translocations. The goal of this part of the project is to automate the manipulation of the liquid sample to enable multiplexing.

Part V of the project aims at development of a label-free sensor for DNA hybridisation. In this part the short DNA sequences representing the translocation are also used. The goal is to develop a reliable method of electrical sensing of the hybridisation event. Silicon nanowires, as well as gold and conductive polymer electrodes are used for electrical measurements.

In **Part VI** of the project we aim at integration of the selected sensor in the centrifugal platform. To achieve that a novel measurement setup is build and tested to allow real time detection while spinning.

7. Structure of the Thesis

This thesis leads the reader through the steps taken to develop a device for chromosome translocation detection during my PhD project. The thesis is divided into Parts that focus on individual research projects.

In **Part I** the motivation of the PhD project is introduced with a brief explanation of chromosomes and cytogenetic analyses, and the importance of lab-on-a-chip systems. The Part I is wrapped up by clear statement of the goals of the project.

Part II is based on Paper I, which describes the existing microchips for fluorescent *in situ* hybridisation in a form of a review paper. Part II begins with a brief Introduction followed by the attached review article.

Part III describes the efforts towards development of an all-polymer device for complete cytogenetic analysis. This Part begins with an Introduction, followed by the scientific article (Paper II) and is summarized with Conclusions and Project Summary.

In **Part IV**, an alternative approach towards detection of chromosome translocations is presented. The work presented here formed a basis for a Master thesis of Anna Line Brøgger. This Part is based on Paper III, which describes the development of a centrifugal microfluidic platform for DNA hybridisation detection. It begins with an Introduction after which the scientific article is attached. At the end of this Part, the project is summarized and concluded.

In **Part V** the various label-free sensors developed in this project are gathered. The label-free sensing technique is introduced with all used sensors briefly described with a theoretical background to the sensing principle. The scientific results for each used sensor are thoroughly described in this Part. This Part is summarized and concluded at the end.

Part VI is based on the work done by a Master student Sune Zoëga Andreasen. This part describes the development of a platform allowing for electrochemical measurements during spinning. This Part begins with an Introduction after which the results are presented. Finally, the Part is summarized and concluded.

Part VII includes a project summary and outlook.

The appendices are included in **Part VIII**.

Bibliography

Alberts, B.; Johnson, A.; Lewis, J.; Raff, M.; Roberts, K.; Walter, P., *Chapter 4. in Molecular Biology of the cell*, Edited by Anderson, M.; Granum, S., Taylor and Francis Group, ISBN 978-0-8153-4106-2, (2008)

Campbell, L.J., *Chapter 2. in Methods in Molecular Medicine, Vol. 125: Myeloid Leukemia: Methods and Protocols*, Edited by Iland, H.; Hertzberg, M. Marlton, P., Humana Press, (2005)

Chin, C.D.; Linder, V.; Sia, S.K., *Commercialization of microfluidic point-of-care diagnostic devices*, Lab on a Chip, **12**, 2118-2134 (2012)

Chudoba, I., *Chapter 18. in Chromosomal Alterations: Methods, Results and Importance in Human Health*, Edited by Gunter Obe and Vijayalaxmi, Springer, (2007)

Ford, C.E.; Jones, K.W.; Polani, P.E.; Dealmeida, J.C.; Briges, J.H., *A sex-chromosome anomaly in a case of gonadal dysgenesis (turners syndrome)*, Lancet, **1**, 711-713 (1959)

Gersen, S.L., *Chapter 1. in The Principles of Clinical Cytogenetics 2nd edition*, Edited by Steven L. Gersen and Martha B. Keagle, Humana Press, ISBN 978-158-82-9300-8 (2005)

Ghallab, Y.H.; Badawy, W., *Chapter 1. in Lab-On-A-Chip: Techniques, Circuits, and Biomedical Applications (Integrated Microsystems)*, Artech House, ISBN 978-159-69-3418-4 (2010)

Gu, Y.; Cimino, G.; Alder, H.; Nakamura, T.; Prasad, R.; Canaani, O.; Moir, D.T.; Jones, C.; Nowell, P.C.; Croce, C.M.; Canaani, E., *The (4;11)(q21;q23) chromosome translocations in acute leukemias involve the VDJ recombinase*, PNAS, **89**, 10464-10468 (1992)

Harper, M.E.; Saunders, G.F., *Localization of single copy DNA sequences on G-banded human chromosomes by in situ hybridization*, Chromosoma, **83**, 431-439 (1981)

Hert, D.G.; Fredlake, C.P.; Barron, A.E., *Advantages and limitations of next generation sequencing technologies:A comparison of electrophoresis and non-electrophoresis methods*, Electrophoresis, **29**, 4618-4626 (2008)

Hong, J.W.; Quake, S.R., *Integrated nanoliter systems*, Nature Biotechnology, **21**, 1179-1183 (2003)

Jacobs, P.A.; Baikie, A.G.; Brown, W.C.; Strong, J.A., *The somatic chromosomes in mongolism*, Lancet, **1**, 710 (1959)

Janasek, D.; Franzke, J.; Manz, A., *Scaling and the design of miniaturized chemical-analysis systems*, Nature, **442**, 374-380 (2006)

Lagos, S.M.R.; Jimenez, N.E.R., *Chapter 1 in Recent Trends in Cytogenetic Studies - Methodologies and Applications*, Edited by Tirunilai, P., INTECH, ISBN 978-953-51-0178-9, (2012)

Lion, N.; Reymond, F.; Girault, H.H.; Rossier, J.S., *Why the move to microfluidics for protein analysis?*, Current Opinion in Biotechnology, **15**, 31-37 (2004)

Macville, M.; Veldman, T.; Padilla-Nash, H.; Wangsa, D.; O'Brien, P.; Schrock, E.; Ried, T., *Spectral karyotyping, a 24-colour FISH technique for the identification of chromosomal rearrangements*, Histochemistry and Cell Biology, **108**, 299-305 (1997)

Manz, A.; Eijkel, J.C.T., *Miniaturization and chip technology. What can we expect?*, Pure and Applied Chemistry, **73**, 1555-1561 (2001)

Nath, J; Johnson, K.L.,*A Review of Fluorescence in Situ Hybridization (FISH): Current Status and Future Prospects*, Biotechnic and Histochemistry, **75**, 54-78 (1999)

Pinkel, D.; Straume, T.; Gray, J.W., *Cytogenetic analysis using quantitative, high-sensitivity, fluorescence hybridization*, PNAS, **83**, 2934-2938 (1986)

Ried, T.; Schrock, E.; Ning, Y.; Wienberg, J., *Chromosome painting: a useful art*, Human Molecular Genetics, **7**, 1619-1626 (1998)

Rowley, J.D., *A new consistent chromosomal abnormality in chronic myelogenous leukemia identified by quinacrine fluorescence and giemsa staining*, Nature, **243**, 290-293 (1973)

Serakinci, N.; Kølvraa, S., *Chapter 1. in Fluorescence in situ hybridization (FISH) - Application Guide*, Edited by Liehr, T., Springer-VBH, (2009)

Shendure, J.; Ji, H., *Next-generation DNA sequencing*, Nature Biotechnology, **26**, 1135-1145 (2008)

Shendure, J.; Lieberman, A.E., *The expanding scope of DNA sequencing*, Nature Biotechnology, **30**, 1084-1094 (2012)

Shulman, S.C.; Katzenstein, H.; Bridge, J.; Bannister, L.L.; Qayed, M.; Oskouei, S.; Shehata, B.M., *Ewing Sarcoma with 7;22 Translocation: Three New Cases and Clinicopathological Characterization*, Fetal and Pediatric Pathology, **31**, 341–348 (2012)

Silva, D.S.B.S.; Sawitzki, F.R.; De Toni, E.C.; Graebin, P.; Picanco, J.B.; Abujamra, A.L.; de Farias, C.B.; Roesler, R.; Brunetto, A.L.; Alho, C.S., *Ewing's sarcoma: Analysis of single nucleotide polymorphism in the EWS gene*, Gene, **509**, 263-266 (2012)

Telleman, P., *Chapter 1. in Microsystem Engineering of Lab-on-a-Chip Devices*, Edited by Geschke, O.; Klank, H.; Telleman, P., Wiley-VCH, ISBN 978-3-527-31942-8 (2008)

Venter, J.C.; Adams, M.D.; Myers, E.W., et al., *The sequence of the human genome*, Science, **291**, 1304-1351 (2001)

Volpi, E.V.; Bridger, J.M., *FISH glossary: an overview of the fluorescence in situ hybridization technique*, Biotechniques, **45**, 385-409 (2008)

Part II

Chromosomes, Fluorescent *In Situ* Hybridisation and Microtechnologies

8. Introduction

At the beginning of the project a literature review was conducted for a better understanding of cytogenetic analysis and techniques currently used. This literature study formed a basis of the Review Article 'Advanced Microtechnologies for fluorescent in situ hybridisation'. It describes the principles behind FISH as a standard analysis performed in cytogenetics. It introduces the application of microtechnologies for miniaturization of the protocols and their optimiziation in relation to analysis time and costs.

8.1 Paper 'Advanced Microtechnologies for fluorescent in situ hybridisation'

In this section the manuscript 'Advanced Microtechnologies for fluorescent in situ hybridisation' is included. The concluding remarks related to the literature review are summarized in Chapter 9.

Biomed Microdevices
DOI 10.1007/s10544-011-9622-7

Advanced microtechnologies for detection of chromosome abnormalities by fluorescent *in situ* hybridization

Dorota Kwasny · Indumathi Vedarethinam · Pranjul Shah · Maria Dimaki · Asli Silahtaroglu · Zeynep Tumer · Winnie Edith Svendsen

Abstract Cytogenetic and molecular cytogenetic analyses, which aim to detect chromosome abnormalities, are routinely performed in cytogenetic laboratories all over the world. Traditional cytogenetic studies are performed by analyzing the banding pattern of chromosomes, and are complemented by molecular cytogenetic techniques such as fluorescent *in situ* hybridization (FISH). To improve FISH application in cytogenetic analysis the issues with long experimental time, high volumes of expensive reagents and requirement for trained technicians need to be addressed. The protocol has recently evolved towards on chip detection of chromosome abnormalities with the development of microsystems for FISH analysis. The challenges addressed by the developed microsystems are mainly the automation of the assay performance, reduction in probe volume, as well as reduction of assay time. The recent focus on the development of automated systems for performing FISH on chip is summarized in this review.

Keywords Fluorescent *in situ* hybridization · FISH on chip · Microsystems · Cytogenetic analysis

D. Kwasny · I. Vedarethinam · P. Shah · M. Dimaki · W. E. Svendsen (✉)
Department of Micro- and Nanotechnology, Technical University of Denmark, Ørsteds Plads, 2800 Kgs. Lyngby, Denmark
e-mail: wisv@nanotech.dtu.dk

D. Kwasny
e-mail: dorota.kwasny@nanotech.dtu.dk

A. Silahtaroglu
Department of Cellular and Molecular Medicine, Faculty of Health Sciences, University of Copenhagen, Copenhagen, Denmark

Z. Tumer
Center for Applied Human Molecular Genetics, The Kennedy Center, Glostrup, Denmark

Present Address:
P. Shah
Luxembourg Centre for Systems Biomedicine, University of Luxembourg, Campus Belval 7, Avenue des Hauts-Fourneaux, 4362 Esch-sur-Alzette, Luxembourg

1 Introduction

The incidence of chromosome abnormalities in live births is around 0.7% (Hsu 1998) and specific chromosome abnormalities are responsible for more than 100 identifiable syndromes (Jackson 2002). Chromosome disorders are hence a major category of genetic disorders (Jackson 2002) and cytogenetic studies, including conventional cytogenetics and the complementary fluorescence *in situ* hybridization (FISH) analyses, are valuable diagnostic tests. FISH complements the conventional cytogenetics, creating a bridge between cytogenetics and molecular genetics. Despite its diagnostic value, FISH analysis is laborious and automating this technique will be beneficial for the routine diagnostic studies. Recently researchers have focused on the development of integrated, miniaturized systems for more sensitive and rapid analysis of biological samples at low cost. Lately some efforts have been made towards fabrication of systems for chromosome and FISH analyses aiming to automate the assay and to reduce cost, sample volume, and hybridization time related. In this

Published online: 06 January 2012

paper, we review the current state of the microsystems developed to detect chromosome abnormalities.

2 Implementation of microdevices for cytogenetic analysis

Chromosome analysis is the first type of whole genome analysis and together with FISH it is still one of the main routine analyses in diagnostic laboratories. Microtechnolgies and microdevices, which became an integral part of different biological protocols, are also being introduced in cytogenetic analyses. The main focus on miniaturizing cytogenetic protocols has been on automation of the process and cost reduction. The main steps in cytogenetic analyses can be divided into the following steps (Fig. 1):

1. Cell culturing, including cell growth stimulation and arrest of cell division in metaphase
2. Spreading metaphase chromosomes on glass slides
3. Visualization by:
   - Chromosome banding using various staining methods
   - Fluorescence *in situ* hybridization

All these steps are amenable for miniaturization allowing reduced work load, shorter analyses time, reduction in the amount of reagents used per analysis and increase in throughput.

3 Microdevices for preparing metaphase chromosomes

Preparation of the metaphase chromosomes is the common step for karyotyping and FISH analyses. This step requires stimulation of cell division of lymphocytes (also called cell culturing in practice) and capturing of cell division in metaphase. Cell division is stimulated by phytohemagglutinin (PHA) leading to increased amount of cells, and thus to obtain more chromosome spreads on a glass slide. Cell culturing is traditionally performed in cell culture flasks using patient's blood sample in volumes of the milliliter order. The sample can be either used directly or purified to culture T-lymphocytes only. At the end of culturing the cells are arrested in metaphase by treatment with colchicine. After three days the cell suspension is collected and centrifuged to change the medium to hypotonic buffer and further to fixative. During the solution changes, few centrifugation steps are performed during which a cell loss is observed. Moreover, manual cell handling

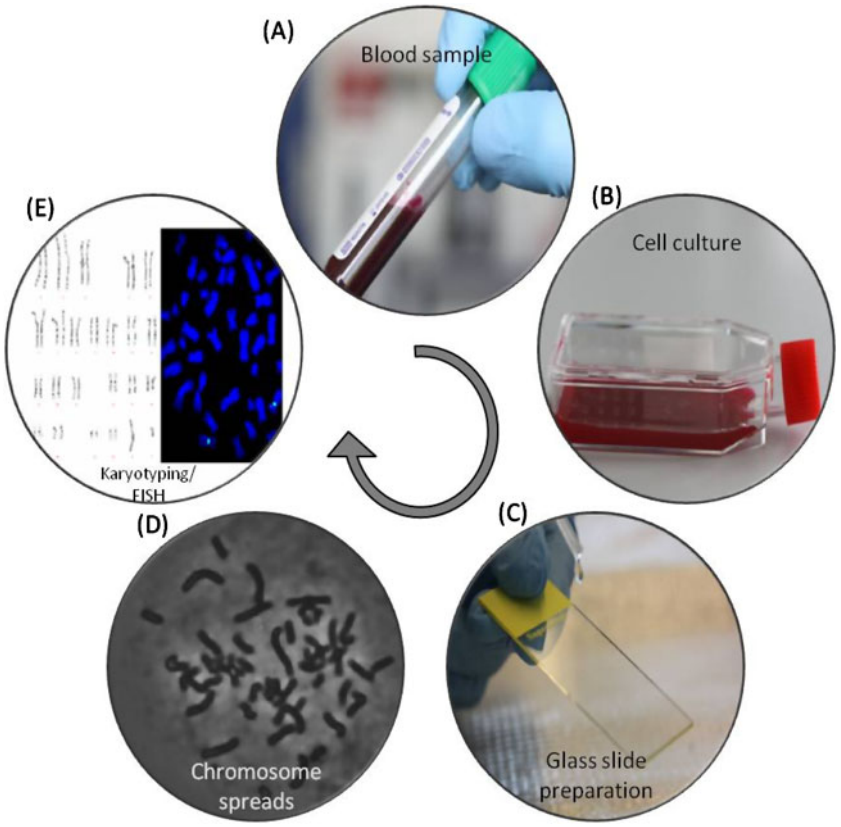

Fig. 1 The cytogenetics analysis protocol. Blood sample is collected from the patient (**A**) and cultured with growth stimulation for 3 days at 37° C (**B**). Colchicine is added at the end of the culture period to arrest the cells in metaphase. Followed by hypotonic treatment, the cells are dropped on a glass slide (**C**) to obtain metaphase chromosome spreads (**D**). At this point the chromosome spreads can either be analyzed by karyotyping or FISH (**E**)

can cause sample contamination and is labour intensive. Microdevices for cell culturing can reduce the contamination risk and significantly decrease the volume of the reagents. Due to miniaturized sizes they can also reduce the time necessary for culturing as the cells are enclosed in chambers of micro dimensions, which is similar to their *in vivo* environment. Furthermore, microfluidic devices offer easy changing of the solutions without the cell loss. The continuous cell perfusion with the medium supplying nutrients provides a better control over cell-to-cell interactions and by-products removal (Kim et al. 2007). Such devices offer possibility to automate the process and set several cultures in parallel thus increasing the throughput.

Liu and co-workers developed a simple cell culture chip suitable for suspension cells (Liu et al. 2008). The device minimizes the shear stress that is applied to the cells, as it is considered a major disadvantage of the microfluidic systems. They fabricated a microfluidic chip composed of two PDMS layers bonded to a glass slide. The PDMS layer consists of a main microfluidic channel with side cell culture chambers. The main channel serves as a medium supply, which provides cells with nutrients due to convective and diffusive mass transfer into the side chambers. They presented culturing of both adhesion and suspension cells without cell damage or loss during the culture period, with a possibility of starting perfusion immediately after cell loading. The main disadvantage of the design with side channels was the cell unloading from the chip for further analysis.

Another solution to culture of suspension cells was currently presented by Svendsen et al. (2011). They developed a membrane based microfluidic bioreactor for suspension cell cultures, which makes preparation of chromosome spreads much easier (Svendsen et al. 2011; Shah et al. 2011b). The proposed diffusion based microreactor facilitates culturing of lymphocytes but also expansion, hypotonic treatment, and fixation of cells with the possibility to avoid several tedious centrifugation steps (Svendsen et al. 2011). Svendsen and others developed a bioreactor for a suspension cells culture on the membrane with a microfluidic channel for media perfusion. To ensure compatibility with the standard laboratory procedures, a pipette access hole was designed for cell loading, which was sealed manually with a PCR tape during cell culturing. All other steps in the procedure where performed on chip without a human intervention, which greatly reduced the contamination risk. The medium flow can be started even before the cells settle on the membrane, due to physical separation of both parts of the device. This is also helpful in protecting the cells from air bubbles that can be formed in the medium. The medium flow ensures continuous delivery of necessary nutrients to the cells by diffusion through the membrane. Although no reduction in culture time was presented the authors proved that a three days culture of lymphocytes in the membrane based bioreactor was comparable to the cell growth in a well-plate.

The membrane based bioreactor was further modified by Shah et al. (2011b). They redesigned the perfusion channel into a meander to improve the nutrients transport across the membrane. This allows for faster change of the cell medium to hypotonic solution and fixative without the cell loss. Also cell loading and unloading was changed to syringe injection through the cell chamber inlet with a 3-port valve for easy bubble removal. Moreover, by performing CellTrace™ CFSE cell staining protocol it was demonstrated that cell proliferation on chip is better than in control experiment in a well plate culture with a possible time reduction required for cell culture.

4 Microsystems developed for FISH analysis

FISH analysis is based on the sequence specific hybridization of fluorescently labeled DNA probe to chromosome preparations fixed on a glass slide (Fig. 2). First, the chromosomes are pretreated with RNAse, dehydrated by ethanol treatment and washed in buffer solutions in coplin jars. Afterwards, both the probe and chromosomes on the slide are heat denatured to enable hybridization of complementary sequences. After incubation, the unbound and unspecifically bound probe is washed away. The hybridization signals are observed under a fluorescent microscope and identify

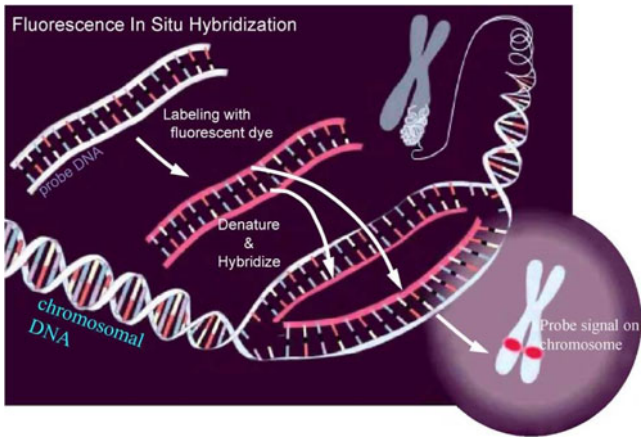

Fig. 2 Fluorescent *In Situ* Hybridization principle. The fluorescently labeled DNA probe is denatured and hybridized to the denatured chromosomal DNA on a glass slide (used with permission from (Smeets 2004))

the presence of the sequence targeted by the applied probe.

The major drawback of FISH analysis is the cost of the reagents used for the assays, mainly the fluorescent probes. In standard lab protocols 10μl of probe are used per slide containing metaphase spreads or interphase nuclei (Lee et al. 2007; Vedarethinam et al. 2010). Such analysis is normally performed on a single patient's sample, thus the cost of a single analysis is extremely high. The development of a high throughput device for metaphase or interphase FISH analysis would reduce the volume of the probe used per single sample, at the same time reducing the cost of an experiment. Also, addressing the need for reduction in probe volume for single analysis would greatly increase the application of FISH in routine analysis. Another bottleneck of the analysis is the long experiment time. To perform a complete FISH analysis, even well trained technicians spend several hours in sample preparation as well as the waiting time in between each pre- and post- hybridization washes. There are at least different washes in a standard routine test that in total takes about 45 min. Apart from the cell culture work, the hybridization time is a very long process. At minimum, performing a FISH analysis with centromeric probes (repetitive sequences), will take 2–4 h. Furthermore, in some FISH experiments the hybridization of a probe requires overnight incubation. The automation of sample preparation, probe delivery, imaging and analysis would result in molecular cytogenetic analysis to be performed routinely at the doctor's office as a point-of-care diagnosis.

One of the many advantages of microdevices for complete chromosome analysis is the possibility to automate the entire biological protocols. It has been demonstrated that FISH protocol can also me miniaturized and possibly automated in the future. Some examples of miniaturized devices for suspension cells culturing have been demonstrated. Moreover, slide preparation and the probe hybridization in microdevices have also been shown. Combining all these steps in one high throughput, automatic microsystem has a potential to establish FISH as a leading cytogenetic technique. Thus, speeding up the process of the cytogenetic analysis and providing fast, reliable results. In recent years the integration and automation of cytogenetic techniques has gained more attention. Most reports in this field focus on the development of an integrated microfluidic chip for interphase FISH analysis. To our knowledge there has been only one report on a microfluidic platform for metaphase FISH on chip.

In 2007, Lee and co-workers presented one of the first examples of miniaturized devices for performing FISH analysis (Lee et al. 2007). The presented work allows for high throughput FISH analysis on a cell array. The typically performed analysis lacks the possibility of conducting high throughput analysis as there is limited amount of samples available. To address this problem, the authors showed the possibility to array cells by spotting the small amounts of cell specimens onto a supporting matrix, which enables high throughput analysis. For the preparation of the chip, a glass slide was used as a supporting matrix. 1 mm thick perforated PDMS was bonded to a glass slide to form 96 cavities of 1.5 mm in diameter for spotting cells (Fig. 3). To enable microscopic cell identification a matrix corresponding to the 96 PDMS wells was microfabricated by photolithograpy on a glass slide. They have showed that 1μl samples can be spotted onto each PDMS well followed by air drying and removal of PDMS cover. Due to PDMS cover, the spotted specimens were confined in a small

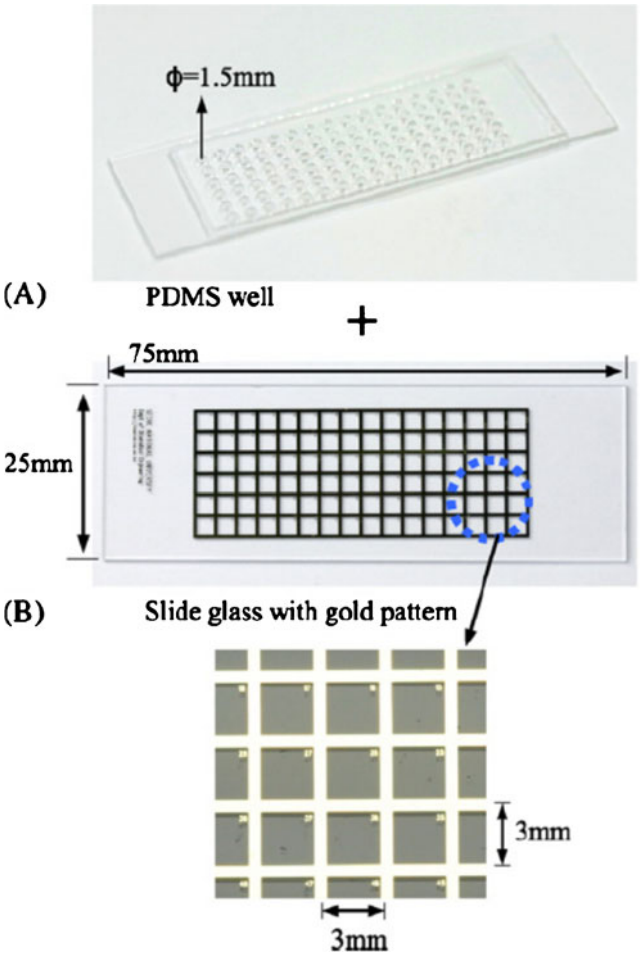

Fig. 3 Fabricated bio-cell chip slide. (**A**) A PDMS layer with 96 wells for multiple cell analysis. (**B**) A glass slide with a gold pattern for sample numbering (used with permission from (Lee et al. 2007))

square area without mixing. Afterwards a conventional FISH protocol was performed on the glass slide. Having 96 different samples spotted on the glass slide they were able to use only 10μl of probe to analyze all of them. This is advantageous in comparison to standard slide preparation as usually this volume of probe is used to analyze only one sample.

The device is very useful in mass sample analysis for the samples screening, in which the probe reduction is relevant. The authors have mentioned the probe volume reduction, but other major issues such as manual intervention and time consumption were not stated. No FISH images were presented but the authors stated that the chip was suitable for FISH analysis of multiple specimens. The authors mentioned a possibility to replace PDMS with paper stickers. Such solution is applicable to current laboratory settings and may be easily used.

The first implementation of interphase FISH protocol on chip was showed in Sieben et al. (2007). They have adapted the conventional FISH protocol into miniaturized format except for the cell immobilization step, which was achieved using temperature treatment. They also investigated a method to reduce hybridization time by probe recirculation with on-chip peristaltic pumps, and electro-kinetic transport of probes by introducing the electrodes into the end-wells. By these two methods, they found out that electro-kinetic transport of the probes was slightly better than recirculation method. In addition, the electro-kinetic chip design is simpler than the recirculating micropump, which involves valves and complex micro fabrication. Nevertheless, by performing the analysis at microfluidic volumes, they were able to achieve a tenfold reduction in DNA probe reduction per test, with an equivalent cost reduction.

In 2008, Sieben and others published another paper in which all previously performed steps with microfluidic FISH were integrated onto one chip and automated (Sieben et al. 2008). Similar to the recirculating design, the new chip consisted of a PDMS layer sandwiched between two glass layers, one of which carried fluids, while the other transmitted air pressure for valve control, e.g. for peristaltic pumping, which is a very complex fabricated system. With the valves operated by computer, preloaded reagents could be multiplexed through the hybridization chamber at appropriate intervals for each step of FISH. A copper thin-film heater was built into the design as well, for the cell-immobilization and denaturation steps (Fig. 4(A), (B)). Unlike the previous designs, this new device did not focus on the reduction in hybridization time, but instead focused mainly on minimizing the labor time and automation of the microfluidics FISH chip. One of the issues with the conventional FISH is that it takes more than an hour of on-and-off attention of a skilled technician, using their time inefficiently. The automated microfluidic FISH device would reduce human intervention and only involve the technicians work during reagent preparation, and image analysis. The authors demonstrated the applicability of the fabricated device for use with cell lines and patient samples for interphase FISH analysis (Fig. 4(C)). The FISH signals

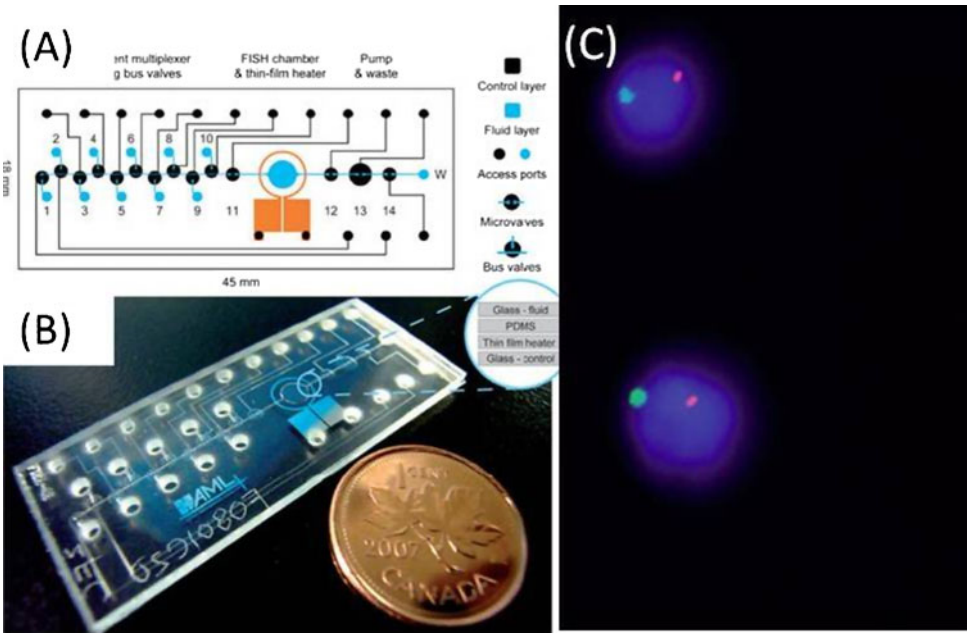

Fig. 4 (**A**) The mask layouts and dimensions of an integrated FISH microchip. The microchip includes a reagent multiplexer, a cell chamber with an integrated thin-film heater, and a peristaltic pump. (**B**) Image of a complete integrated FISH chip. (**C**) Interphase FISH results of a male sample showing signals from one X and one Y chromosomes (used with permission from (Sieben et al. 2008))

obtained in the microchip were comparable to the conventional method with the advantage of using less probe and technician work.

The most recent advances in integrated interphase FISH analysis were presented in Zanardi et al. (2010). They focused on the development of an analytical tool for performing interphase FISH on both living and fixed cells. The application of microfluidic technologies might reduce costs and improve assay performance by development of microchannels for easy reagent loading and cell immobilization. However, the fluid flowing in the microchannels causes intense shear stress on cells; this may result in their disruption or detachment from the surface. In this paper the authors' addressed this particular problem in the application of microfluidics for FISH. By changing the surface chemistry they enhanced the cell immobilization on the surface that significantly reduced the cells detachment due to shear stress. In this article, the entire glass slide is coated with nano structured TiO_2 using cluster beam technology which adds significant costs to the device owing to the need for access to cleanroom and costs of additional material deposition. Moreover, routine genetic labs do not necessarily have access to cleanroom facilities, which makes the method very difficult to implement on a larger scale. Besides, the authors do not mention the lifetime of the applied surface coating. The commonly applied coatings have a relatively short lifetime, which makes them unsuitable for long term storage of the devices. The top cover bonded to the modified glass slide contains a microfluidic channel that is used for loading cells and other reagents in FISH protocol. The channel has pipette access holes as an inlet and an outlet, which is applicable to standard laboratory procedures. Such a simple design facilitates handling of the fluids without generating bubbles that could affect assay performance. Moreover, due to channel dimensions the cells are confined in a small space, which makes the image analysis faster. The authors demonstrated the use of the miniaturized FISH device for the entire protocol performed on several cell samples with different FISH probes applied. The channel was closed with a drop of mineral oil to prevent probe evaporation during overnight hybridization. The miniaturized interphase FISH results were comparable to conventional FISH technique. The main advantage of the device is the reported probe reduction of 10- to 30- folds, which significantly reduces the experiment costs.

In 2010, Vedarethinam and colleagues developed the first metaphase FISH device, which can be used to detect the microdeletion or specific translocation with high resolution (Vedarethinam et al. 2010). Unlike interphase FISH, metaphase FISH is difficult to adapt to a closed microfluidic system. The chromosome immobilization needs preparation of chromosome spreads, which rely on certain factors, such as controlled angle of spotting (Deng et al. 2003), temperature gradient and humidity (Henegariu et al. 2001). Recently, Qu and others devised a chromosome dropper tool, which demonstrates that the dropping angle and height are the important factors getting good metaphase spreads on glass slides (Deng et al. 2003; Qu et al. 2008).

Based on these factors Vedarethinam and others made a novel splashing device with an open chamber, which allows for easy evaporation of the fixative (Fig. 5(A)). The device provides 11 mm dropping height with two inlets-one for cold water and one for the fixed mitotic cells suspension. The microFISH device is a PDMS lid with two channels and a reaction chamber for metaphase FISH. The bonding of the PDMS chip to the glass slide is achieved by the double side adhesive tape with laser ablated channels and chamber structure. This rapid and easy assembly protocol for the microFISH device allows for quick transformation of a simple glass slide into a microFISH device, which makes it a solution for integration into existing work routines at cytogenetic labs (Fig. 5(B)). Nevertheless, the authors have mainly focused on adapting the conventional metaphase FISH to lab-on-a-chip method. The average numbers of spreads obtained using the splashing device are comparatively lower and the splashing device does not improve the chromosome spreading. However, it produces reliable metaphase spreads on a glass slide (Fig. 5(C)), which is sufficient for conducting routine FISH analysis. The microFISH device was used for miniaturized metaphase FISH protocol and produced FISH signals comparable to the conventional method (Fig. 5(D)). Even though the microFISH device allows for an optimized metaphase FISH protocol on a chip with over 2-fold reduction in the reagent volume, the reduction of probe volume, which is the most expensive part of the process, is not very large. One of the device advantages is the simplicity of chip assembly on a glass slide. However, for the controlled reagents loading a syringe pump should be used, which is not standard cytogenetic lab equipment. If complete automation of the microFISH device is possible with further probe volume reduction, it should improve the use of metaphase FISH for widespread genetic testing of unknown translocations making it more accessible in a clinical setting (Theodosiou et al. 2007).

Recently a FISHprep device was developed by Shah et al. (2011a). It combines a membrane based cell culture device (Shah et al. 2011b) with the splashing device (Vedarethinam et al. 2010) that are separated by

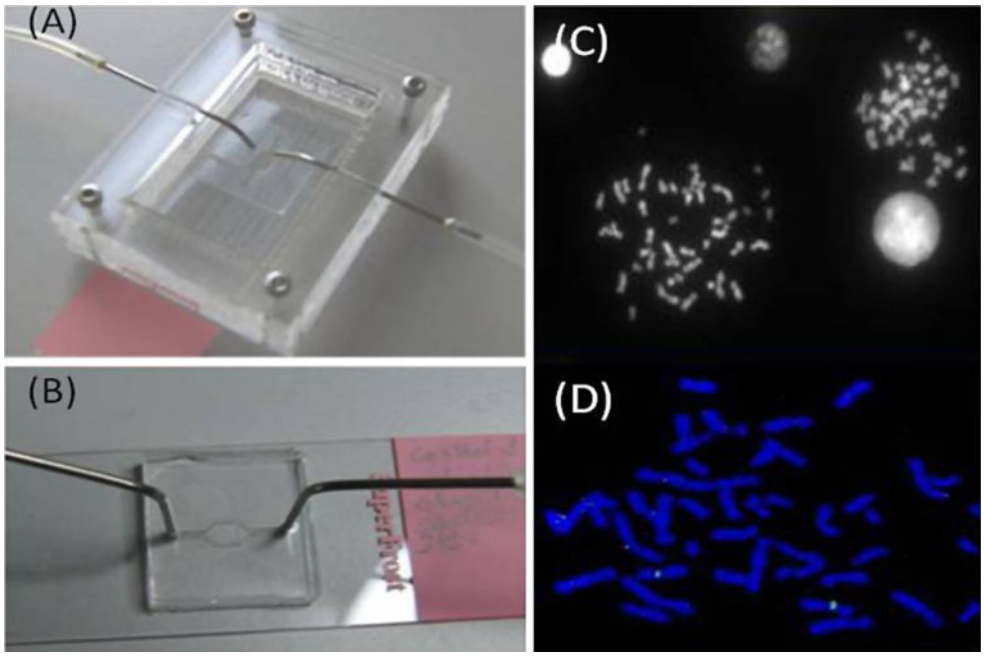

Fig. 5 (**A**) The PMMA splashing device with two inlets for glacial water and cell suspension. (**B**) Fully assembled microFISH device with a PDMS chamber on a glass slide with chromosome spreads. (**C**) Chromosome spreads obtained from a splashing device. (**D**) Metaphase FISH performed in a microFISH device (used with permission from (Vedarethinam et al. 2010)).

a clip valve that controls fluid flow. It is an example of formation of an almost complete system for metaphase FISH on chip analysis. The device consists of the membrane based cell culture chip, on which T-lymphocytes were cultured for 72 h with CFSE staining to determine the proliferation rate. After the culturing step was completed, the clip valve was removed to allow the fixed cells to be passed to the splashing device and dropped on a glass slide. The metaphase spreads obtained in this device were comparable to those obtained by manual dropping. This FISHprep device is the first example of integration of different cytogenetic analysis steps in one system. The last step of actual FISH protocol can be easily incorporated into the system by placing the double sided adhesive tape stencil on a glass slide and bonding microFISH devices. Thus, FISHprep offers a possibility of automating the metaphase FISH analysis in future.

5 Future prospects

The miniaturization of the integrated platforms for molecular cytogenetics will progress in the nearest future. The devices for culturing of lymphocytes are available, which offers reduction of the reagents volume and better nutrients supply. Combining the cell culture device with sample preparation and miniaturized FISH is a next step towards automating the FISH analysis and using it routinely all over the world. Most of the work done in the microcytogenetics field has addressed the probe volume used and further development will be directed towards automation of the available systems. The interphase FISH has been almost completely automated by means of microsystems, but some work still needs to be done in order to reduce the assay time.

The advantages of making analysis on metaphase chromosomes are enormous and the development of microsystems for their preparation and analysis is of utmost importance. The presented splashing device by Vedarethinam and co-workers has a potential of being automated and can be coupled to cell culture microdevice as presented by Shah and others. However, the chromosome spreads are formed in an open chamber, which requires some manual handling of the glass slide. For the future of metaphase FISH analysis it is crucial to fabricate a closed or semi-closed microdevice in which metaphase spreads are easily formed. Some chemical modifications of the substrate surface could help in obtaining high quality metaphase spreads even in confined channels.

Most of the cytogenetic techniques require a use of glass slides. Fabrication of microdevices on a glass requires use of expensive cleanroom technology adding significant costs to the final analysis. Some efforts need to be taken in order to introduce polymers into the cytogenetic analysis. Most of the reviewed microdevices for FISH protocol used PDMS as a part of the device. However, in all cases the PDMS lid was bonded to the glass slide. Other polymers should also be considered for fabrication of a complete polymeric chip, with the interphase nuclei or metaphase chromosomes prepared

on a polymer slide. Such device would be disposable and benefit from lower costs of production, leading to inexpensive analysis.

All of the presented devices offer miniaturization of the standard FISH protocol. The presented microdevices enable detection of the abnormalities on the available patient samples at a reduced probe volume, allowing their common application in the cytogenetic analysis. However, the analysis of the results is performed manually under a fluorescent microscope. Future work should focus on the integration of the microfluidic devices with an automatic readout of the hybridization signal. Moreover, as the FISH analysis can only be used in detection of known chromosome abnormalities using available fluorescent probes, some efforts should be made to enable determination of unknown chromosome disorders, such as chromosome translocations. There is a great need for a system that can enable determination of unknown translocations and still a lot of work needs to be done to achieve their reliable analysis.

6 Conclusions

Cytogenetic analysis is an important tool commonly used in clinical diagnosis and treatment monitoring. FISH has a numerous applications in molecular biology, including gene mapping, diagnosis of chromosome abnormalities, and cancer detection. In clinical research, FISH can be used for prenatal diagnosis of inherited chromosomal aberrations, postnatal diagnosis of carriers of genetic disease, diagnosis of infectious disease, viral and bacterial disease, tumor cytogenetic diagnosis, and detection of aberrant gene expression. Technical complexity of conventional FISH protocol has slowed down the usage of the technique in clinical settings. Significant effort has been put into enabling fast, reliable and high throughput analysis of samples. The assays and devices presented in this review can be easily incorporated in cytogenetic laboratories to improve the quality of analysis and reduce the time necessary to obtain significant results. The presented bioreactors for cell cultures offer the automation of the preparation of metaphase spreads on glass slides without the need for centrifugation steps. Most of the mentioned work was done to improve the interphase FISH analysis with just one work presenting metaphase FISH analysis. These platforms offer great advantages over conventional methods in regards to reduction of probe volume per analysis used as well as the possibility to automate the protocol. Nevertheless, there is still a gap between developing the technology and usage of these systems as a routine diagnostic tool in cytogenetic laboratories.

Acknowledgement The authors would like to thank the Danish Council for Strategic Research for financial support.

References

W. Deng, S.W. Tsao, J.N. Lucas, C.S. Leung, A.L.M. Cheung, Cytometry **51A**, 46–51 (2003)
O. Henegariu, N.A. Heerema, L.L. Wright, P. Bray-Ward, D.C. Ward, G.H. Vance, Cytometry **43**, 101–109 (2001)
L. Hsu, Prenatal diagnosis of chromosomal abnormalities through amniocentesis. in *Genetic Disorders and the Fetus*, 4th edn. (The Johns Hopkins University Press, Baltimore, 1998)
L. Jackson, Clin. Obstet. Gynecol. **45**, 622–639 (2002)
L. Kim, Y.-C. Toh, J. Voldman, H. Yu, Lab Chip **7**, 681–694 (2007)
D.S. Lee, J.H. Lee, H.C. Min, T.Y. Kim, B.R. Oh, H.Y. Kim, J.Y. Lee, C.K. Lee, H.G. Chun, H.C. Kim, J. Biotechnol. **127**, 355–360 (2007)
K. Liu, R. Pitchimani, D. Dang, K. Bayer, T. Harrington, D. Pappas, Langmuir **24**, 5955–5960 (2008)
Y.Y. Qu, L.Y. Xing, E.D. Hughes, T.L. Saunders, J. Histotechnol. **31**, 75–79 (2008)
P. Shah, I. Vedarethinam, D. Kwasny, L. Andresen, S. Skov, A. Silahtaroglu, Z. Tumer, M. Dimaki, W.E. Svendsen, Micromachines **2**, 116–128 (2011a)
P. Shah, I. Vedarethinam, D. Kwasny, L. Andresen, M. Dimaki, S. Skov, W.E. Svendsen, Sens. Actuators B Chem. **156**, 1002–1008 (2011b)
V.J. Sieben, C.S.D. Marun, P.M. Pilarski, G.V. Kaigala, L.M. Pilarski, C.J. Backhouse, IET Nanotechnology **1**, 27–35 (2007)
V.J. Sieben, C.S. Debes-Marun, L.M. Pilarski, C.J. Backhouse, Lab Chip **8**, 2151–2156 (2008)
D.F.C.M. Smeets, Clin. Biochem. **37**, 439–446 (2004)
W.E. Svendsen, J. Castillo-Leon, J.M. Lange, L. Sasso, M.H. Olsen, M. Abaddi, L. Andresen, S. Levinsen, P. Shah, I. Vedarethinam, M. Dimaki, Sens. Actuators A Phys. **172**, 54–60 (2011)
Z. Theodosiou, L.N. Kasampalidis, G. Livanos, M. Zervakis, L. Pitas, K. Lyroudia, Cytometry **71A**, 439–450 (2007)
I. Vedarethinam, P. Shah, M. Dimaki, Z. Tumer, N. Tommerup, W.E. Svendsen, Sensors **10**, 9831–9846 (2010)
A. Zanardi, D. Bandiero, F. Bertolini, C.A. Corsini, G. Gregato, P. Milani, E. Barborini, R. Carbone, BioTechniques **49**, 497–504 (2010)

9. Conclusions

The literature review of the microtechnologies applied to cytogenetics was performed at the beginning of the project. It was conducted to determine the activities in the field and its size. There is a relatively little interest in the development of the microdevices for cytogenetic analysis with the main focus on FISH. Only few groups devote their efforts towards improvement of the existing protocols by their miniaturization. Their main advantage is the reduced reagents use and minimal sample handling. Most of the reviewed articles focused on the application of the standard FISH protocol with little input on the new approaches towards detection of the chromosome translocations. Furthermore, the presented devices are often only applicable to interphase FISH procedure and are rarely used for metaphase chromosome spreads. The metaphase FISH would be beneficial for detection of complex rearrangements as SKY or multiplex-FISH could be used for detection. In case of the existing metaphase FISH devices the chromosome spreads are prepared manually, while it would be advantageous to obtain chromosome spreads in a controlled way inside a microdevice.

Part III

Chromosome Total Analysis System

Introduction

Part III briefly introduces a previous research project in the group called Chromosome Total Analysis System, which was the base for this entire PhD project. The work related to this project is also described including attempts towards development of a complete polymer device for cytogenetic analysis. The polymer material considerations are described based on the requirements for optimal chromosome spreading. The research related to Part III is presented in a manuscript 'All-polymer semi-closed device for metaphase chromosome spreading' (Paper II). At the end of Part III concluding remarks are given with a brief discussion of the presented work.

10. Chromosome Total Analysis System

The Chromosome Total Analysis System (C-TAS) project in the NaBIS group aimed at developing a miniaturized system for analysis of chromosome abnormalities. The project was based on the conventional protocol for FISH (Campbell, 2005; Harper and Saunders, 1981; Pinkel et al., 1986) focusing on its miniaturization and automation. It has been divided into three separate modules for lysing of red blood cells, culturing of lymphocytes and further analysis of metaphase chromosomes by FISH. The first step is necessary for isolating lymphocytes from a blood sample, which are further cultured for 72 h with a growth stimulation medium in a cell culturing module. The cells are arrested in metaphase and are further suspended in a fixative solution. The fixative is a mixture of methanol and acetic acid that allows the chromosomes to spread on a glass slide. The metaphase chromosome spreads are then used for FISH analysis, which is based on hybridisation of fluorescently labeled sequence specific DNA probes to chromosomes (Campbell, 2005; Harper and Saunders, 1981; Pinkel et al., 1986).

10.1 FISH on Chip Module - Previous Studies

The third module in C-TAS project was aiming at the development of a miniaturized system for detection of chromosome abnormalities using FISH. This tech-

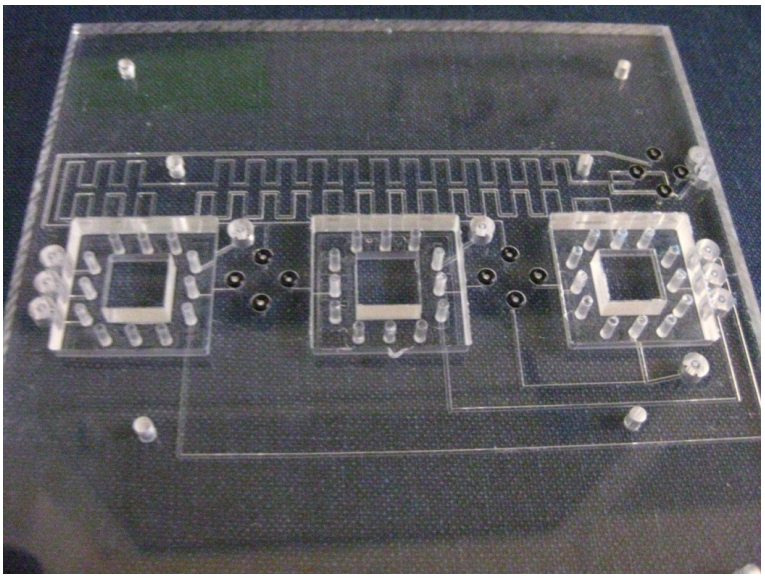

Figure 10.1: Motherboard developed in C-TAS project with a plug and play principle to insert 3 separate modules for chromosome analysis. *Image adapted from Pranjul Shah's PhD thesis.*

nique is commonly used in cytogenetic analysis and includes a series of pre- and posthybridisation steps with a DNA hybridisation step in between (Campbell, 2005; Harper and Saunders, 1981; Pinkel et al., 1986). The prehybridisation steps are performed to prepare the chromosome spreads on a glass slide for application of the fluorescently labeled probe. During the prehybridisation steps the chromosome preparations are washed, dehydrated and denatured for the DNA probe to hybridize. The DNA probe is also denatured as it is normally double stranded. The posthybridisation stringent washes are applied to remove the unspecifically bound DNA probe and to make sure that the only fluorescent signals are occurring due to probe being specifically attached to targeted sequence. The procedure is performed manually and takes about few hours of manpower. Moreover, the large amount of reagents used during the analysis contributes to its cost. The idea behind the miniaturized FISH system was to reduce the analysis time and reagents consumption, by applying a laminar flow to actively exchange all the solutions.

During her PhD project, Indumathi Vedarethinam has successfully miniaturized the FISH assay, reaching 2 fold reduction in the amount of probes used (Vedarethinam et al., 2010). The developed assay was composed of two chips - one for controlled chromosome spreading on a glass slide and a second one for application of FISH reagents. The FISH on Chip was composed of a polydimethylsiloxane (PDMS) gasket with a microfluidic channel and a chamber mounted on a glass slide by means of adhesive tape. Such a mild bonding approach was used in order

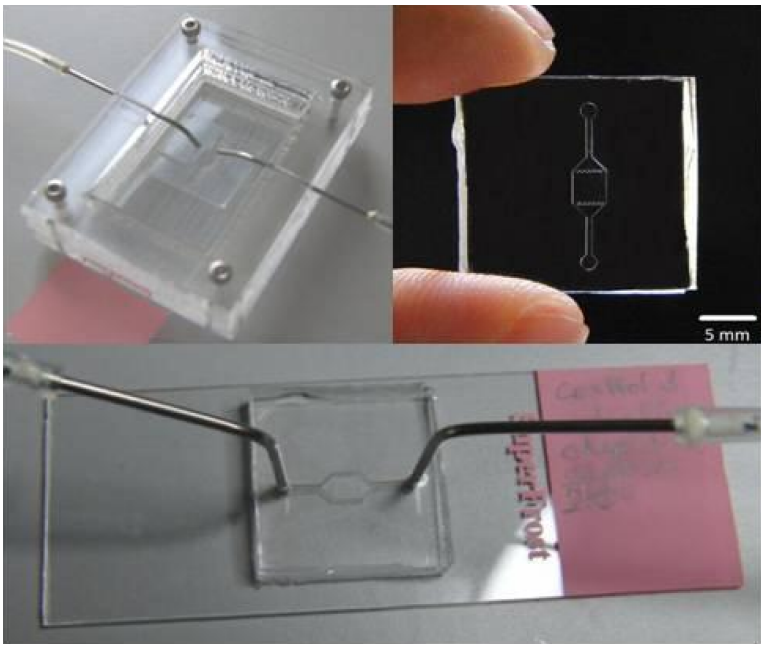

Figure 10.2: The microfluidic device for metaphase FISH analysis developed by Indumathi Vedarethinam. *Image obtained from Indumathi Vedarethinam's PhD Thesis.*

to not destroy the chromosome preparations in a typical PDMS-glass bonding technique by oxygen plasma (Eddings et al., 2008).

Another PhD student involved in C-TAS project, Pranjul Shah, took the chromosome preparation one step further. He integrated the lymphocytes culture microfluidic system (Shah et al., 2011b) with a chromosome spreading device. The device was used for culturing lymphocytes for 3 days under continuous flow conditions, after which the growth medium was exchanged with a hypothonic solution and fixative. The cells in fixative were afterwards dropped in a controlled way, on a glass slide with a double sided adhesive tape stencil for mounting the miniaturized FISH device (Shah et al., 2011a).

Even though the miniaturized assay was successful and readily applicable in a cytogenetic laboratory settings, it was still only a slight modification of standard FISH analysis. The chromosome spreads are typically prepared on untreated glass slides, because of their hydrophilic nature. The fixative solution needs to be quickly evaporated by exposing the glass slide to air. Thus, in the developed miniaturized FISH device the microfluidic pad was attached to the glass slide after preparation of chromosome spreads. However, it would be beneficial for automation of FISH analysis if the formation of chromosome spreads occurs in a controlled manner inside a closed device. This is the approach described in the next Chapter 11.

11. All Polymer Chip for Chromosome Spreading and FISH

In this Part of the thesis the aim is to develop a complete FISH device, that can be operated outside of a specialized laboratory. We aim at fabricating a reliable device for preparation of chromosome spreads inside a microfluidic device that are useful for further cytogenetic analysis. FISH is a sensitive diagnostic tool that can reveal changes in a normal chromosome structure with a higher resolution down to 10-50 kbp (Campbell, 2005; Nath and Johnson, 1999; Serakinci and Kølvraa, 2009). FISH can be applied to interphase or metaphase chromosomes as was shown in Part I in Figure 2.2. In the interphase, chromosomes are present in a cell nuclei as tangled DNA strands (Part I Figure 2.1A). Work with interphase FISH does not require cell culturing, thus it is often performed when a quick analysis is required. This method differs from metaphase FISH, where cells need to be cultured for 3 days and arrested in a metaphase. During metaphase, chromosomes are in their most condensed state (Part I Figure 2.1B). Metaphase FISH can be used to detect more complex chromosome aberrations. It is a powerful technique, but requires several preparation steps. One of the very first steps in metaphase FISH is chromosome spreading on a glass slide. The cell suspension is mixed with a fixative solution (3:1 methanol:acetic acid) and dropped on a glass slide. Due to hydrophilic surface the drops spread very fast allowing formation of chromosome spreads. It is important that the chromosomes spread from a single cell are fixed on a glass slide close to each other but without any overlapping chromosomes. The spreading technique is often regarded as an art more than science and is carefully prepared by trained personnel.

11.1 Chromosome Spreading Principles

The chromosome spreading process has been thoroughly studied since its first successful application for chromosome analysis in 1956 (Claussen et al., 2002). The goal of the chromosome analysis is to achieve the best quality results that are highly dependent on the metaphase chromosome spreads. However, the spreading depends on conditions such as ambient temperature, humidity, the quality of the glass slide and its temperature (Claussen et al., 2002; Spurbeck et al., 1996; Weise and Liehr, 2009). To obtain good chromosome spreads the relative humidity should be kept at a level of 42 %, with a temperature of 27 °C (Lagos and Jimenez, 2012). The rate of chromosome drying is regarded as the main factor influencing the spread quality (Deng et al., 2003; Spurbeck et al., 1996). Other factors such as dropping height, the dropping angle, the pipette tip opening size

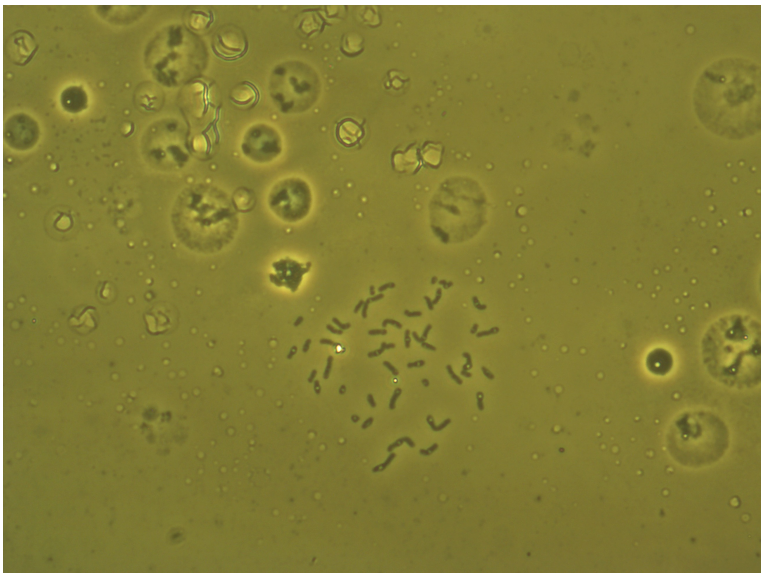

Figure 11.1: Good quality metaphase chromosome spreads formed by a manual dropping technique on a glass slide.

have also been studied for their effect on chromosome spreading. Claussen and others reported that the water content on the glass slide has a major effect on the spreading properties (Claussen et al., 2002). During chromosome drying, first methanol from the fixative solution evaporates thus the acetic acid concentration on the slide increases. It starts digesting the cell structure which results in shrinkage of cells, opening the nuclei and enabling chromosomes to spread uniformly. Only at humidity higher than 21 % the cell swelling was observed, which resulted in chromosome spreads being useful for analysis. Thus it was concluded that the glass slides should be stored in water for the spread preparation, which is a common practice in cytogenetic laboratories. In the present study all the known factors affecting spreads quality were taken into account while designing the all-polymer device for FISH in order to achieve the chromosome spreading as in Figure 11.1. The chromosomes in the spread are well separated without any visible overlaps, at the same time the chromosomes from a single cell are grouped close to each other.

11.2 Testing Various Polymers for FISH

Normally the chromosome spreading is done on glass slides. They are cheap and easily available in any laboratory, however, they are difficult to integrate into a complete microfluidic device. Moreover, polymeric materials have many advantages over glass namely reduced cost, availability and ease of processing for in-

tegration in a microfluidic device. There exist processes for etching and bonding of glass, but they are difficult to control and increase the overall cost of the device (Ilescu et al., 2012). Thus, we decided to develop an all polymer chip for chromosome spreading and FISH analysis. There are several requirements that the selected polymer needs to fulfil to perform well in FISH analysis.

- It needs to be of high optical quality, because the results are analysed using fluorescence microscopy.
- The polymer should not exhibit autofluorescence in any of the used wavelengths, as different fluorophores can be used for probe labeling.
- The polymer needs to withstand the use of harsh chemicals such as acetic acid and methanol.
- The surface wettability, as the chromosomes spread well and uniformly on a hydrophilic surface such as glass.

Several polymers had been investigated during the project to select the best candidate for realization of a chromosome spreading device. Some investigation of polymer optical properties has been reported in literature. Piruska and others (Piruska et al., 2005) has shown that PDMS exhibits a very low autofluorescence as a raw material, which increases slightly in the final device. Hawkins with colleagues (Hawkins and Yager, 2003) also determined autofluorescence of several polymers and proved that long exposure to laser resulted in reduced autofluorescence due to bleaching. Yun Chen and others (Chen et al., 2008) did a thorough study of mechanical, optical and chemical properties of poly(methyl methacrylate) (PMMA) and showed that it has a superior optical property to borofloat glass. However, it is known to be insufficiently stable in case of exposure to typically used solvents such as ethanol, and methanol. Polycarbonate (PC) is known to be more resistant to solvents, however it exhibits a high autofluorescence excited by a blue light, which is often used to visualize the DNA probes hybridisation. Another commonly used polymer is cyclic olefin copolymer (COC) also known by the trade name Topas®, which has very good optical properties, is resistant to various solvents, does not autofluoresce and can be structured by micromilling. We have chosen Topas® as the best candidate for fabrication of the device for metaphase chromosome analysis. Though Topas® seems like an obvious choice for preparation of a device for FISH analysis, its main drawback is the hydrophobicity of the surface. We have addressed it by applying various modifications to the surface to change the hydrophobicity for long term device use. The modifications were applied to fabricate a hydrophilic semi-closed device for faster evaporation of the fluid from microfluidic chambers. We studied a possibility of applying such a device for reliable metaphase chromosome spreading to be further used in cytogenetic analysis. The research findings were described in the article 'All-polymer semi-closed device for metaphase chromosome spreading' - manuscript submitted to *Biomedical Microdevices*. The article text is included in Section 11.3.

11.3 Paper 'All-Polymer Semi-Closed Device for Metaphase Chromosome Spreading'

Following the assay design consideration described above, the project was concluded with a manuscript 'All-Polymer Semi-Closed Device for Metaphase Chromosome Spreading'. The concluding remarks related to the work described in the manuscript and the discussion preceding it are summarized in Chapter 12.

Biomedical Microdevices manuscript No.
(will be inserted by the editor)

All-polymer semi-closed device for metaphase chromosome spreading

Dorota Kwasny · Olga Mednova · Indumathi Vedarethinam · Maria Dimaki · Asli Silahtaroglu · Zeynep Tümer · Kristoffer Almdal · Winnie E. Svendsen

Received: date / Accepted: date

Abstract Metaphase chromosome spreding is the most crucial step required for succesful karyotyping and FISH analysis. These two techniques are routinely used in cytogeneticsto assess the chromosome abnormalities. The spreading process has been studied for years but it is still considered an art more than science. The chromosome spreading greatly depends on the environmental conditions such as humidity and temperature, which govern the evaporation of fixative, in which the cells are suspended. The spreading is normally performed manually on glass slides, which are hydrophilic, and thus allow for better quality spreads. Further cytogenetic analysis depends on the quality of the spreads, which is dependent on the skills of the personnel and is thus limited to laboratory settings. We present here an all-polymer Topas® semi-closed microfluidic chip for preparation of the metaphase spreads for further cytogenetic analysis. The device consists of a microfluidic chamber with perfusion holes that facilitate the evaporation of fixative. To improve the usability of the spreads the surface of Topas® slide is rendered more hydrophilic by oxygen plasma treatment coupled with photografting. The usability of the chromosome spreads was investigated and they were further used for performing FISH analysis.

Keywords cytogenetic analysis · evaporation · chromosome spreading · microfluidic chip

Dorota Kwasny · Olga Mednova · Maria Dimaki · Kristoffer Almdal · Winnie E. Svendsen
Department of Micro- and Nanotechnology, Technical University of Denmark, Orsteds Plads, 2800 Kgs. Lyngby, Denmark
E-mail: wisv@nanotech.dtu.dk

Indumathi Vedarethinam
Center for Molecular Biology 'Severo Ochoa', UAM campus Cantoblano, Madrid, Spain

Asli Silahtaroglu
University of Copenhagen, Faculty of Health Sciences, Department of Cellular and Molecular Medicine, Copenhagen, Denmark

Zeynep Tümer
Applied Human Molecular Genetics, Kennedy Center, Copenhagen University Hospital, Rigshospitalet, Glostrup, Denmark

1 Introduction

The ability to assess chromosome abnormalities based on the analysis of metaphase chromosome spreads can reveal various genetic disorders or haematological malignancies. The chromosomes need to be spread sufficiently without overlaps for their individual analysis, however keeping them close enough to identify the interchromosomal changes such as translocations. Traditionally, the metaphase spreads are prepared manually by dropping the cell suspension in a mixture of methanol and acetic acid, called fixative, on a glass slide. Due to the substrate hydrophilicity and exposure to ambient air the drop spreads quickly, thus allowing the thin layer of fixative to evaporate within a minute. Chromosome spreading depends on many conditions such as temperature, humidity, the quality of the glass slide and its temperature (Claussen, 2002; Deng, 2003; Henegariu, 2001; Qu, 2008; Spurbeck, 1996). Making good spreads is often regarded as an art more than science and is carefully prepared by trained personnel. There has been few reports on performing cytogenetic analysis using microfabricated devices (Shah, 2011a,b; Sieben, 2007, 2008; Vedarethinam, 2010). They offer a

reduction in the reagents volume with great focus on minimizing the amount of the DNA probe used. Those devices start to make their way into the cytogenetic field as they allow for performing the standardized protocols at a smaller scale. However, they are mostly based on chromosome preparations on glass slides prepared in specialized laboratories. Thus, the chromosome analysis, even if performed using a microdevice, is still reserved for laboratory settings.

Spreading depends mostly on the fixative evaporation rate. The evaporation of solution is an extremely challenging task for closed microfluidic devices. It has been addressed by few groups in order to achieve protein crystallization (Yu, 2012) or sample preconcentration (Zhang, 2013). These devices incorporate active gas flow to facilitate the evaporation, with a main application of concentrating analytes, microspheres, bacteria, virus or proteins (Zhang, 2013). The solution we investigate in this paper incorporates passive evaporation to initiate the chromosome spreading on the surface.

To develop an inexpensive all polymer device for cytogenetic analysis, the proper polymer needs to be selected. The selection criteria are based on the resistance to chemicals used in the fixative, optical properties, ease of structuring and surface wettability (Vedarethinam, 2010). Some of the commonly used polymers such as polycarbonate (PC) or polymethylmethacrylate (PMMA) are good candidates for microfluidic devices, however not for this particular application, as PC autofluoresces and PMMA is not resistant to ethanol. Cyclic Olefin Copolymer (COC), also known by the trade name Topas®, is another polymer that can be used for microfabrication. Due to its hydrophobic nature it needs to be modified to achieve proper chromosome spreading. We tested various surface treatments to decrease the contact angle with long-term stability to apply for chromosome spreading (data not shown).

The fabrication of an all-polymer microfluidic device has been proposed to simplify the whole FISH procedure. In this paper we report the application of a semi-closed microfluidic chip for fast evaporation of the fixative solution. We investigate the possibility of obtaining metaphase chromosome spreads in such a semi-closed device for further analysis of the chromosomes by banding or FISH. We applied a chemical surface modification method for altering the long term-wettability of Topas® to improve the spreading capability on a polymer surface.

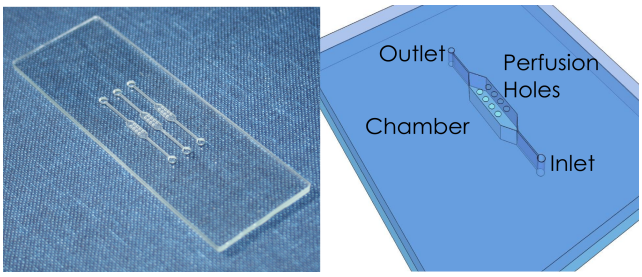

Fig. 1 A semi-closed device for fast evaporation of the fixative - device image on the left and outline on the right.

2 Experimental

2.1 Materials and Chemicals

COC microscope slides were acquired from ChipShop (Jena, Germany) and were used for the device fabrication. They will further be called Topas® slides. The chemicals used for modification of Topas® were purchased from Sigma-Aldrich. Oxygen gas was provided from AGA S/A and used in low pressure plasma chamber (Plasma Cleaner Atto, Diener Electronic). Cell samples were obtained from Panum Institute (Copenhagen University, Denmark). All reagents for FISH protocol such as saline sodium citrate (SSC) and phosphate buffered saline (PBS) buffer were purchased from Invitrogen and Sigma-Aldrich. The X-Chromosome centromere specific probe was purchased from Kreatech Diagnostics (Amsterdam, The Netherlands).

2.2 Device Fabrication

The device was designed in AutoCad2000 and fabricated by micromilling in Topas®. The final device and its outline are depicted in Figure 1. It consists of a bottom unstructured microscope slide size Topas® thermally bonded to a top slide with structured microfluidic channels and chambers with perfusion holes. The holes are placed over the chamber to allow for fast fixative evaporation and better visualization of chromosome spreads.

2.3 Topas® modification

To improve surface hydrophilicity of Topas®, the slides were treated with oxygen plasma followed by immediate UV photografting of a hydrophilic 2-hydroxyl acrylate (2-HEA). Prior to modification, the slides were cleaned with a mixture of isopropanol/acetone in an ultrasonic bath at 40 °C for 30 minutes and dried with N_2. First, oxygen plasma under work pressure of 0.2-0.5 mbar was

applied for 3 minutes. Afterwards, Topas® samples were soaked in an acetone solution of 3 M 2-HEA and 0.2 M benzophenone (BP) and placed in a UV-photoreactor at 50 °C. UV photografting was performed in a photoreactor with 360 nm wavelength lamps and 5 cm distance from the treated slides. Total irradiation was set to 7 mW/cm^2 at 50 °C. After treatment, the slides were washed in isopropanol/acetone bath followed by 24 hr washing in MilliQ water on a magnetic stirrer. The measurements of the water contact angle was performed on the prepared Topas® slides using Contact Angle System (OCA-15, DataPhysics). Deionized 1 μL water drops were deposited and contact angles have been recorded in a sessile drop regime after 30s. For comparison of the Topas® modification methods four different slides were used for chromosome spreading testing - conventional glass slide as a control, unmodified Topas® slide, Topas® slide treated with oxygen plasma and Topas® slide modified by oxygen plasma and photografting (see Figure 3). Additionally, a glass and a Topas® slide treated with oxygen plasma and photografting were assembled as a bottom substrate for a semi-closed device and tested for chromosome spreading. Prior to spreading all slides were immersed in water at 50 °C and stored in this way, which is a standard procedure for metaphase spreading on glass slides.

2.4 Chromosome spreading

The cell suspensions used for preparation of the spreads were acquired from the chromosome lab within the health sciences faculty at Panum Institute (Copenhagen University). Before spreading, the cell suspensions were centrifuged and a fresh portion of fixative containing methanol and acetic acid in 3:1 ratio was slowly introduced drop by drop while mixing the solution to resuspend the cell pellet. As a control the standard spreading protocol was carried out on clean glass and Topas® slides kept in ice cold water in water. The same was repeated for Topas® slides treated with oxygen plasma and oxygen plasma coupled with photografting. The cell suspension was dropped on the control slides and air dried. To test the metaphase spread formation in the semi-closed device, 10 μl of the cell suspension was introduced to the channel filled with ice cold water. The semi-closed device was placed at 40 °C for 10-15 minutes to allow evaporation of the fixative. The spreads were analyzed using a bright-field optical microscope (Olympus). The average spread area on each sample was analyzed by measuring the area in ImageJ.

2.5 FISH protocol

The complete FISH protocol was performed on both control glass slides and a modified Topas® slide with assembled semi-closed FISH device. The inlet was connected to the syringe by a fixed silicone tubing and the chamber perforation was closed with a tape typically used for polymerase chain reaction (PCR) to allow easy exchange of the FISH reagents and probes. The spreads denaturation was performed by heat treatment on a hot plate at 75 °C. Firstly RNAse (10μg/μl) was diluted 100x in 2 x SSC and injected through the inlet and the slides were incubated in a humidity chamber at 37 °C for 1 hour. Following the RNAse treatment, the metaphase spreads were washed with 2 x SSC solution at room temperature. Dehydration was carried out with increasing concentrations of ethanol (70, 80 and 90 %). Subsequently, the slides were heated at 75 °C for 5 minutes on a hot plate to denature the chromosomal DNA. DNA probe denaturation was performed simultaneously at 75 °C for 5 minutes in a water bath. After the probe solution was injected into the device, the inlet and outlet were closed to prevent drying of the probe solution. The device was incubated overnight at 37 °C in a humidity chamber to allow for the probe hybridization to chromosome spreads. Subsequently, 50 % formamide was introduced as post hybridization wash at 42 °C. Final washing was performed with 0.1 x SSC at 60 °C, 4 x SSC and 1 x PBS at room temperature. For the analysis of signals using Olympus fluorescent microscope the chromosomal DNA was stained with diamidino-2-phenylindole (DAPI).

3 Results and Discussion

3.1 Topas® modification

The initial water contact angle for Topas® is around 100 °, which is not sufficient for efficient spreading of chromosomes. The Topas® modification applied in this paper was based on the reports by Jena and others regarding the photografting solution composition (Jena, 2011). For a stable treatment, it was coupled with an oxygen plasma, which is a frequently used method for changing surface properties. Plasma surface treatment tunes the surface properties to promote adhesion, diminish the surface roughness and enhance wettability (Guimond, 2004). However, active radicals on plasma treated surface reduce the treatment stability and hydrophobicity recovers to the initial value during two weeks observation period in case of argon and oxygenated-argon plasma (Sunanda, 2010; Tsao, 2007). In the present investigation several of

the Topas® slides were only treated with oxygen plasma to compare the recovery rates and long term stability with the proposed combined technique. The stability was investigated by measurements of the water contact angle repeated over time and the results are presented in Figure 2. As a control, changes in the measured contact angle over time were also performed on the untreated Topas®. The values of the contact angle were not varying significantly thus data shown in Figure 2 as blue triangles have small error bars. It can be seen that just after treatment the contact angle value for oxygen plasma treated sample is around 30 °, which increases rapidly a few days after the treatment. Whereas for slides modified with a combined method the initial value of the water contact angle is higher, around 53 °, but stable over the 3 weeks time. The highly reactive surface radicals formed during plasma treatment were further bound to the monomers applied during photografting, which prolongs the stability of the treatment. The photografting was conducted at elevated temperature for a better efficiency (deSmet, 2009).

3.2 Chromosome spreading

The chromosome spreading was performed on various slides with different surface properties. As a control, the cell suspension sample was dropped on a glass slide, untreated Topas® slide and also on Topas® slide treated with oxygen plasma coupled with photografting. Untreated Topas® surface has a water contact angle of 100 ° in contrast to glass, which has a hydrophilic surface. The wettability of the surface is crucial during preparation of metaphase chromosome spreads as it allows for the cell suspension drop

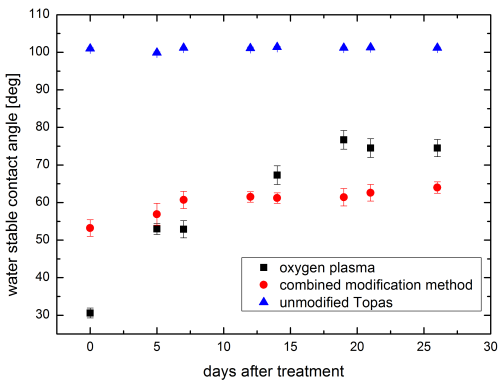

Fig. 2 The graph of stability of hydrophilic treatment over time.

to spread quickly over the surface. Such a spread drop has a much bigger surface area and thus the fixative evaporation occurs faster resulting in well spread chromosomes with few overlaps (Figure 3 Glass). Contrary, the cell suspension placed on an untreated Topas® slide forms a standing drop, which prolongs the evaporation. Moreover, the chromosomes do not have enough space to properly spread. The visual inspection of the spreads on hydrophobic Topas® surface revealed the presence of cell clusters at the edges of the drop (Figure 3 Topas). The chromosomes spread well after treating Topas® with oxygen plasma and also after additional photografting. However, the slides after photografting have an unclear appearance, which can be reduced by optimizing the post-photografting washing procedure. Furthermore, the spreading in a semi-closed device was done with evaporation enhancement through perforation and keeping the devices at elevated temperature. To ensure that the spreading is not only affected by the surface properties, both glass slide and the modified Topas® slide were used as a bottom for the semi-closed device. In both cases the spreads were formed in the chamber below the perforation. Although, in case of modified Topas® slides the area of each spread was smaller and their quality was worse. As the spreads were formed properly in a semi-closed device with a glass bottom we suspect that the surface treatment of Topas® might not have been sufficient to achieve good quality spreads. The evaporation in the device for spreads formation was successful although the performance of the device with a glass bottom was superior. The average spread area on each sample was measured in ImageJ. The graph with the analyzed results is shown in Figure 4. The chromosome spreads have the largest area on a control glass sample, which is comparable to the average area of spreads in a semi-closed glass device. This shows that the evaporation of the fixative solution does not hinder the spreads formation. Furthermore, there were many spreads available for the analysis. On a control Topas® the chromosomes were spread on an untreated Topas® slide. Only few spreads were found on the surface and they are very condensed what is reflected by a small average area. The chromosome spreads had a bigger area on a Topas® slide treated with oxygen plasma, with the value of 878 μm^2, which is close to the one for control glass slide. The modified Topas® slide performed relatively well both as an open slide and as a bottom of semi-closed modified Topas® device. The spreads occupy a larger area in comparison to the untreated Topas® but the value is much smaller than the one for glass slide. There were only few spreads available for the analysis and their area varied greatly.

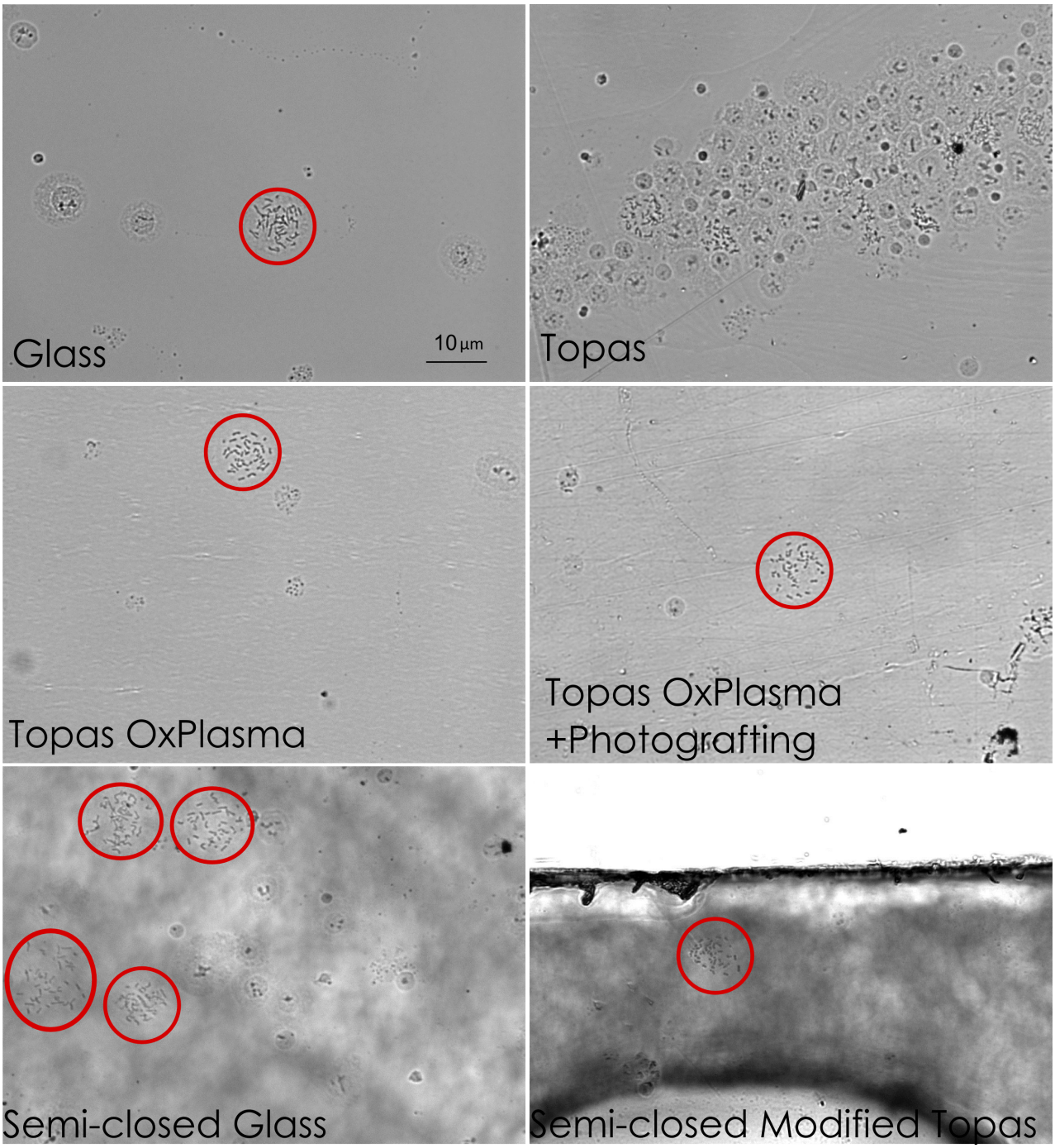

Fig. 3 Chromosome spread poorly on untreated Topas® surface (Topas), while their quality was comparable on Glass, Topas® treated with oxygen plasma (Topas OxPlasma) and Topas® modified by oxygen plasma coupled with photografting. The spreads prepared in semi-closed device on glass bottom (Semi-closed Glass) are of good quality, whereas on Topas® bottom (Semi-closed Modified Topas) they are more condensed. The circles in the pictures surround the metaphase chromosome spreads.

3.3 FISH analysis

After preparation of the chromosome spreads we performed FISH analysis using an X chromosome centromeric probe to check usability of the prepared metaphase chromosome spreads. We used sample from a male patient with 46,XY karyotype and a single positive signal corresponding to the only X chromosome was observed. The entire protocol was applied for both semi-closed devices with a glass and modified Topas® as a bottom. The probe was labeled with

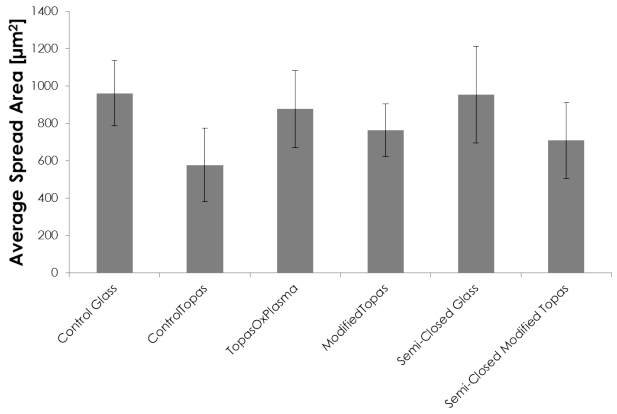

Fig. 4 The graph presents the results of the analysis of average spread area on each tested sample.

fluorescein isothiocyanate (FITC) thus it appears green in the picture. The chromosomal DNA was stained with DAPI, which intercalates between the two DNA strands and appears blue under a fluorescent microscope. The visual inspection of stained chromosomes revealed that only interphase FISH signals could be found on semi-closed Topas® device (Figure 5). None of the metaphase chromosome spreads obtained in the semi-closed Topas® device had FISH signals. In case of a semi-closed glass device some of the metaphase spreads showed positive FISH signals, which is an indication that the chromosomes were spread better allowing the probe to bind the matching sequence on the chromosomes. Interphase signals were also obtained in the semi-closed glass device. In case of semi-closed Topas® device, the few obtained metaphase spreads are too condensed and thus prevent any hybridization of the probe. The presence of interphase signals proves that the FISH protocol was conducted properly.

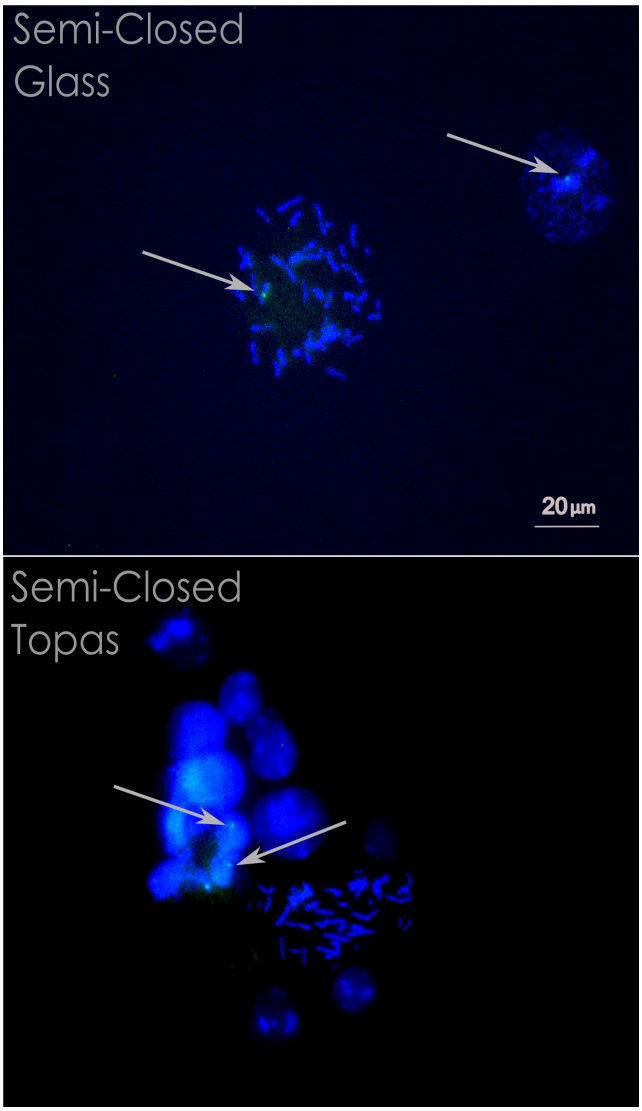

Fig. 5 FISH validation of spreads usability. The metaphase signals of X centromeric probe can be seen on spreads prepared in a glass semi-closed device. For the semi-closed Topas® device only interphase signals were obtained. The arrows point at the FISH signals.

4 Conclusions

We have developed a simple microfluidic device to facilitate fast evaporation of the solution from the device. The device was fabricated completely in Topas®, which was modified by oxygen plasma and photografting to achieve long-term hydrophilic properties. We investigated that the treatment is stable over 3 weeks while oxygen plasma treatment gradually diminishes. The design incorporated perfusion holes placed over a chamber to allow for reliable chromosome spreading during evaporation of the fixative. The openings proved to be sufficient for solution evaporation after a short time at 40 °C, which was tested for both glass and Topas® semi-closed devices. Although it was possible to achieve proper spreading the quality of the chromosomes was questionable. The average spread area was compared on all tested samples and it showed that the cells spread equally well in a semi-closed device as well as in an open system. It can be the consequence of low quality cell suspension sample but also might arise from the insufficiently fast fixative evaporation and the surface properties. Moreover, the stable Topas® modification with oxygen plasma and photografting resulted in unclear surface, which formed obstacles for the proper chromosome spreading. The FISH protocol was used for chromosome usability validation. It was completed in both semi-closed Topas® and semi-closed glass device. Both surface allowed for preparation of metaphase chromosome spreads but the positive

metaphase FISH signals were observed only in case of a glass bottom device. Such a validation method was chosen to assess the metaphase spreads usability and showed that chromosomes on treated Topas® slide are not spread sufficiently well to be used in further cytogenetic analysis.

5 Acknowledgements

The authors would like to thank the Danish Council for Strategic Research (via the NanoKaryotyping project) and the Villum Kann Rasmussen Centre of Excellence NAMEC under Contract No.65286 for financial support.

References

Claussen, U.; Michel, S.; Muhlig, P.; Westermann, M.; Grummt, U.W.; Kromeyer-Hauschild, K.; Liehr, T., Cytogenetic and Genome Research, **98**, 136-146 (2002)

Deng, W.; Tsao, S. W.; Lucas, J. N.; Leung, C.S.; Cheung, A. L. M., Cytometry, **51A**, 46-51 (2003)

Guimond, S.; Wertheimer, M.R., Journal of Appied Polymer Science, **94**, 1291 (2004)

Henegariu, O.; Heerema, N. A.; Wright, L. L.; Bray-Ward, P.; Ward, D. C.; Vance, G. H., Cytometry, **43**, 101-109 (2001)

Jena, R.; Yue, C.; Anand, L., Sensors and Actuators B:Chemical, **157**, 518-526 (2011)

Qu, Y. Y.; Xing, L. Y.; Hughes, E. D.; Saunders, T. L., Journal of Histotechnology, **31**, 75-79 (2008)

Shah, P.; Vedarethinam, I.; Kwasny, D.; Andresen, L.; Skov, S.; Silahtaroglu, A.; Tumer, Z.; Dimaki, M.; Svendsen, W. E., Micromachines, **2**, 116-128 (2011)

Shah, P.; Vedarethinam, I.; Kwasny, D.; Andresen, L.; Dimaki, M.; Skov, S.; Svendsen, W.E., Sensors and Actuators B:Chemical, **156**, 1002-1008 (2011)

Sieben, V. J.; Marun, C. S. D.; Pilarski, P. M.; Kaigala, G. V.; Pilarski, L. M.; Backhouse, C. J., IET Nanotechnology, **1**, 27-35 (2007)

Sieben, V. J.; Debes-Marun, C. S.; Pilarski, L. M.; Backhouse, C. J., Lab on a Chip, **8**, 2151-2156 (2008)

de Smet, N.; Rymarczyk-Machal, M.; Schacht, E., Journal of Biomaterials Science, **20**, 2039-2053 (2009)

Spurbeck, J.L.; Zinsmeister, A.R.; Meyer, K.J.; Jalal, S.M., American Journal of Medical Genetics, **61**, 387.393 (1996)

Sunanda, R.; Yue, C.E.; Lam, Y.C.; Wang, Z.Y.; Huifang, H., Sensors and Actuators B:Chemical, **150**, 537-549 (2010)

Tsao, C.W.; Hromada, L.L.; Liu, J., Lab on a Chip, **7**, 499-505 (2007)

Vedarethinam, I.; Shah, P.; Dimaki, M.; Tumer, Z.; Tommerup, N.; Svendsen, W. E., Sensors, **10**, 9831-9846 (2010)

Yu, Y.; Wang, X.; Oberthur, D.; Meyer, A.; Perbandt, M.; Duan, L.; Kang, Q., Journal of Applied Crystallography, **45**, 53-60 (2012)

Zanardi, A.; Bandiero, D.; Bertolini, F.; Corsini, C. A.; Gregato, G.; Milani, P.; Barborini, E.; Carbone, R., BioTechniques, **49**, 497-504 (2010)

Zhang, J.Y.; Mahalanabis, M.; Liu, L.; Chang, J.; Pollock, N.R.; Klapperich, C.M., Diagnostics, **3**, 155-169 (2013)

12. Conclusions and Project Summary

In this Part the attempt on making a complete polymer device for metaphase spreading was described. The manuscript on 'All-polymer semi-closed device for metaphase chromosome spreading' was preceded by a discussion of the chromosome spreading principles and the requirements for the polymeric device. Topas® was selected as the most appropriate polymer substrate due to its chemical resistance, no autofluorescence and ease of properties modification. The device properties were altered by oxygen plasma and chemical modification by photografting to obtain a stable hydrophilic surface. The device composed of Topas® bottom and lid with micromilled microfluidic chambers with perforation (semi-closed), was bonded and used for chromosome spreading. To enhance the evaporation of the fixative the device was kept in a preheated oven, which resulted in better quality of chromosome spreads. After visual inspection of the spreads' a FISH protocol was performed for further validation of the metaphase spreads usability. The FISH protocol was conducted properly as interphase FISH signals were visible, though no metaphase signals were found on the Topas® semi-closed device. A possible explanation for unsuccessful metaphase FISH was the quality of the prepared chromosomes on the modified Topas® surface. The chromosomes on Topas® slides were in general more condensed and shorter, occupying a smaller area. To prove that the evaporation in the semi-closed device is in fact sufficient to obtain good chromosome spread, we made a device with a glass bottom. In this device, it was possible to obtain well spread chromosomes, that gave metaphase signals after performing FISH protocol. We concluded, that with further optimization of the Topas® modification the realization of reliable all-polymer device for chromosome spreading will be possible.

Bibliography

Claussen, U.; Michel, S.; Muhlig, P.; Westermann, M.; Grummt, U.W.; Kromeyer-Hauschild, K.; Liehr, T., *Demystifying chromosome preparation and the implications for the concept of chromosome condensation during mitosis*, Cytogenetic and Genome Research, **98**, 136-146 (2002)

Campbell, L.J., *Chapter 2 in Methods in Molecular Medicine, Vol. 125: Myeloid Leukemia: Methods and Protocols*, Edited by Iland, H.; Hertzberg, M. Marlton, P., Humana Press, (2005)

Chen, Y.; Zhang, L.; Chen, G., *Fabrication, modification, and application of department of analytical poly(methyl methacrylate) microfluidic chips*, Electrophoresis, **29**, 1801-1814 (2008)

Deng, W.; Tsao, S.W.; Lucas, J.N.; Leung, C.S.; Cheung, A.L.M., *A New Method for Improving Metaphase Chromosome Spreading*, Cytometry Part A, **51A**, 46-53 (2003)

Eddings, M.A.; Johnson, M.A.; Gale, B.K., *Determining the optimal PDMS–PDMS bonding technique for microfluidic devices*, Journal of Micromechanics and Microengineering, **18**, (2008)

Harper, M.E.; Saunders, G.F., *Localization of single copy DNA sequences on G-banded human chromosomes by in situ hybridization*, Chromosoma, **83**, 431-439 (1981)

Hawkins, K.R.; Yager, P., *Nonlinear decrease of background fluorescence in polymer thin-films - a survey of materials and how they can complicate fluorescence detection in μTAS*, Lab on a Chip, **3**, 248-252 (2003)

Iliescu, C.; Taylor, H.; Avram, M.; Miao, J.; Franssila, S., *A practical guide for the fabrication of microfluidic devices using glass and silicon*, Biomicrofluidics, **6**, 016505 (2012)

Nath, J; Johnson, K.L.,*A Review of Fluorescence in Situ Hybridization (FISH): Current Status and Future Prospects*, Biotechnic and Histochemistry, **75**, 54-78 (1999)

Pinkel, D.; Straume, T.; Gray, J.W., *Cytogenetic analysis using quantitative, high-sensitivity, fluorescence hybridization*, PNAS, **83**, 2934-2938 (1986)

Piruska, A.; Nikcevic, I.; Lee, S.H.; Ahn, C.; Heineman, W.R.; Limbach, P.A.; Seliskar, C.J., *The autofluorescence of plastic materials and chips measured under laser irradiation*, Lab on a Chip, **5**, 1348-1354 (2005)

Serakinci, N.; Kølvraa, S., *Chapter 1 in Fluorescence in situ hybridization (FISH) - Application Guide*, Edited by Liehr, T., Springer-VBH, (2009)

Shah, P.; Vedarethinam, I.; Kwasny, D.; Andresen, L.; Skov, S.; Silahtaroglu, A.; Tumer, Z.; Dimaki, M.; Svendsen, W. E., *FISHprep: A Novel Integrated Device for Metaphase FISH Sample Preparation*, Micromachines, **2**, 116-128 (2011)

Shah, P.; Vedarethinam, I.; Kwasny, D.; Andresen, L.; Dimaki, M.; Skov, S.; Svendsen, W.E., *Microfluidic bioreactors for culture of non-adherent cells*, Sensors and Actuators B:Chemical, **156**, 1002-1008 (2011)

Spurbeck, J.L.; Zinsmeister, A.R.; Meyer, K.J.; Jalal, S.M., *Dynamics of Chromosome Spreading*, American Journal of Medical Genetics, **61**, 387-393 (1996)

Lagos, S.M.R.; Jimenez, N.E.R., *Chapter 1 in Recent Trends in Cytogenetic Studies - Methodologies and Applications*, Edited by Tirunilai, P., INTECH, ISBN 978-953-51-0178-9, (2012)

Vedarethinam, I.; Shah, P.; Dimaki, M.; Tumer, Z.; Tommerup, N.; Svendsen, W. E., *Metaphase FISH on a Chip: Miniaturized Microfluidic Device for Fluorescence in situ Hybridization*, Sensors, **10**, 9831-9846 (2010)

Weise, A.; Liehr, T., *Chapter 10 in Fluorescence in situ hybridization (FISH) - Application Guide*, Edited by Liehr, T., Springer-VBH, (2009)

Part IV

NanoKaryotyping on Lab-on-a-Disc

13. Introduction

This Part of the thesis is partially based on a Master's thesis project performed by Anna Line Brøgger supervised by me in collaboration with Nanoprobes group at DTU Nanotech.

In Part III of this thesis, a device for complete FISH analysis was demonstrated with its advantages and drawbacks. The quality of metaphase chromosome spreads was questionable so we decided to take an alternative path towards solving the task of chromosome translocation detection. From previous projects in the group we knew how difficult it is to handle chromosomes in microfluidic channels. They consist of proteins called histones that keep the chromosome structure intact, but are at the same time very 'sticky', which results in high levels of clogging of microfluidic devices (Inoue et al., 2008). Moreover, the chromosomes are exposed to high shear stress due to applied flow, causing decomposition of their structure.

In this part of the project we decided to make use of a microarray principle with DNA probes immobilized on a solid support to hybridize the target DNA. The chromosome translocation detection, however, requires a double hybridisation assay, as it is important to determine whether the target DNA contains sequence coming from two chromosomes. The applied detection principle is illustrated in Figure 13.1. The detection in this part of the project was based on fluorescence. In the presence of a DNA fragment with translocation the positive signal is visible on both chips with two different DNA probes immobilized. In case of a normal DNA fragment, the hybridisation occurs only on the first chip as the DNA target and DNA probe sequence on the second chip are not matching.

To enable easy and reliable handling of the double hybridisation a lab-on-a-disc assay was developed. The specific design consisting of two chambers in each channel allows for two separate hybridisation steps to be controlled independently. The liquid movement in the disc assay is controlled by centrifugal pumping, and the liquid can be held in one of the chambers due to the presence of capillary burst valves. Due to changes in capillary forces the liquid stops at the entrance to the chamber because of a sudden expansion of the channel. The liquid is moved from 1st chamber to the 2nd chamber by a simple rotating stage.

14. Lab-on-a-Disc

Lab-on-a-chip technology aims to develop complete analysis systems to miniaturize the conventional protocols and to minimize the requirement for manual sample handling (Chin et al., 2012; Hong and Quake, 2003; Manz and Eijkel, 2001). It enables easier manipulation and detection of analytes, often in a shorter time with less volume used. Such devices are portable and are a basis of point-of-care technology (Madou et al., 2001). However, they often require external equipment such as power supplies or syringe pumps, which hinder their application as complete point-of-care systems. One of the few commercially available hand held devices is the glucose meter. It uses batteries as power supply and capillary forces to transfer the blood sample from a finger prick into the sensor site. A good example of powerless analytical devices are paper based assays known as dip sticks such as

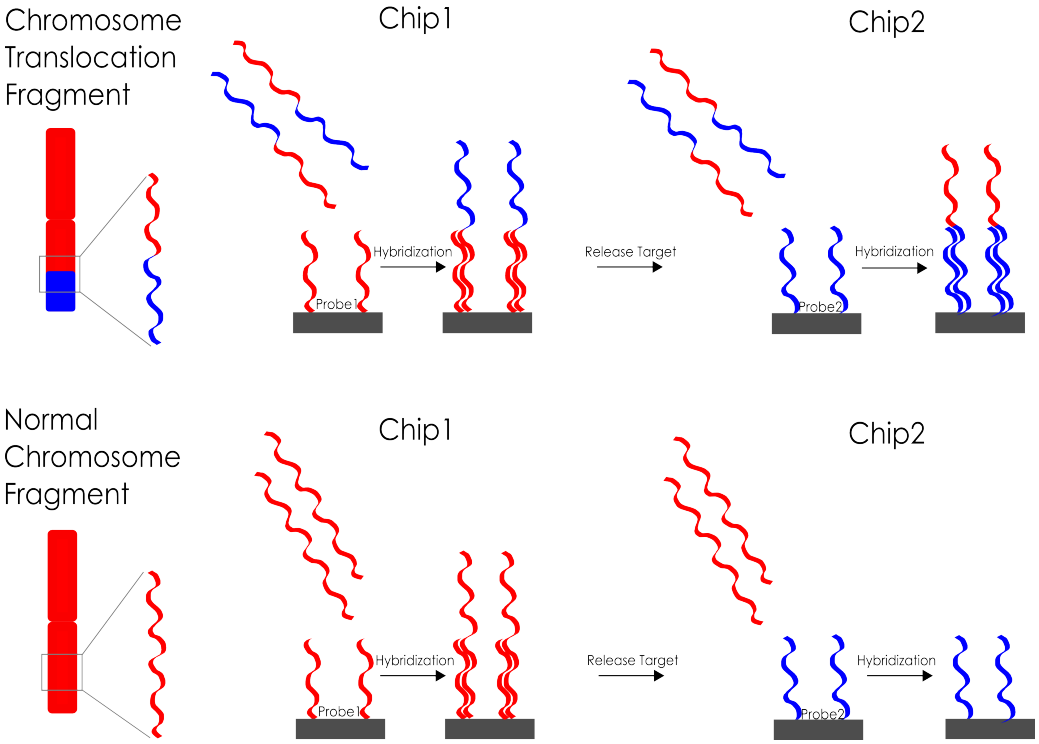

Figure 13.1: Chromosome translocation detection is based on a double hybridisation assay on two separate chips, which can reveal whether the DNA sequences were connected in a genome. A chromosome fragment with translocation will give a positive signal on both chips, while a normal chromosome fragment will result in hybridisation only on one chip.

pregnancy tests. Such tests incorporate capillary forces as transfer mechanism to determine whether human chorionic gonadotropin (HCG) is present in the sample. It is worth noticing that a control line is present to validate the test performance and to avoid false negatives. Such simple analytical tests can be used in less developed countries, where access to specialized laboratories and power supplies is limited. There is a need for fast and accurate point-of-care systems that work optimally in low-resource settings.

Lab-on-a-disc or centrifugal microfluidic platforms are centrifugally driven lab-on-a-chip systems (Duffy et al., 1999; Gorkin et al., 2012; Madou and Kellogg, 1998). The field of research was started in 1960s when a centrifugal analyzer has been developed (Gorkin et al., 2010) and gained more popularity by the end of 90s (Madou and Kellogg, 1998). The platforms are composed of circular systems, the size of a compact disc, with a centrifugal force driving the liquid flow. The only parameter that is adjusted during operation is a rotational speed, which controls the flow rate of the liquid. The lab-on-a-disc platforms can integrate various microfluidic functions such as valving, mixing, flow splitting, etc (Duffy et al., 1999; Madou and Kellogg, 1998; Madou et al., 2001). During spinning, the centrifugal force causes the liquid flow from center of rotation towards the edge of the disc. The liquid motion can be controlled by incorporating various structures such as meanders as mixers or capillary burst valves as passive ways of holding the liquid. The lab-on-a-disc can be coupled with the detection systems such as laser from a DVD platform (Bosco et al., 2011). In this way not only pumping can be realized without any peripheral equipment, but detection of analytes can be achieved using the same equipment. Some commercial centrifugal microfluidic platforms are available from Abaxis (Figure 14.1A) or Gyros AB (Figure 14.1B), however most of them are only used in academia. The main advantage of these systems com-

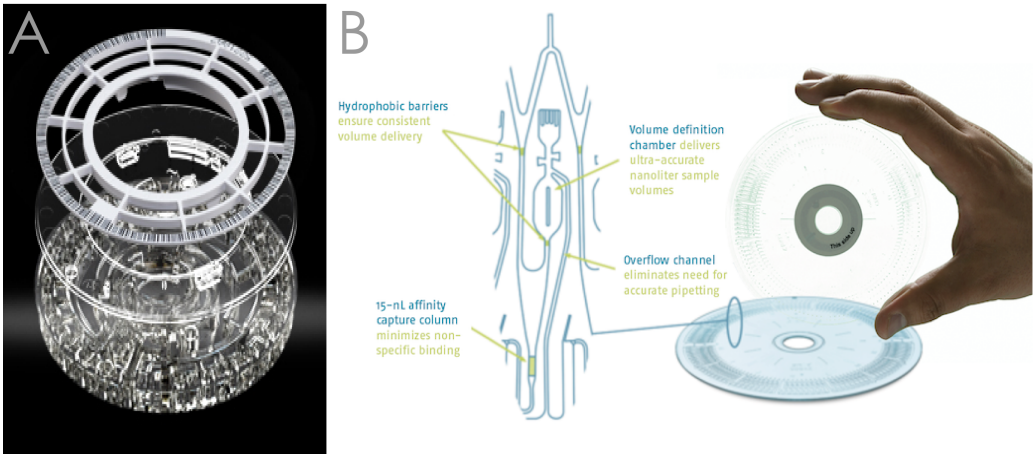

Figure 14.1: Commercially available lab-on-a-disc platforms from Abaxis (A) *(adapted from piccoloxpress.com)* and Gyros (B) *(adapted from gyros.com)*.

pared to paper microfluidics is application in multiplexing and high-throughput diagnostic screening, while being disposable. A small sample volume can be analysed at low-cost using inexpensive and uncomplicated analysis scheme for parallel detection (Madou et al., 2001, 2006). Lab-on-a-disc platforms have various applications ranging from ions detection (Johnson et al., 2001), immunoassays (Lee et al., 2009), microarray based DNA hybridisation (Peytavi et al., 2005), whole blood analysis (Lee et al., 2009; Steigert et al., 2006), polymerase chain reaction (PCR) (Amasia et al., 2012; Gorkin et al., 2010; Madou et al., 2006).

14.1 Capillary Burst Valves

One of the key features of microfluidic devices is the presence of valves, which can control the liquid flow (Cho et al., 2004; Gorkin et al., 2010; Madou et al., 2006). Different solutions have been proposed for achieving reliable and easy to integrate valving on chip, with the most popular being Solenoid valves (Hulme et al., 2008) or diaphragm valves (Melin and Quake, 2007). Although versatile and easy to operate, they require external equipment for operation, which often uses high power sources, which is less favorable in point-of-care applications. Different approaches towards valving have been realized on centrifugal microfluidic platforms such as hydrophobic patches (Gorkin et al., 2010), siphon (Gorkin et al., 2012, 2010) or capillary burst valves (Duffy et al., 1999; Gorkin et al., 2010). To develop a hydrophobic valve, additional surface treatment is required, whereas

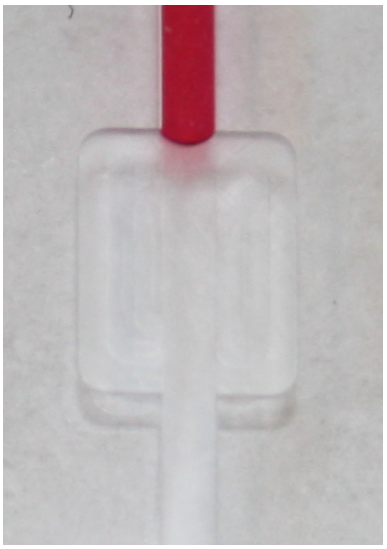

Figure 14.2: An example of capillary burst valve design. The liquid is moving in the narrow channel until a sudden expansion causes it to stop. *Courtesy of Anna Line Brøgger.*

siphon valves operate only on hydrophilic surfaces as they need to be primed with liquid (Gorkin et al., 2010). The most elegant solution is to develop capillary burst valves, in which the liquid is stopped at a sudden expansion of the channel width due to capillary pressure barrier as illustrated in Figure 14.2 (Cho et al., 2004; Duffy et al., 1999; Madou and Kellogg, 1998; Madou et al., 2006). During spinning at a burst frequency the capillary pressure is overcome by centrifugal force and the liquid proceeds further. The centrifugal force is used conventionally in lab-on-a-disc field to describe the force acting on the liquid. From this a centrifugally induced pressure, $\Delta P_{centrifugal}$ can be derived by integrating the force per volume over the radial spread of the liquid from the center.

$$\Delta P_{centrifugal} = \frac{1}{2}\rho\omega^2(r_2^2 - r_1^2) \tag{14.1}$$

where ω is the angular velocity, ρ is a liquid density, r_1 is the distance from the center to the inlet, and r_2 is the distance from the center to the capillary burst valve. Thus, the derived pressure is dependent on the design of the lab-on-a-disc device, the liquid used and the spinning disc velocity.

Burst valves remain closed until a centrifugal pressure is greater than the pressure at which the valve bursts open. The valves operate due to the capillary pressure, which is the difference in pressure at the interface between two immiscible liquids. In this particular case the interface is formed between liquid and air. The capillary burst valve is characterized by the angle of expansion, β and the physical dimensions such as width (w) and height (h). At the sudden expansion of the channel the liquid movement in the channel is stopped due to the capillary pressure. This depends on the surface tension γ_{lg} and the advancing contact angle θ_A which is an angle between the liquid front and the channel side, top and bottom walls. The value of θ_A is 80° for PMMA (Marco et al., 2010), which was used in the experiments.

For a straight channel the $\Delta P_{capillary}$ is

$$\Delta P_{capillary} = 2\gamma_{lg}(\frac{cos\theta_A}{w} + \frac{cos\theta_A}{h}) \tag{14.2}$$

At the valve position the burst pressure is given by

$$\Delta P_{burst} = 2\gamma_{lg}(\frac{cos(\theta_A + \beta)}{w} + \frac{cos\theta_A}{h}) \tag{14.3}$$

In order to burst the liquid an external pressure in the form of $\Delta P_{centrifugal}$ needs to be applied.

$$|\Delta P_{centrifugal}| \geq |\Delta P_{burst}| \tag{14.4}$$

and from this we get a value of the angular velocity to apply to open the valve

$$\omega_B = |\frac{4\gamma_{lg}}{\rho(r_2^2 - r_1^2)}(\frac{cos(\theta_{A,w} + \beta)}{w} + \frac{cos\theta_{A,h}}{h})|^{\frac{1}{2}} \tag{14.5}$$

The value of ω_B is given in radians per second, which can be converted to frequency f (in Hz) by dividing ω_B by 2π and to revolutions per minute (RPM) by multiplying f by 60. RPM is the most commonly used unit in the centrifugal microfluidics field.

The capillary burst valves can be operated in series by varying the channel dimensions and distance from the center of rotation (Cho et al., 2004; Johnson et al., 2001). In most cases, the detection window is positioned at the edge of the disc and the valves burst sequentially - starting from the one furthest away from the center. In the design proposed here, the valves burst from the center outwards to allow for transfer of target DNA from first to second chamber. To achieve this, we have modified the channel dimensions so that the outlet channel of the first chamber is much broader than the outlet of the second chamber with a difference of 180 RPM in bursting frequency. Such a design allowed us to realize two independent hybridisation steps in order to detect the presence of DNA fragment with chromosome translocation.

14.2 Detection Principle on Lab-on-a-Disc

The developed centrifugal microfluidic system consists of 9 channels that allows statistical analysis of the performed experiments. Each channel is composed of two chambers separated by a capillary burst valve. Such a prototype is used to demonstrate the potential for multiplexed detection. The envisioned system is presented in the Figure 14.3. The system consist of 8 channels but can be expanded to 24 channels, where all individual chromosomes can be separated into designated chambers. By immobilizing the chromosome specific centromeric probes in individual chambers (pink), the chromosomes extracted from a patient sample can be sorted. Such a separation of the chromosomes maintains the main advantage of karyotyping, which is the ability to visualize the entire karyotype at the same time. After the chromosomes have been separated based on their centromeres in the first set of chambers, they are released and transferred to the second set of chambers (yellow/green) by spinning of the disc. In those chambers the subtellomeric probes specific for all the other chromosomes are immobilized, which means that if chromosome 3 was captured in the first chamber, probes for chromosomes 1-2, 4-22 and the two sex chromosomes are immobilized in the second chamber. If the chromosome translocation is present between chromosome 3 and one of the others, the probes in the second chamber will catch it and detect another target chromosome sequence. Such a double positive hybridisation in the

first and second chamber is only possible in presence of chromosome translocation, while normal chromosomes will only be detected in the first set of chambers.

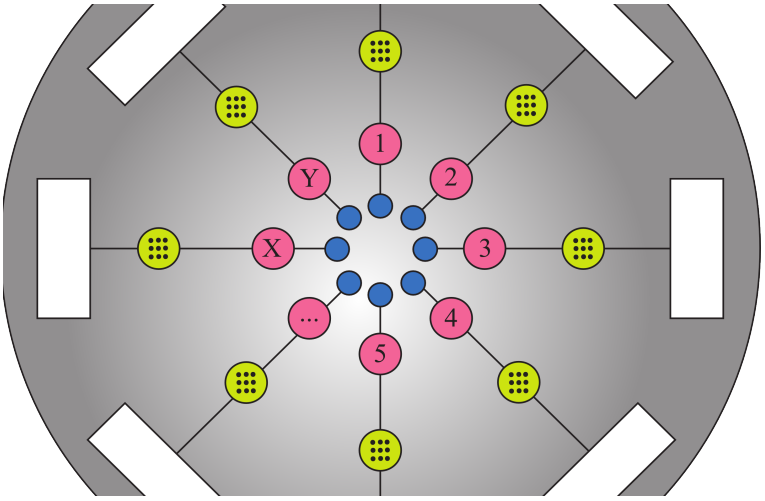

Figure 14.3: The envisioned centrifugal microfluidic system for multiplexed analysis of chromosome translocations. The system consists of 8 channels (expandable to 24) for separation of each chromosome into a separate location. In the first chamber (pink) the chromosome specific centromeric probes are used to capture the specific chromosomes in a way sorting them. In the second set of chambers (yellow/green) the subtellomeric probes are immobilized targeting all other chromosomes than the one captured in the first level chamber. If the probes in the second chamber capture a chromosome fragment it means there was a translocation present. *Courtesy of Anna Line Brøgger.*

14.3 Paper 'Centrifugally Driven Microfluidic Disc for Detection of Chromosomal Translocation'

The research related to Part IV was presented in a scientific paper 'Centrifugally driven microfluidic disc for detection of chromosomal translocation'. The concluding remarks related to the discussion and the work described in the article are summarized in Chapter 15.

Lab on a Chip

View Online / Journal Homepage
Dynamic Article Links

Cite this: DOI: 10.1039/c2lc40554g

www.rsc.org/loc

PAPER

Centrifugally driven microfluidic disc for detection of chromosomal translocations

Anna Line Brøgger,†[a] Dorota Kwasny,†[a] Filippo G. Bosco,[a] Asli Silahtaroglu,[b] Zeynep Tümer,[c] Anja Boisen[a] and Winnie E. Svendsen*[a]

Received 15th May 2012, Accepted 10th July 2012
DOI: 10.1039/c2lc40554g

Chromosome translocations are a common cause of congenital disorders and cancer. Current detection methods require use of expensive and highly specialized techniques to identify the chromosome regions involved in a translocation. There is a need for rapid yet specific detection for diagnosis and prognosis of patients. In this work we demonstrate a novel, centrifugally-driven microfluidic system for controlled manipulation of oligonucleotides and subsequent detection of chromosomal translocations. The device is fabricated in the form of a disc with capillary burst microvalves employed to control the fluid flow. The microvalves in series are designed to enable fluid movement from the center towards the periphery of the disc to handle DNA sequences representing translocation between chromosome 3 and 9. The translocation detection is performed in two hybridization steps in separate sorting and detection chambers. The burst frequencies of the two capillary burst microvalves are separated by 180 rpm enabling precise control of hybridization in each of the chambers. The DNA probes targeting a translocation are immobilized directly on PMMA by a UV-activated procedure, which is compatible with the disc fabrication method. The device performance was validated by successful specific hybridization of the translocation derivatives in the sorting and detection chambers.

1 Introduction

Chromosomal abnormalities are numerical or structural changes of the normal chromosome content or composition, which can either be inherited or can occur later in life. Chromosomal translocations are one of the many possible abnormalities, and are characterized by interchange of genetic material between two non-homologous chromosomes, resulting in two derivative chromosomes. They are the cause of many genetic diseases among which cancer is one of the most common. Therefore, rapid yet specific detection is essential for diagnosis, prognosis, management, treatment and follow-up of the patients.[1]

Currently, chromosome translocations are detected by karyotyping or fluorescent *in situ* hybridization (FISH). Karyotyping involves the use of stains such as Giemsa stain to specifically label chromosome regions by banding. Each chromosome has a unique banding pattern, and a thorough analysis of a stained karyotype can reveal changes in a normal chromosome content. A main advantage of this technique is a possibility to visualize the entire karyotype at once to detect abnormalities. However, the resolution of this technique is limited and usually at a level of 5–10 Mbp. An alternative technique is based on the application of sequence-specific, labeled FISH probes to target selected chromosome regions. Although this technique can detect chromosome translocations at a high resolution it is limited to translocations with known breakpoints, as it requires targeting of the specific sequences. Moreover, the available methods are complex, expensive and require specialized expertise or prior knowledge of the karyotype.[2] In recent years some attempts to miniaturize cytogenetic analyses have been presented, but they mainly focused on implementing the existing protocols such as FISH on microdevices to reduce the analysis time and volume of reagents.[3] However, none of the work was aiming at a new way to detect chromosomal translocations. Therefore, it is highly desirable to develop a novel, inexpensive method which enables the rapid, parallel, reliable and automated detection of the different translocations in the same sample.

Microfluidic devices integrate several laboratory processing steps into a single portable platform, where miniaturization enables highly parallelized, multiplexed and fast detection processes.[4] These systems, often referred to as lab-on-a-chip devices, typically contain several reaction chambers for sample and reagent handling together with actuation and detection mechanisms. Microfluidic devices make it possible to automate tedious experimental processes and they are increasingly being used for life science research and *in vitro* diagnostics.

[a]*Technical University of Denmark, Ørsteds Plads, 345 B, 2800 Kgs. Lyngby, Denmark. E-mail: Winnie.Svendsen@nanotech.dtu.dk; Fax: +45 4588 7762; Tel: +45 4525 5731*
[b]*Copenhagen University, Blegdamsvej 3, 2200 København N, Denmark*
[c]*Kennedy Center, Gl. Landevej 7, 2600 Glostrup, Denmark*
† These authors contributed equally to this work.

Centrifugally driven microfluidic platforms facilitate precise handling of fluidic samples at the microscale. Liquid is moved by the centrifugal pressure generated by spinning the disc at specific rotational frequencies.[5,6] The advantage of this kind of device is the elimination of bulky external pumps (and generated mechanical noise) for the manipulation of liquids. Only a low-power and low-cost rotational motor is required for spinning the disc. These microfluidic platforms are generally referred to as "lab-on-a-disc" devices.[7] It has been shown that flow rates from 5 nL s^{-1} to over 0.1 mL s^{-1} can be centrifugally generated,[8] and that the flow rate is extremely robust to physico-chemical variations such as ionic strength, pH, conductivity or presence of analytes.

Different kinds of valves have been proved to work in centrifugally driven microfluidic discs.[9] Among them, the simplest and most used is the capillary burst microvalve.[10] This type of valve is characterized by an abrupt geometric channel expansion. When liquid reaches the section expansion, it stops due to the capillary pressure at the liquid front meniscus. By spinning the disc at sufficiently high speeds, the centrifugal force induces a pressure on the liquid, which exceeds the capillary pressure, leading the meniscus to burst, hence the valve opens and the liquid advances. The advantages of the capillary burst microvalve are the simplicity of the fabrication and the lack of external actuation, which consequently enables cheaper and smaller device design. The limitations of this kind of valve are the irreversibility, which means that it cannot close when it has opened, and the need of relatively high surface tension of the liquid sample.

Here we present the use of a specifically designed centrifugal microfluidic device for the detection of chromosomal translocations where the fluid manipulation is driven by a combination of centrifugal forces and sets of capillary burst microvalves.

2 Centrifugal platform design

Fig. 1(a) schematically illustrates the lab-on-a-disc device, which was designed, fabricated and employed in translocation detection experiments. It consists of 9 channels for statistical purposes, with 9 inlets near the center of the disc. Each inlet leads to a system of two chambers, where the first functions as a sorting chamber and the second as a detection chamber. As a simple model for chromosome translocation detection, 40 bp long oligonucleotides were used. They consist of a sequence spanning over the breakpoint in the translocation of chromosome 3 and 9, representing derivative 3 and derivative 9. For derivative 3 detection, in the sorting chamber, 20 bp probes targeting the chromosome 3 sequence are immobilized. In the detection chamber, 20 bp probes targeting the chromosome 9 sequence are immobilized. In the case of translocation the positive signal will appear in both chambers, while for the normal chromosome 3 fragment a signal appears only in the sorting chamber.

The liquid handling system, which consists of capillary burst microvalves, allows the target suspension to be hybridized in the sorting chamber. By denaturation the target oligonucleotides are released from the probes, and by spinning the disc the targets (in suspension) flow to the detection chamber. Again, a capillary burst microvalve stops the liquid after the detection chamber to allow the target to hybridize with the second set of probes. Fig. 1(b) shows the schematic layout of the individual microchannel.

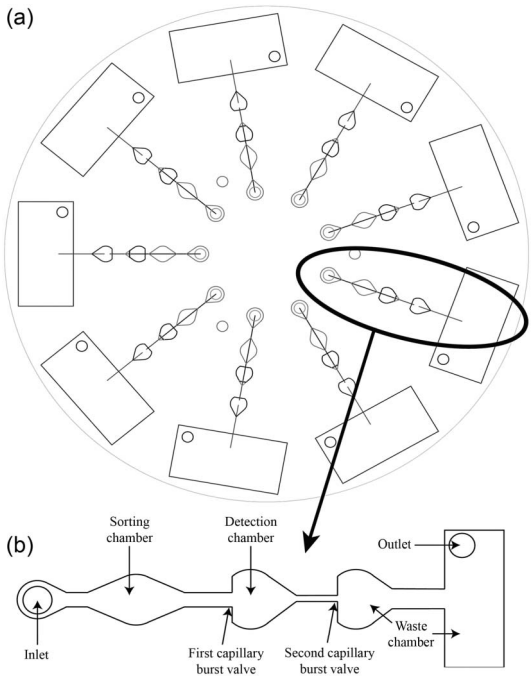

Fig. 1 (a) Schematics of the device for detection of chromosomal translocations. There are 24 channels, representing the 24 different chromosomes in the human karyotype, and each channel can detect one specific translocation. (b) The zoom shows the sorting chamber, followed by the first capillary burst valve. Then the detection chamber, followed by a second capillary burst valve and, finally, a waste reservoir.

The requirement of the two valves is that they burst sequentially and with the highest burst speed difference as possible. The design considerations of the valves were based on a theoretical analysis to ensure sequential bursting. In a centrifugally driven microfluidic platform the centrifugally induced pressure ($\Delta P_{\text{centrifugal}}$) is given by

$$\Delta P_{\text{centrifugal}} = \frac{1}{2}\rho\omega^2\left(r_2^2 - r_1^2\right) \quad (1)$$

where ρ is the density of the liquid, ω is the angular spinning speed, r_2 is the distance from the center of the disc to the front position of the liquid (typically at the valve) and r_1 is the distance to the rear position of the liquid. This means that the centrifugal force increases as the valve moves closer to the periphery of the disc, which as a result decreases the angular burst speed. This is not desirable for sequential bursting and has to be minimized by design. The capillary pressure difference ($\Delta P_{\text{capillary}}$) of the meniscus in a rectangular microchannel is given by the Young–Laplace equation[11–13]

$$\Delta P_{\text{capillary}} = -2\gamma_{\text{la}}\left(\frac{\cos\theta_{\text{A}}}{w} + \frac{\cos\theta_{\text{A}}}{h}\right) \quad (2)$$

where γ_{1a} is the surface tension for the liquid–air interface, θ_A is the advancing contact angle, and w and h are the width and height of the channel leading up to the valve, respectively. In the transition regime where the channel suddenly expands and forms

Table 1 DNA samples representing the normal chromosome 3 (3.1;3.2) and 9 (9.1;9.2) and the derivative chromosome 3 (3.1;9.2) and the derivative chromosome 9 (9.1;3.2). The colors of the sequences correspond to the colors in Fig. 2

Oligonucleotides	Sequence
Normal chromosome 3 fragment (3.1;3.2)	Cy3-5′-AGA ATA TAA GAA AAT GTA CAT TAA CTT TTA AAA ATA GCT T-3′-Cy3
Normal chromosome 9 fragment (9.1;9,2)	Cy3-5′-CGG GAT ACA ATT GGT GTT GGG TGT TTG TCA GGG AGG TTT T-3′-Cy3
Derivative chromosome 3 (3.1;9.2)	Cy3-5′-AGA ATA TAA GAA AAT GTA CAT GTC CTG TTT TCT AAA TTG T-3′-Cy3
Derivative chromosome 9 (9.1;3.2)	Cy3-5′-CGG GAT ACA ATT GGT GTT GGA CTT TTA AAA ATA GCT TTT A-3′-Cy3
Probe 3.1	FITC-5′-TGT ACA TTT TCT TAT ATT CT-3′-NH_2
Probe 3.2	NH_2-5′-TAA AAG CTA TTT TTA AAA GT-3′-FITC
Probe 9.1	FITC-5′-CCA ACA CCA ATT GTA TCC CG-3′-NH_2
Probe 9.2	NH_2-5′-ACA ATT TAG AAA ACA GGA CA-3′-FITC

the capillary burst valve, the contact angle with the straight channel wall is increased from θ_A to $\theta_A + \beta$ in the width direction, which is written as

$$\Delta P_{\text{capillary}} = -2\gamma_{\text{la}}\left(\frac{\cos(\theta_A+\beta)}{w} + \frac{\cos\theta_A}{h}\right) \quad (3)$$

where β is the valve angle, which in this design is 90°. When the disc is spinning the centrifugally driven pressure will increase and the capillary pressure decrease. When the centrifugally driven pressure exceeds the capillary driven pressure, the valve bursts and the liquid moves forward into the chamber. From eqn (3), it can be deduced that when the channel width is decreased the capillary pressure is increased, leading to a higher angular burst speed. This can be exploited when designing the valves, by decreasing the width of the channel leading to the second capillary burst valve, compared to the channel leading to the first. This approach enables controlled movement of hybridization solution from the sorting chambers to the detection chambers.

3 Materials and methods

3.1 Chemicals

The following chemicals were employed in the sample preparation and immobilization steps: Saline Sodium Citrate buffer (SSC), 20× SSC (Gibco, UltraPure), diluted. The phosphate buffer (0.1 M, pH 8.0) was made from 1.682 g sodium phosphate dibasic dihydrate, $Na_2HPO_4{\cdot}2H_2O$ (Sigma-Aldrich, CAS: 10028-24-7) and 0.0749 g potassium dihydrogenphosphate, KH_2PO_4 (Sigma-Aldrich, CAS: 7778-77-0) dissolved in 100 mL Milli-Q water.

3.2 DNA samples

To test the device performance we used a patient with a t(3;9) translocation, where the translocation breakpoints were sequenced on the basepair level. Synthetic oligonucleotides (40 bp) representing the normal chromosomes 3 and 9, and the derivative chromosomes der(3) and der(9) were labeled with Cy3 at both ends to enhance the fluorescence signal (DNA technology, Risskov, DK). As immobilized probes, we used 20 bp synthetic oligonucleotides modified with amine to enable direct immobilization on the PMMA disc and they were labeled with the FITC fluorophore. The oligonucleotides are summarized in Table 1 and schematically illustrated in Fig. 2 with matching colors.

3.3 Disc fabrication and probes immobilization

The fluidic system was designed using AutoCAD and EZcam software. The microchannels and chambers were patterned in a 2 mm thick PMMA disc (Nordisk Plast) by CNC-assisted micromilling technology. Several end mills with diameters ranging from 300 μm to 2 mm were used. The depth of the structures was kept constant at 500 μm. The device is built by two PMMA discs (95 mm in diameter) – one structured with microfluidic components and one employed as a lid. After milling, the discs were cleansed with commercial soap, then washed with Milli-Q water, followed by blow drying with compressed air.

Once the channels and chambers were structured, the DNA immobilization on PMMA was executed based on a previously reported method.[14–16] The procedure has been optimized for the purpose of these experiments and the probe immobilization efficiency has been validated by fluorescence microscopy. The DNA probes (0.3 μL), suspended in 100 mM phosphate buffer at a concentration of 50 μM, were manually spotted using an automatic pipette into the chambers. No additional control over the drop shape was applied.

After the spotting, the two PMMA plates were assembled by UV-activated thermal bonding. The discs were swiped with ethanol and exposed to UV light for 2 min (Dymax 5000-EC, UV-A wavelength range 320–390 nm, intensity = 225 mW cm^{-2}). The UV exposure both activates the surface for PMMA–PMMA bonding and for PMMA–probe immobilization enhancement. During this process the probe solution dries and is immobilized on the PMMA surface. Afterwards, the two discs were aligned, assembled and pressed at 85 °C under a constant force of 12 kN for 1 h in a bonding press (P/O/Weber PW). After bonding the channels were washed with 0.1× SSC in order to remove unattached probes. The disc was thereafter blow dried with nitrogen and investigated under a fluorescent microscope (U-MWB2 (Olympus) filter) to validate successful probe immobilization. A picture of a fabricated disc is shown in Fig. 3(a). It contains 9 different channels for statistical purposes. The device

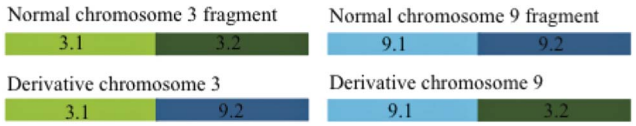

Fig. 2 Schematics of DNA samples representing the normal chromosome 3 and 9 and the derivative chromosome 3 and the derivative chromosome 9. The colors of the strands correspond to the colors in Table 1

was of high quality in terms of optics and channel geometry definition, and no leakage was observed. As seen in Fig. 3(b) the valve angles are well defined at 90°, which leads to more accurate and precise angular burst speeds. The sorting chamber is diamond-shaped (also illustrated in Fig. 1) to avoid an unwanted capillary burst valve before the chamber and also to lead the liquid on to the next chamber without leaving any liquid behind. The detection chamber is drop-shaped since, here, a capillary burst valve is required before the chamber.

3.4 Hybridization, denaturation and detection

The DNA targets, suspended in 1× SSC at a concentration of 1 μM, were manually injected in the channels. The liquid sample front stops at the first capillary burst valve, thus just reacting in the first sorting chamber. The hybridization is left to proceed for 2 h, before the channel is washed by flushing of 0.1× SSC in order to remove unattached probes. No temperature control during the hybridization step is applied. The microchannels are thereafter blow dried with nitrogen flow for a few minutes. The double-stranded DNA is then denatured by heating the disc at 95 °C for 5 min on a hot plate. This step is performed when the chambers and channels are dry. After the heating, 1× SSC, which is at room temperature, is manually injected through the inlets. The liquid again stops at the first capillary burst valve, filling the first chamber and letting the denaturated DNA suspend in the liquid solution. The disc is then spun at 360 rpm for 200 revolutions in order to burst the first capillary valve and let the sample to flow towards the second one. In this way the suspension of denatured DNA probes is moved from the sorting chamber to the detection chamber. It is important to perform this step as fast as possible to avoid rehybridization of the target DNA suspension in the sorting chamber.

The disc's rotational acceleration time, the number of revolutions and the rotational speed are controlled with software (Immediate Motion Creator V1.41). The spinning range was set between 0.6 and 1500 rpm, with acceleration and deceleration times in the range of seconds. The suspension of DNA is subsequently allowed to cool down and hybridize with the probes in the detection chamber for an incubation time of at least 2 h. No temperature control during the hybridization step is applied. Thereafter, the channel is washed by flushing of 0.1× SSC with a syringe to remove unattached probes and then blow dried with nitrogen. The fluorescence-based detection of the hybridized DNA strands is performed after each step of the procedure – hybridization in the sorting chamber and second hybridization in the detection chamber, with a U-MWIY2 (Olympus) filter.

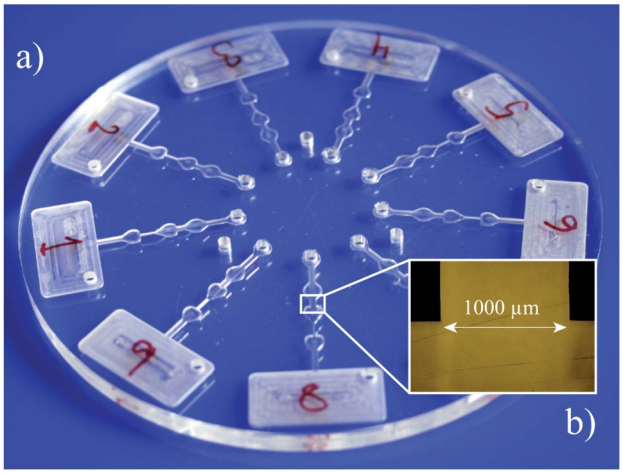

Fig. 3 (a) Image of the fabricated disc in PMMA with 9 different channels for statistical purposes. (b) Magnification of a valve with a width expansion from 1000 μm at a 90° angle.

4 Results and discussion

4.1 Sequential bursting

From these equations a design where the two valves burst at different angular spinning speeds is developed. The specifications of the valves are shown in Table 2 and the theoretical as well as experimentally found angular burst speeds are illustrated in Fig. 4. The experiments were repeated nine times for each valve. The first capillary burst valve bursts at 236 rpm ± 9.8 rpm, while the second valve bursts at 416 rpm ± 26.5 rpm as illustrated in Fig. 4. This yields a bursting difference of 180 rpm and no overlap in the statistical errors. Thus, by spinning the disc at 360 rpm the first capillary burst valve bursts while the second valve remains closed. This ensures that the liquid does not move to the waste chamber but stays in the second detection chamber for the second hybridization.

4.2 Immobilization, hybridization and denaturation

The immobilization method was selected based on the compatibility with the disc fabrication procedure. The requirement was to obtain a high-density immobilization of amine-modified probes on PMMA without losing the probe ability to hybridize to complementary targets. Immobilization of the probes in the sorting chamber is shown in Fig. 5(a) with U-MWB2 as a detection filter. The image shows a high fluorescence intensity, indicating a dense immobilization, which is achieved only by UV activation of the surface and without any chemical treatment. The non-uniform drop shape is a result of manual spotting and roughness of the milled surface. Hybridization of the target probe is shown in Fig. 5(b) and is indicated by the color change from green to yellow since the probe is labeled with FITC and the target with Cy3. Denaturation of the double-stranded DNA is shown in Fig. 5(c) and is indicated by a color change from yellow to green.

In the performed hybridization experiments the complementary DNA fragment was successfully hybridized to the immobilized probe. Each experiment was performed at least 3 times to determine the reproducibility of the results. The fluorescent signals of the immobilized probe and complementary DNA are colocalized indicating a specific hybridization, with no unspecific binding to the surface. The presented results prove that with the

Table 2 Specifications of the two capillary burst valves in series

	$r_{1,n}$/mm	$r_{2,n}$/mm	w_n/μm	h/μm	β/°
Valve 1 (n = 1)	11	22	1000	500	90
Valve 2 (n = 2)	13[a]	28	300	500	90

[a] Approximated value.

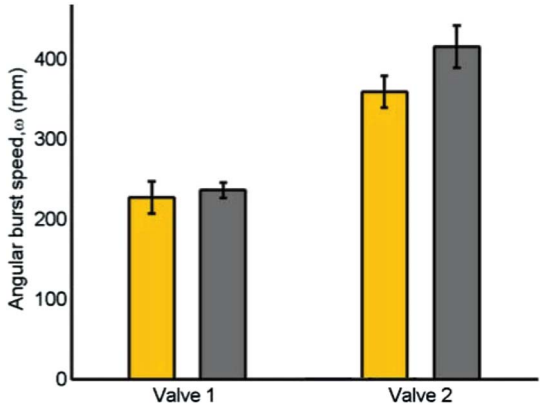

Fig. 4 Theoretical (yellow) and experimental (grey) angular burst speeds for both valves. The experimental results are a mean of nine measurements.

developed procedures, it is possible to denature the DNA without detaching the probes from the PMMA, which indicates that the immobilization is strong enough for the purpose of the device. For the device optimal performance it is important to release only the target DNA during denaturation and transfer it to the detection chamber. The initial denaturation procedure was performed with 1× SSC buffer present in the channel during heating at 95 °C on a hot plate. This led to partial evaporation of the liquid, which interfered with the performance of the capillary burst valve. To achieve better control over device handling a denaturation procedure in dry conditions was applied. During heating, the target DNA is released from the immobilized probe. By fast injection of the 1× SSC buffer and disc spinning the target DNA suspension was transferred to the detection chamber and allowed to hybridize while cooling down. The immobilization procedure was optimized for the purpose of the device. The previously reported methods for immobilization and hybridization included surfactants in the buffer solutions. The capillary burst microvalves rely on the surface tension of the liquid and since the surfactants lower the surface tension of the liquid, it is not possible to contain the liquid in the two chambers. The capillary burst microvalves are not working under these conditions and therefore the surfactants were excluded from the hybridization procedure, without altering the immobilization and hybridization efficiency. Moreover, by excluding the surfactants from the immobilization solution the spotted drop was more confined and was only spreading due to the surface roughness.

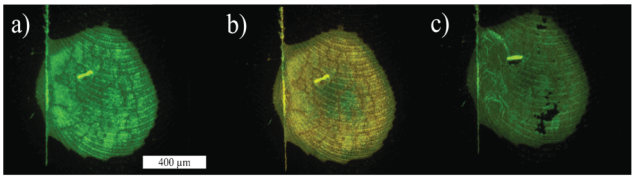

Fig. 5 (a) Immobilization of the FITC-labeled DNA probe on PMMA. (b) Subsequent hybridization of the Cy3-labeled target DNA. (c) Denaturation of the double-stranded DNA. The fluorescence is detected with the filter U-MWB2.

4.3 Translocation detection

The experiments for translocation detection were performed in triplicates for statistical purposes. The sample of results for the chromosome translocation experiments are shown in Fig. 6. The first rows of pictures are from the sorting chamber, while the second rows show pictures from the detection chamber. The first column shows the result after immobilization of the probes. The

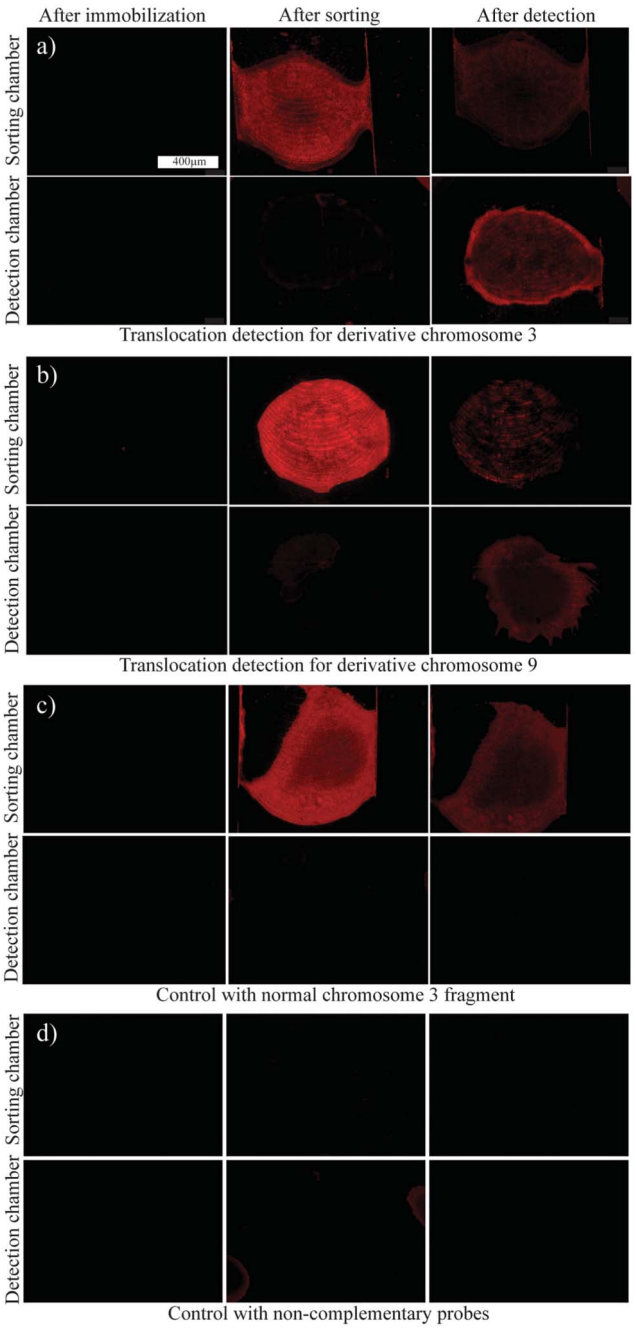

Fig. 6 (a) Translocation detection for derivative chromosome 3: probe 3.1 in the sorting chamber, probe 9.2 in the detection chamber. (b) Derivative chromosome 9: probe 9.1 in the sorting chamber, probe 3.2 in the detection chamber. (c) Control with the normal chromosome 3 fragment: probes 3.1 in the sorting chamber, probe 9.2 in the detection chamber. (d) Control with derivative 9: probe 3.1 in the sorting chamber, probe 9.2 in the detection chamber.

second column shows the results after hybridization in the sorting chamber and the third column shows the results after denaturation in the sorting chamber and re-hybridization in the detection chamber.

In Fig. 6(a) and (b) are shown the results for derivative chromosome 3 and derivative chromosome 9. The sorting chamber contains probes targeting the first 20 bp sequence on each derivative chromosome. The detection chamber contains probes for the remaining 20 bp fragment on each derivative. In the second column, the hybridization of the derivatives to the probes in the sorting chamber is shown. Due to the valves, the hybridization suspension is confined to the sorting chamber, so no hybridization is observed in the detection chamber. After denaturation and spinning of the disc, the liquid is partially transferred to the detection chamber where the probes targeting the second part of the derivative are immobilized. Due to sequence complementarity, hybridization in the detection chamber occurs. After the immobilization, there is no fluorescence observed, due to the filter used.

To ensure the specificity of the binding, necessary controls were performed. In Fig. 6(c) a control experiment with a normal chromosome 3 fragment as the target is shown. The probes 3.1 and 9.2 are immobilized in the sorting chamber and detection chamber, respectively. This means that the probes and targets are complementary in the sorting chamber, while they are non-complementary in the detection chamber. The same experiment was performed with normal chromosome 9 fragment using 9.1 and 3.2 probes, with similar results (data not shown). In Fig. 6(d) a control non-complementary experiment is shown. The target used was the derivative chromosome 9 while the immobilized probes are 3.1 and 9.2.

The presented results proved the principle of translocation detection on the disc. The successful consecutive hybridization in the two chambers was only observed for the derivative chromosomes, which indicates the specificity of the performed experiments. It also proves that it is possible to detect the translocation. The normal chromosome fragments were only hybridizing in the sorting chamber without giving a signal in the detection chamber. No observed hybridization in the non-complementary experiment proves that the probes are specifically targeting selected translocation. Both controls indicate the possibility of sorting the chromosomal fragments into separate chambers.

During disc handling, it was noticed that proper drying of the channels after washing steps is critical for the valve performance. The valves are controlled by the contact angle between the liquid and channel wall and by wetting the channel, the properties of the valve are changed. Due to the thin water layer in the channel, the valve act as open and does therefore not constrain the sample suspension in the sorting and detection chambers.

In the images after the second hybridization, fluorescence is detected in both chambers. After the spinning, the solution containing the target is moved to the detection chamber. Because the volume in the sorting chamber is larger than the volume in the detection chamber, some of the liquid remains in the sorting chamber. This results in hybridization in both chambers in the second step. The observed fluorescence intensity is consequently reduced in the detection chamber. Another possible explanation for the lowered intensity is the thermal instability of Cy3.[17]

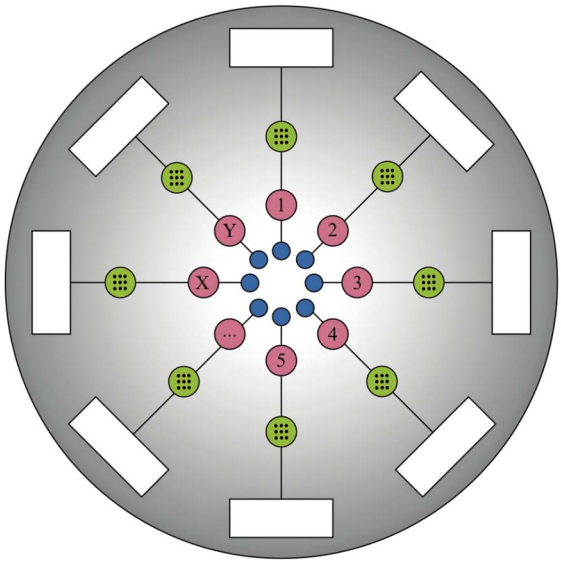

Fig. 7 Schematics of the device for detection of chromosomal translocations. There are 24 channels, representing the 24 different chromosomes in the human karyotype, and each channel can detect one specific translocation.

During heating of the disc, the Cy3-labeled target might lose most of its intensity. In the future, a more stable fluorophore should be chosen.

5 Outlook

The obtained results prove the working principle of translocation detection in the lab-on-a-disc device. It can be further modified to enable detection of the chromosome translocations in patient samples. Fig. 7 schematically illustrates the working principle of the device. Near the center of the disc, 24 inlet reservoirs (blue) are structured (for the 22 autosomes and two sex chromosomes of the human karyotype). Each inlet leads to a system of two chambers, where the first functions as a sorting chamber (pink) and the second as a detection chamber (green). In each sorting chamber, probes for a specific chromosome centromere are immobilized. As a result, each chromosome is then sorted into each of the 24 channels. In this way the whole karyotype is divided into its individual chromosomes represented by their centromeres, each located into a specific sorting chamber. In the detection chamber a microarray of probes for the remaining 23 chromosome chromatids is immobilized. If there is a translocation present, one of the specific probes for the remaining chromosomes will hybridize with a target chromosome. Due to the low flow rates used in the device the chromosome shearing is minimized.

6 Conclusions

Centrifugally driven microfluidics offers inexpensive, simple and fast device actuation. Moreover, being compatible with standard CD disc players and laboratory centrifuges it offers a possibility to become a portable point-of-care device. Capillary burst microvalves are some of the most widely used valve systems. They do not require any additional chemical modification steps

to control liquid flow, only a design with an abrupt geometrical expansion of the channel. In the work shown here we presented a design with two capillary burst microvalves placed in series. To our knowledge it is the first example of valves bursting sequentially from the center towards the periphery of the disc. The burst speed of the two valves is separated by 180 rpm, which allows precise control of valve opening. The design was applied to handle DNA samples to achieve two consecutive hybridizations for the detection of chromosome translocation. Nowadays, the most commonly used technique for translocation detection is FISH, which can only detect known translocations. The main advantage of the presented device over FISH is a possibility to study the chromosome translocations without prior knowledge of the karyotype. The demonstrated assay provides a fast and reliable diagnostic method, which could in the future compete with currently used cytogenetic methods. In this work we selected a known translocation to validate the device performance; however, the device is versatile and will be expanded towards targeting several common translocations. The device is easy to use, enabling introduction of this type of assay in everyday cytogenetic analysis.

Acknowledgements

The authors would like to thank the Danish Council for Strategic Research-Programme Commission for Growth Technologies for financial support (project MUSE and Nano-Karyotyping).

References

1 L. Jorde, J. Carey, M. Bamshad and R. White, *Medical Genetics*, Mosby, St. Louis, MO, 2003, pp. 107–135.
2 M. Speicher and N. Carter, *Nat. Rev. Genet.*, 2005, **6**, 782–792.
3 D. Kwasny, I. Vedarethinam, P. Shah, M. Dimaki, A. Silahtaroglu, Z. Tumer and W. Svendsen, *Biomed. Microdevices*, 2012, **14**, 453–460.
4 S. J. Trietsch, T. Hankemeier and H. J. van der Linden, *Chemom. Intell. Lab. Syst.*, 2011, **108**, 64–75.
5 M. J. Madou, L. J. Lee, S. Daunert, S. Lai and C. H. Shih, *Biomed. Microdevices*, 2001, **3**, 245–254.
6 M. Madou and G. Kellogg, *Proceedings of Systems and Technologies for Clinical Diagnostics and Drug Discovery*, 1998, **3259**, 80–93.
7 M. Madou, J. Zoval, G. Jia, H. Kido, J. Kim and N. Kim, *Annu. Rev. Biomed. Eng.*, 2006, **8**, 601–628.
8 D. Duffy, H. Gillis, J. Lin, N. Sheppard and G. Kellogg, *Anal. Chem.*, 1999, **71**, 4669–4678.
9 R. Gorkin, J. Park, J. Siegrist, M. Amasia, B. S. Lee, J.-M. Park, J. Kim, H. Kim, M. Madou and Y.-K. Cho, *Lab Chip*, 2010, **10**, 1758–1773.
10 T. Leu and P. Chang, *Sens. Actuators, A*, 2004, **115**, 508–515.
11 H. Cho, H.-Y. Kim, J. Y. Kang and T. S. Kim, *J. Colloid Interface Sci.*, 2007, **306**, 379–385.
12 H. Cho, H. Kim, J. Kang and T. Kim, *Technical Proceedings of the 2004 NSTI Nanotechnology Conference and Trade Show*, Nano Science and Technology Institute, Cambridge, MA, 2004, vol. 1, pp. 263–266.
13 J. M. Chen, P.-C. Huang and M.-G. Lin, *Microfluid. Nanofluid.*, 2008, **4**, 427–437.
14 Y. Sun, I. Perch-Nielsen, M. Dufva, D. Sabourin, D. D. Bang, J. Hogberg and A. Wolff, *Anal. Bioanal. Chem.*, 2012, **402**, 741–748.
15 F. Fixe, M. Dufva, P. Telleman and C. Christensen, *Lab Chip*, 2004, **4**, 191–195.
16 F. Fixe, M. Dufva, P. Telleman and C. Christensen, *Nucleic Acids Res.*, 2004, **32**, e9.
17 W. Liu, J. Wu, E. Li and E. Selamat, *Appl. Environ. Microbiol.*, 2005, **71**, 6453–6457.

15. Conclusions and Project Summary

We have developed a lab-on-a-disc system for fluorescent detection of chromosome translocation fragments. The work was carried out on a simple, synthesized DNA fragment that contains a real translocation sequence. The principle of detection by surface immobilized DNA probes has been demonstrated and realization of double hybridisation assay was successful. To multiplex the assay to allow for detection of various chromosomal translocations in a patient sample it would be necessary to form an array of probes on the disc surface. However, the requirement for DNA probes specific for the entire human genome sequence prevents us from demonstrating the multiplexing ability of the device. Furthermore, the principle was shown on short synthetic DNA fragments, while it is necessary to achieve hybridisation of longer PCR amplified DNA fragments and a total DNA extracted from a patient carrying a translocation. An attempt to amplify the 1 kbp DNA spanning over the translocation breakpoint was made. Although it was possible to amplify the desired DNA fragment, it was challenging to incorporate fluorescent labels and to validate the successful hybridisation to surface immobilized probes.

Bibliography

Amasia, M.; Cozzens, M.; Madou, M.J., *Centrifugal microfluidic platform for rapid PCR amplification using integrated thermoelectric heating and ice-valving*, Sensors and Actuators: B. Chemical, **161**, 1191-1197 (2012)

Bosco, F.G.; Hwu, E.-T.; Chen, C.-H.; Keller, S.; Bache, M.; Jakobsen, M.H.; Hwang, I.-S.; Boisen, A., *High throughput label-free platform for statistical biomolecular sensing*, Lab on a Chip, **11**, 2411-2416 (2011)

Chin, C.D.; Linder, V.; Sia, S.K., *Commercialization of microfluidic point-of-care diagnostic devices*, Lab on a Chip, **12**, 2118-2134 (2012)

Cho, H.; Kim, H.-Y.; Kang, J.Y.; Kim, T.S., *Capillary Passive Valve in Microfluidic System*, NSTI-Nanotech, **1**, ISBN 0-9728422-7-6, 263-266 (2004)

Duffy, D.C.; Gillis, H.L.; Lin, J.; Sheppard, N.F.; Kellogg, G.J., *Microfabricated Centrifugal Microfluidic Systems: Characterization and Multiple Enzymatic Assays*, Analytical Chemistry, **71**, 4669-4678 (1999)

Gorkin, R.; Park, J.; Siegrist, J.; Amasia, M.; Lee, B.S.; Park, J.-M.; Kim, J.; Kim, H.; Madou, M.; Cho, Y.-K., *Centrifugal microfluidics for biomedical applications*, Lab on a Chip, **10**, 1758-1773 (2010)

Gorkin, R.; Soroori, S.; Southard, W.; Clime, L.; Veres, T.; Kido, H.; Kulinsky, L.; Madou, M., *Suction-enhanced siphon valves for centrifugal microfluidic platforms*, Microfluidics and Nanofluidics, **12**, 345-354 (2012)

Hulme, S.E.; Shevkoplyas, S.S.; Whitesides, G.M., *Incorporation of prefabricated screw, pneumatic, and solenoid valves into microfluidic devices*, Lab on a Chip, **9**, 79-86 (2008)

Hong, J.W.; Quake, S.R., *Integrated nanoliter systems*, Nature Biotechnology, **21**, 1179-1183 (2003)

Inoue, T.; Fujita, Y.; Uchiyama, S.; Doi, T.; Fukui, K.; Yokoyama, H., *Chapter 4 in Chromosome Nanoscience and Technology*, Edited by Fukui, K. and Ushiki, T., Taylor and Francis Group, ISBN 978-1-4200-4491-1 (2008)

Johnson, R.D.; Badr, I.H.A.; Barret, G.; Lai, S.; Madou, M.J.; Bachas, L.G., *Development of a fully integrated analysis system for ions based on ion-selective optodes and centrifugal microfluidics*, Analytical Chemistry, **73**, 3940-3946 (2001)

Lee, B.S.; Lee, J.-N.; Park, J.-M.; Lee, J.-G.; Kim, S.; Cho, Y.-K.; Koa, C., *A fully automated immunoassay from whole blood on a disc*, Lab on a chip, **9**, 1548-1555 (2009)

Madou, M.J.; Kellogg, G.J., *LabCD: a centrifuge-based microfluidic platform for diagnostics*, Proceedings of Systems and Technologies for Clinical Diagnostics and Drug Discovery, **3259**, 80-93 (1998)

Madou, M.J.; Lee, J.J.; Daunert, S.; Lai, S.; Shih, C.-H., *Design and Fabrication of CD-like Microfluidic Platforms for Diagnostics: Microfluidic Functions*, Biomedical Microdevices, **3**, 245-254 (2001)

Madou, M.J.; Zoval, J.; Jia, G.; Kido, H.; Kim, J.; Kim, N., *Lab on a CD*, Annual Review of Biomedical Engineering, **8**, 601-628 (2006)

Manz, A.; Eijkel, J.C.T., *Miniaturization and chip technology. What can we expect?*, Pure and Applied Chemistry, **73**, 1555-1561 (2001)

Marco, C.D.; Eaton, S.M.; Suriano, R.; Turri, S.; Levi, M.; Ramponi, R.; Cerullo, G.; Osellame, R., *Surface properties of femtosecond laser ablated PMMA*, ACS Applied Materials and Interfaces, **2**, 2377-2384 (2010)

Melin, J.; Quake, S.R., *Microfluidic Large-Scale Integration: The Evolution of Design Rules for Biological Automation*, Annual Review of Biophysics and Biomolecular Structure, **7**, 213-231 (2007)

Peytavi, R.; Raymond, F.R.; Gagne, D.; Picard, F.J.; Jia, G.; Zoval, J.; Madou, M.; Boissinot, K.; Boissinot, M.; Bissonnette, L.; Ouellette, M.; Bergeron, M.G., *Microfluidic device for rapid (< 15 min) automated microarray hybridization*, Clinical Chemistry, **51**, 1836-1844 (2005)

Steigert, J.; Grumann, M.; Brenner, T.; Riegger, L; Harter, J.; Zengerle, R.; Ducree, J., *Fully integrated whole blood testing by real-time absorption measurement on a centrifugal platform*, Lab on a Chip, **6**, 1040-1044 (2006)

Part V

Label Free Detection of Chromosome Translocation

16. Introduction

In the previous parts of the thesis different methods for performing chromosome translocation detection were investigated. The lab-on-a-disc proved to be the most useful in realizing the two independent DNA hybridisation steps necessary for the translocation detection. However, the detection was done with fluorescently labeled DNA by fluorescent microscopy, which is a bulky and expensive technique. The ideal solution would be to fabricate a label-free sensor for DNA hybridisation, which would facilitate the creation of a point-of-care system and reduce the reagents costs. In this Part V the application of three different electrical sensors for DNA hybridisation sensing will be described.

Biosensors are devices that are able to recognize the specific binding event between an analyte and a biological recognition element (Figure 16.1) (Daniels and Pourmand, 2007). These biological recognition elements can be of vast variety such as cells, antibodies, antigens, aptamers, DNA probes, etc (Guan et al., 2004; Hunt and Armani, 2010). They are immobilized on a surface of a transducer, which translates the binding event into a measurable signal as seen in Figure 16.1 (Drummond et al., 2003). In the presence of a specific analyte the binding to the biological recognition layer takes place. This induces the changes in a transducer, which results in a measurable signal. In the presence of a mismatching sample there is no specific binding event thus no signal should be measured (Daniels and Pourmand, 2007). Biosensors can be categorized based on the biological element or the transducer. The transduction mechanism can be optical, magnetic, mechanical or electrical (Daniels and Pourmand, 2007; Drummond et al., 2003; Hunt and Armani, 2010). Optical sensors are based on the use of optical fibers, wave guides or a surface plasmon resonance (Hunt and Armani, 2010). Magnetic sensors often require magnetic particles with immobilized biorecognition element (Daniels and Pourmand, 2007; Hunt and Armani, 2010). Mechanical sensors such as cantilevers are often fabricated by lithography and can be used in vibration or deflection mode, which occurs due to the binding event on their surface (Hunt and Armani, 2010). Electrical sensors are based on measuring the changes in the electrical properties due to the biorecognition (Hunt and Armani, 2010). The subject of this Part of the thesis is the electrical biosensing of DNA hybridisation.

The biorecognition events have been studied for years in biochemistry or molecular biology. However, they often involve use of labeling molecules that are most commonly fluorophores (Daniels and Pourmand, 2007). Detection is based on the analysis of fluorescence signal by either plate readers, scanners, flow cytometers or fluorescent microscopes. All these equipments are expensive and bulky, which reserves the analysis to specialized laboratories (Drummond et al., 2003). Furthermore, the labeling often requires modification of the target by adding the

fluorophore, which adds cumbersome washing steps to the entire procedure. Besides, the labeling may have an influence on the structure of the analyzed molecule which may alter the molecular binding (Daniels and Pourmand, 2007). Labeling of the target can be omitted by the use of secondary recognition elements that are labeled instead. They also bind specifically to the target and after washing steps their fluorescence signal is measured (Daniels and Pourmand, 2007). The ideal solution would be to use label-free sensing for direct measurement of the binding event. Label-free sensors do not need any additional labels as they can recognize the binding due to the changes occurring on the tranducer surface (Daniels and Pourmand, 2007). Consequently, the assay cost and time can be greatly reduced since no additional labeling steps are needed.

The advances in a sequencing technology generated a great amount of data, which need to be analyzed in a simple, fast and reliable way (Cosnier and Mailley, 2008; Drummond et al., 2003; Hunt and Armani, 2010; Teles and Fonseca, 2008). Sequencing of genomes allowed identification of gene mutations that cause various diseases, thus it is know possible to develop sensors detecting those abnormalities (Hunt and Armani, 2010; Teles and Fonseca, 2008). DNA hybridisation sensors, so called genosensors have been of great interest in the scientific world. The increasing popularity of microarrays in diagnostics, showed that there is a need for hybridisation sensors that are realized without fluorescent labels (Teles and Fonseca, 2008). The microarrays, being very useful, are still expensive and used only in specialized laboratories. The advantage of using DNA hybridisation sensors is the fact that the biorecognition occurs directly on the transducer surface. DNA sensors consist of a DNA (probe) immobilized on the surface that is specific towards a complementary DNA target (analyte) (Cosnier and Mailley, 2008; Teles and Fonseca, 2008). The underlying mechanism of detection is based on the specific hybridisation between these two strands. The double strand (duplex) formation can be recognized directly or using a hybridisation indicator or mediator (Drummond et al., 2003). The recognition between two DNA strands occurs in nature in solution, which is a fast process. Hybridisation on a solid support as is the case for a biosensor occurs much more slowly due to decreased mobility of

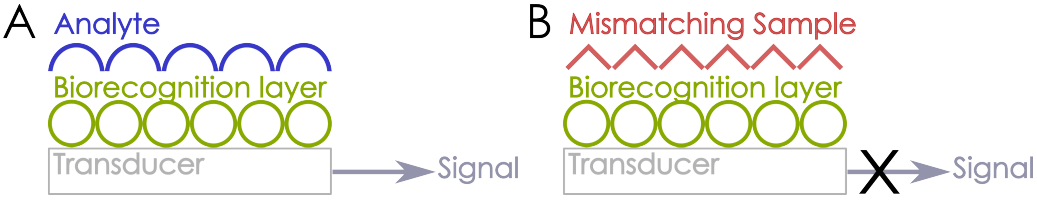

Figure 16.1: Schematic representation of a biosensor working principle. In A, an analyte present in the sample binds specifically to the biorecognition layer on a transducer surface, which leads to a detectable signal. In B, the sample contains mismatching molecules which do not bind to the biolayer and thus no readable signal is observed.

the immobilized strands (Teles and Fonseca, 2008). Although there are different transduction mechanisms used for detection of DNA hybridisation the main focus of this thesis is the electrical detection. Electrical biosensors offer low cost, low power devices that are amenable for miniaturization at the same time allowing fast analysis times (Daniels and Pourmand, 2007). In this Part of the project three different electrical sensors were used, namely silicon nanowires as biological field effect transistors (BioFET), metallic and conductive polymer electrodes used as tranducers for impedance spectroscopy measurements.

17. Detection of DNA Hybridisation Using SiNWs as BioFETs

This chapter is partially based on a Master's thesis project performed by Kasper Bayer Frøhling and supervised by me.

Silicon nanowires (SiNWs) are silicon structures with a critical dimension of the order of nanometers at which effects of quantum mechanics have to be considered. The diameter of a nanowire is usually between 10-100 nm, which means that most of the atoms are close to the surface. Thus, minute changes in charge on the surface of a nanowire can be detected. Due to the semiconducting properties nanowires can be used for novel electronic components but also as biosensors in a similar way to Field Effect Transistors (FET). The BioFETs detect the changes in the nanowire conductance due to the biorecognition event. SiNWs as biosensors have been reported for detection of virus particles, cancer biomarkers, DNA hybridisation (Chen et al., 2013; De et al., 2013; Lin et al., 2009; Mescher et al., 2013; Patolsky et al., 2004; Shen et al.;, 2012; Wenga et al., 2013). The main advantage of using SiNW sensors is their small size and high sensitivity to the charged particles mainly attributed to their large surface-to-volume ration (De et al., 2013). They are especially useful for detection of such molecules as proteins or DNA due to their charged surface. The measurements can be performed in real time and a typical measurement takes about 100-500 seconds (Gao et al., 2011; Hahm and Lieber, 2004; Li et al., 2004). They are amenable for multiplexing and are cost-efficient due to their reusability (Chen et al., 2011; Zhang et al., 2010). The peripheral equipment necessary for the electrical detection is limited to a potential source and an amperometer. The potential source can be as simple as a battery, which greatly reduces the costs of the biosensor and the amperometer can be integrated that enables miniaturization.

17.1 Theory

The detection principle for SiNW biosensor is based on the current measurements in the nanowire, which can be influenced by the charge of the analyte and ions in the solution (Wenga et al., 2013). The typical SiNW biosensor consists of a p- or n-doped SiNW connected to a source and drain metal electrodes (Chen et al., 2013). The nanowire is isolated from the silicon substrate with a silicon oxide and its conductance can be adjusted by a back gate situated below the oxide layer (Mescher et al., 2013). A typical scheme of detection is presented in Figure 17.1. As an example a p-type SiNW with a native oxide is used with

the charged molecules immobilized on the surface of the nanowire. The holes are responsible for conducting current in a p-type SiNW that flows from source to drain. When a negatively charged species are introduced in the vicinity of the nanowire, more holes will be attracted from the bulk of the silicon, resulting in an increased current and thus resistance drop (Chen et al., 2013). The detection is based on electrostatic forces, thus the closer the charges on the surface, the bigger the effect (Wenga et al., 2013). The charge based detection depends on the ability of the analyte to significantly change the conductivity of the nanowire. Otherwise, the noise level can prevent any readable signal. The charged molecules are often present in a buffer solution thus the analyte is surrounded by a cloud of counter ions from the bulk of the solution, which screens the charges (Chen et al., 2013). To achieve the best sensitivity, the amount of ions in the solution needs to be reduced, at the same time allowing the target molecule to remain in a native state.

17.2 Chip Design and Fabrication

For the device fabrication a new approach has been applied. Another project in the research group involved investigation of various properties of diphenylalanine peptide tubes. Based on the results the diphenylalanine tubes were selected for fabrication of the nanowires as etching masks (Andersen et al., 2012; Larsen et al., 2011). The fabrication scheme is briefly described here with a thorough explanation included in Appendix B. The design of the mask is highly dependant on the peptide tubes alignment technique by spin casting. During the spin casting the peptide tubes align radially from the center of rotation. Thus, to use them as etching mask for the SiNW fabrication, the contacting electrodes need to be placed perpendicular to the tubes orientation. To better visualize the chips setup a schematic is shown in Figure 17.2. The nanowires are formed across the channel made in the passivation layer to isolate the electrodes.

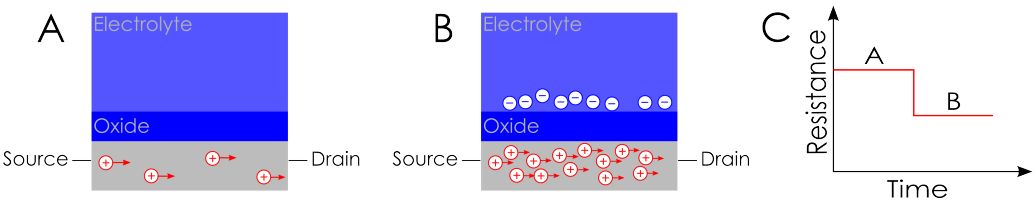

Figure 17.1: Principle of detection with p-type SiNW. The holes as charge carriers appear to be running from source to drain in the p-type nanowire (A). When negatively charged particles are introduced in the electrolyte more holes are attracted from the bulk (B). The nanowire resistance change is shown in C with an initial stable value that decrease when the negatively charged particles are added.

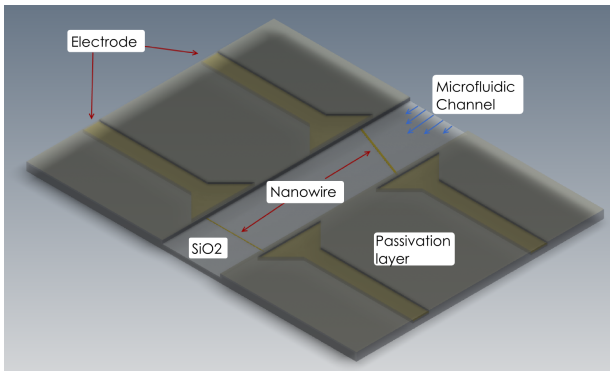

Figure 17.2: A schematic of the silicon nanowire setup with the nanowires bridging the gap between two electrode pads. The passivation layer forms a microfluidic channel placed in between the electrode pads. *Courtesy of Kasper Bayer Frøhling.*

The fabrication process starts with a growth of 500 nm oxide layer. Subsequently a 52 nm p-doped polysilicon as a device layer is deposited. Afterwards the electrodes are patterned by photolithography and a thin metal layer (up to 50 nm) is deposited. The fabrication procedure and allowed materials in the etching machine limited us to the use of aluminium as the metal for electrical connections. After the lift-off process the peptide tubes are spin casted on the wafer. The peptide solution is dropped on the spinning wafer followed by an isopropanol drop to remove the majority of misaligned tubes. Subsequently, the pattern of the peptide tubes is transferred to the polysilicon layer by reactive ion etching (RIE) followed by washing of the peptide tubes with MilliQ water. To ensure that the current is only running through the nanowires and not through the liquid, the chips are passivated with silicon dioxide or titanium oxide, which can be patterned by standard lithography technique. After the cleanroom fabrication was completed the

Figure 17.3: A silicon nanowire chip connected to the ZIF socket. *Courtesy of Kasper Bayer Frøhling.*

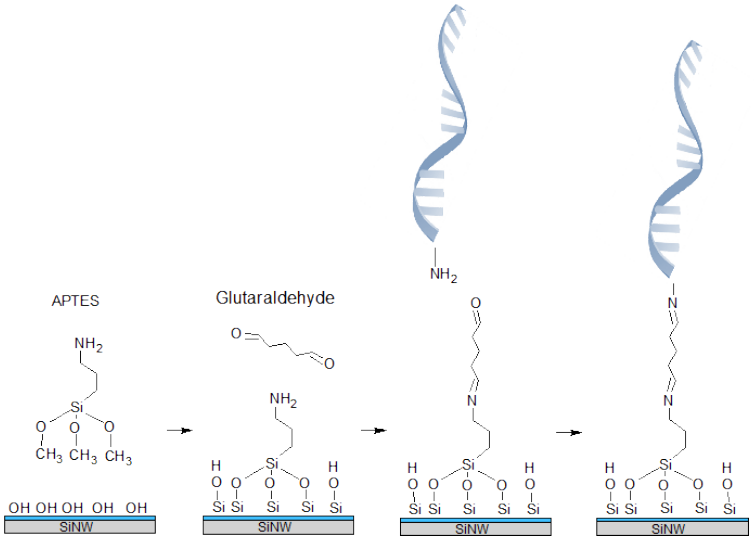

Figure 17.4: Functionalization of SiNW surface with APTES and glutaraldehyde. The surface is first treated with ethanol to create OH groups on the surface that are binding to APTES. Afterwards glutaraldehyde is added as a linker to which amine group at the end of a DNA probe strand binds. *Courtesy of Kasper Bayer Frøhling.*

chips were diced and ready to use. The chips' electrical connections were designed to fit with a standard 10 connection ZIF socket. The picture of the chip connected to a ZIF socket is shown in Figure 17.3. For most of the measurements the devices were used by placing a drop of liquid solution to cover the wires. The measurements were performed using a custom made setup consisting of a manual switching device, current preamplifier with a data acquisition card operated by a LabView program. The readout setup was designed by a Master student in the group Michael Jørgensen.

17.3 Nanowire Functionalization

The functionalization of a silicon surface is often performed by silanization. The basic procedure applied in the experiments is shown in Figure 17.4. In the experiments with SiNWs the modification was done by (3-aminopropyl)triethoxysilane (APTES) attachment. It creates amine (NH_2) modified surface, which can be further modified by adding a glutaraldehyde. The glutaraldehyde surface is terminated with functional carboxyl groups, which can be bound to amine modified molecules. For the purpose of these experiments DNA probes modified with amines were used. The modification started by dipping the chips in absolute ethanol to create silanols on the surface. Afterwards the chips were soaked in 2 % APTES in ethanol solution for 30 minutes followed by washing in ethanol and 1 hour

Table 17.1: DNA samples used in the project for detection of chromosome translocation. Der9 - complementary to probes 9.3 and 9.9; Der3 - non-complementary DNA. The probes with matching complementary fragments are colour coded.

Name	Sequence
Probe 9.9	sequence 5'-CCA ACA CCA ATT GTA TCC CG-NH2-3'
Probe 9.3	sequence 5'-NH2-TAA AAG CTA TTT TTA AAA GT-3'
Der9	Cy3-5'-CGG GAT ACA ATT GGT GTT GGA CTT TTA AAA ATA GCT TTT A-3'-Cy3
Der3	Cy3-5'-AGA ATA TAA GAA AAT GTA CAT GTC CTG TTT TCT AAA TTG T-3'-Cy3

treatement with 2.5 % glutaraldehyde. Subsequently, the chips were washed in PBS before adding a DNA probe with amine end. After overnight incubation in a humidity chamber the chips were washed and ready to be used for the DNA hybridisation experiments. As a control, non-complementary DNA was used to check the specificity of the obtained signal. Following, the complementary DNA strand was used at various concentrations. For detection of the chromosome translocation the double hybridisation assay was used with two chips functionalized with probes matching the two chromosome sequences in a derivative chromosome. The target DNA captured on one chip was denatured at 95 °C and transferred to the second chip and incubated. The sequence of DNA strands used in this part of the project is shown in Table 17.1. The DNA sequences are conventionally written from 5' to 3' end with a complementary strand written from 3' to 5' end.

17.4 Results and Discussion

17.4.1 DNA Hybridisation Sensing

The fabricated SiNWs were used as DNA hybridisation biosensors. As they are p-dopped the resistance of the nanowire was expected to decrease after immobilization of the negatively charged DNA probe and after specific hybridisation with a complementary DNA strand as seen in Figure 17.5. Due to some experimental error the control with non-complementary DNA strand has not been performed on the peptide fabricated nanowires. There is another project in the group that uses nanowire sensors fabricated following the same scheme as described in Section 17.2. The only difference in the fabrication is the use of a photolithography mask to create the nanowire structures, rather than the peptide tubes. The chips fabricated using the mask were also tested and a proper control with a non-complementary strand has been done. The results of this experiment are shown in Figure 17.5. The non-complementary DNA strand is not binding specifically to the DNA probes on the surface and thus should not change the signal significantly. This experiment was repeated several times with contradictory results and

the graph shown in Figure 17.5 represents a single experiment with the expected results. There are several possible reasons for this non reproducibility, namely the functionalization procedure that cannot be precisely controlled. Moreover, with the current procedure the DNA probes are immobilized on the natural silicon oxide present on SiNW, which may shield the effect of the charges redistribution during binding. Furthermore, the entire bottom of the channel is covered with silicon oxide thus APTES functionalization results in the probe immobilization on the entire surface. This may affect the sensitivity of the sensing, as binding will take place not only on the nanowire surface. APTES functionalization is an old method of modifying silicon oxide surfaces that is now being replaced by more reliable methods of direct modification of the silicon surface. Silicon oxide layer is much thinner on the nanowire, so by applying short etching time only silicon wire gets exposed and thus the functionalization takes place on the active area of the sensor.

To ensure that the binding between the probe and the target DNA is specific we validated the results by fluorescence microscopy. We used DNA strands that were fluorescently labeled for proper results visualization. The results are shown in Figure 17.6. The pictures show a device channel across which a nanowire was present. As the entire surface of the channel is covered with silicon oxide the probes are immobilized everywhere. This should not create severe problems during electrical sensing as the nanowires only react to changes in their vicinity. However, it may affect the sensitivity. After immobilization of DNA probe labeled with FITC the green fluorescence appears. It is not changed significantly after incubation with non-complementary DNA labeled with Cy3. A slight change in colour was visi-

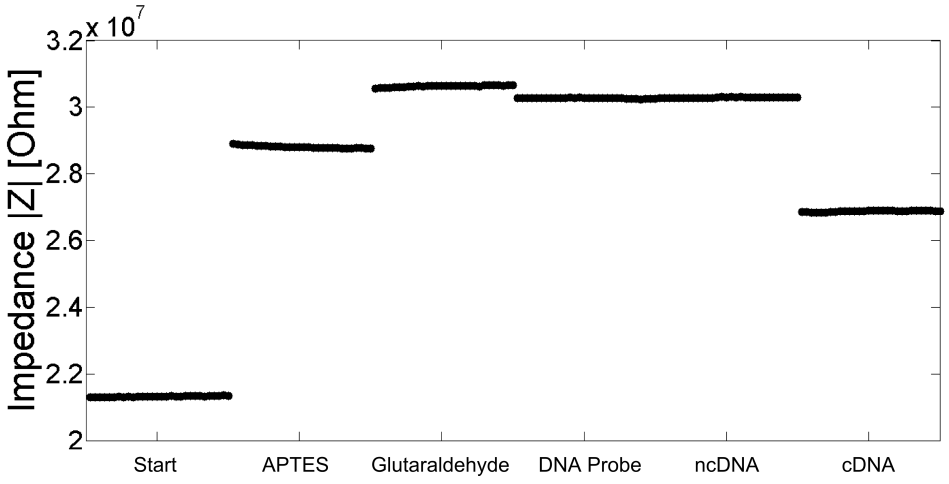

Figure 17.5: A typical graph from the impedance measurements on the SiNW chip with measurements performed at each step of the procedure. The most important step is the change in impedance observed after complementary DNA hybridisation, while no change is observed for the non-complementary strand.

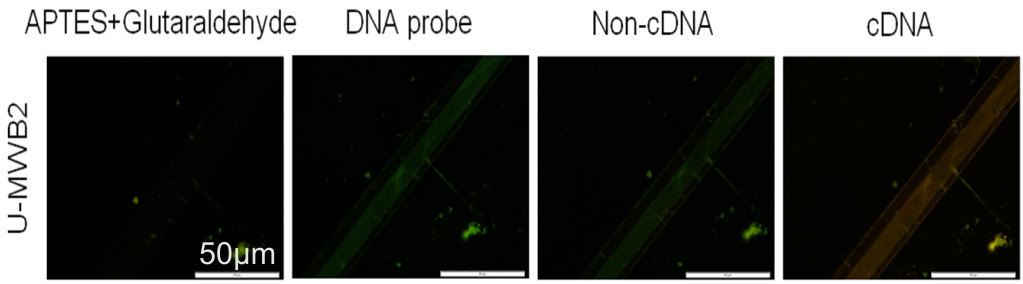

Figure 17.6: Fluorescent pictures of the immobilization and hybridisation procedure. In the pictures the microfluidic channel is visible across which nanowires were present. As the entire surface of the channel was covered with silicon oxide it was used for visualization of the functionalization and binding procedure. The DNA probe was labelled with FITC and the non-complementary and complementary DNA with Cy3. After immobilization of the probe the green fluorescence appears and does not change after incubation with the non-complementary DNA. After incubation with the complementary DNA the fluorescence changes to yellow-orange due to binding of the target DNA with Cy3. *Courtesy of Kasper Bayer Frøhling.*

ble due to a minimal amount of unspecific binding. After subsequent incubation with complementary DNA a colour change to yellow/orange is observed. This is a result of a specific binding between a probe and Cy3 labeled complementary DNA.

17.4.2 Detection Limit

To further characterize the SiNW sensor we tested its sensitivity using increasing concentrations of complementary target DNA. The measured response of the nanowire is shown in Figure 17.7. The columns with a standard deviation show a gradual decrease in the resistance of the nanowire during addition of increasing concentration of a target DNA.

Initially we measured the baseline signal, which is the nanowire modified with the DNA probes. Subsequently, we started adding increasing concentrations of the target DNA and observed a decrease of the nanowire resistance, which is in agreement with the p-doping. The resistance was dropping gradually with the addition of higher concentrations of the target DNA. We have not observed the saturation point, which may indicate that the DNA probes have not been completely occupied. These experiment has been repeated several times with satisfactory results. However, the resistance decrease was different for each tested wire due to their size difference.

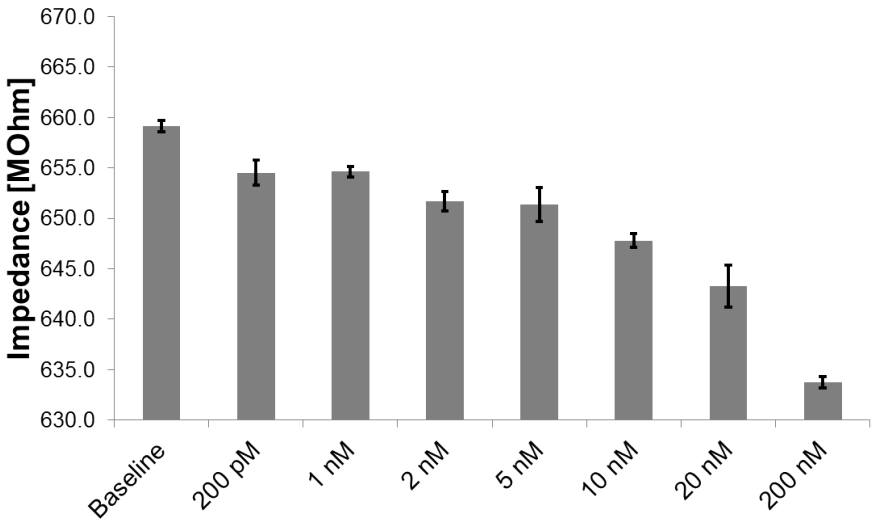

Figure 17.7: The sensitivity of the nanowire was tested by adding increasing concentration of the target DNA.

17.4.3 Translocation Detection

The SiNWs were intended for detection of chromosome translocation. To achieve a double hybridisation assay a denaturation step is needed. To remove the target DNA from first chip and transfer it to another we wanted to use heat by placing the chip on a hot plate. The parameters for thermal denaturation of the target DNA were optimized in the experiments described in Part IV. As explained earlier, for the translocation detection the double hybridisation assay was used. A schematic explanation of the experimental setup is shown in Figure 17.8. The

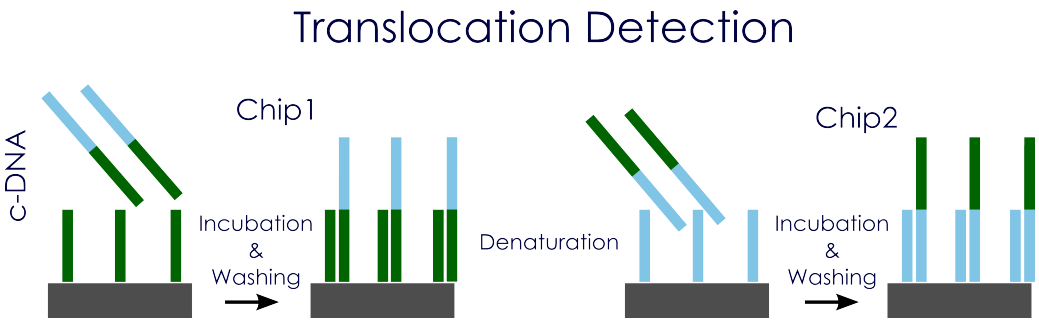

Figure 17.8: Schematic of a double hybridisation assay on silicon nanowires. For the experiment two chips were used with Chip1 covered with 9.3 probes and Chip2 with 9.9 probes. After incubation with a DNA fragment complementary to the probes on Chip1, the captured fragment was released and incubated with the probes on Chip2.

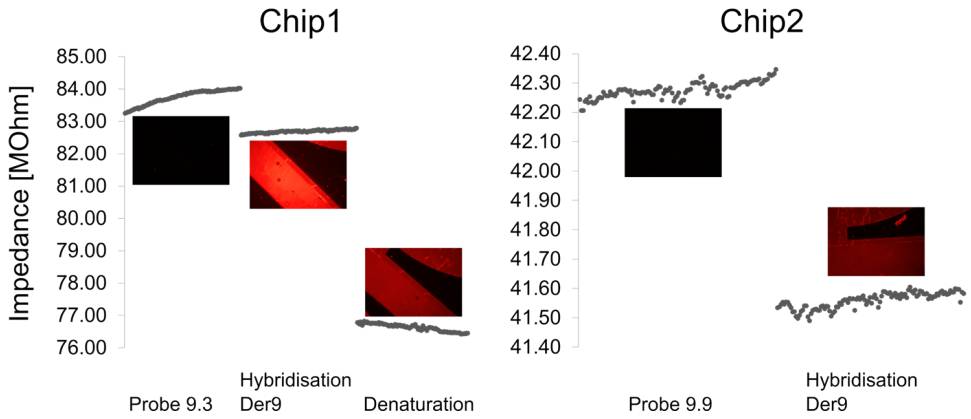

Figure 17.9: The translocation detection was performed on two separate chips. Probes 9.3 were immobilized on Chip1, while Chip2 had probes 9.9. The impedance was measured on both chips first with just the probes. After hybridisation with Der9 on Chip1 the impedance dropped. After heat treatment the released DNA was transferred to Chip2 on which the impedance also dropped after the hybridisation. The process was also followed by fluorescence. Initially there was no fluorescence signal observed as the probes were not labeled. After the hybridisation with Cy3 labeled red fluorescence appeared on Chip1, with the increase intensity after denaturation. The released DNA gave rise to fluorescence signal after incubation on Chip2.

DNA probes immobilized on two separate chips were matching both sequences on a target DNA strand. Chip1 was covered with probes 9.3 and Chip2 with probes 9.9. After a positive hybridisation on the Chip1, it was placed on a hot plate at 95 °C for 10 min. The denatured DNA was transferred manually by pipetting to Chip2 and incubated for hybridisation to take place. The results of the experiment are shown in Figure 17.9. At the beginning of the experiment a baseline with immobilized probes was recorded on Chip1 and Chip2. The subsequent decrease in the nanowire resistance occurs after incubation with a target DNA strand. Following the denaturation the resistance decreases further. The denatured DNA was transferred to Chip2 and again the resistance dropped. The same procedure was performed using fluorescently labeled DNA target to validate the impedance measurements. Initially there is now fluorescence observed on both Chip1 and Chip2 as the immobilized probe was not labeled. After hybridisation with the DNA target labeled with Cy3 the bright red fluorescence appears on Chip1, which decreases after denaturation. The released fragment binds to the probes on Chip2 as the red fluorescence appears.

This experiment was performed as a proof of principle for detection of chromosome translocations represented by a short DNA strand. Both of the immobilized probes were matching the target DNA, thus they were expected to bind it specifically. The decrease in the resistance of the nanowire is in agreement with the previously

obtained results. The additional decrease of the resistance after denaturation of the DNA probably comes from the heat treatment of the nanowires. The positive response of both chips indicates the presence of the translocation. However, all the controls need to be carefully prepared and performed to validate the specificity of the observed decrease in resistance.

17.4.4 Denaturation of the Target

Another approach tested for denaturation of the target DNA was to pass a DC voltage through the nanowire. In this experiment the SiNWs were fabricated using a mask for structuring the nanowires in the photolithography. The graph in Figure 17.10 shows the experimental results from a single experiment with appli-

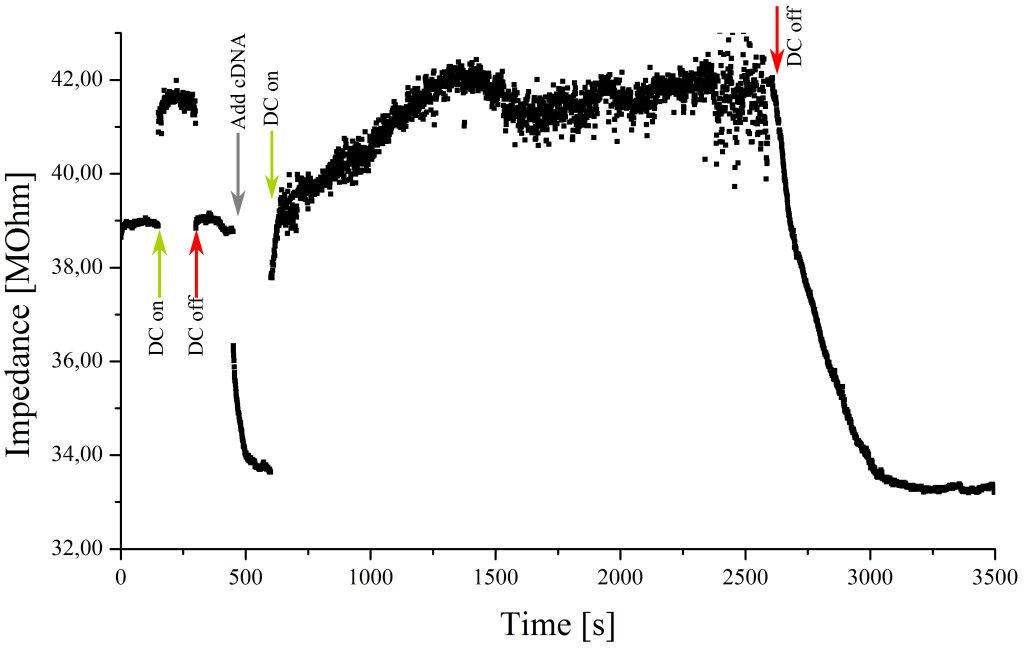

Figure 17.10: Measurements performed with a DC on (green arrows) and DC off (red arrows) for denaturation of the captured DNA. At time 0 the DNA probe has been immobilized on the nanowire and the resistance was measured without a DC offset. At 150 s the DC offset at -1 V was turned on and the measurements continued until 300 s when DC was turned off again. At 450 s the complementary DNA was added to the nanowire and the drop in resistance due to hybridisation was observed. After the signal stabilized at 33.5 MOhm at 600 s the DC was turned on again and the resistance increased to 42 MOhm. After about 30 min the DC was turned off and the signal gradually decrease due to rehybridisation of the target DNA.

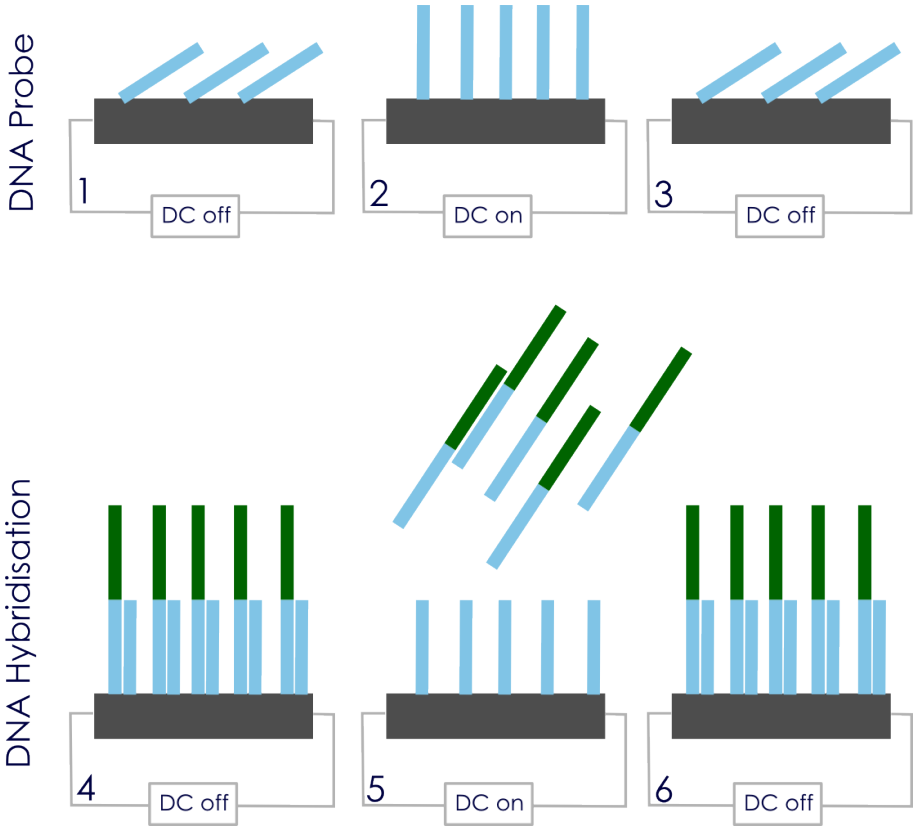

Figure 17.11: The DNA orientation changes due to the applied DC offset and DNA hybridisation. Initially, with a DC offset at 0 V the single stranded is very flexible (1) and is repelled by the applied negative potential (2). With a DC off the DNA probe reorientates on the surface (3). The hybridisation with a complementary DNA results in a rigid duplex formation (4), which is disturbed due to the applied -1 V with the denaturation of the target DNA (5). When the potential is back at 0 V the rehybridisation occurs with a formation of the rigid duplex structure (6).

cation of sinusoidal signal with an amplitude of 0.1 V at a frequency of 1 Hz with a DC offset at -1 V. The measurements started after overnight immobilization of the DNA probe with a recorded resistance around 39 MOhm. After application of a DC offset of -1 V the resistance of the nanowire increases to roughly 42 MOhm. When the DC was turned off the resistance went back to the level after the probe immobilisation. At 450 s 1 µM complementary DNA was added to the nanowire and the resistance drop was monitored over time. Once the signal stabilized the DC offset at -1 V was turned on and the resistance increase to 42 MOhm was observed. When the offset was turned off the resistance dropped down again to around 33 MOhm, which is almost the same as the resistance level after hybridisation.

This experiment was conducted to determine whether it is possible to recover the surface of the silicon nanowire surface by applying a negative potential. Figure 17.11 illustrates the correlation of the applied DC offset with the DNA orientation on the surface of the nanowire. The immobilization of the probe on the nanowire is realized by covalent bonds, which is a strong and stable bond. The single stranded DNA is a flexible molecule, thus it is leaning towards the surface of the nanowire (Figure 17.111 and 3). In such an orientation the negative charges are closer to the nanowire surface and thus the resistance can have a lower value. The application of -1 V DC offset should not destroy the probe layer due to the covalent attachment. However, as the DNA is negatively charged it will be repelled from the surface (Figure 17.112). After DNA hybridisation the double stranded DNA duplex is formed, which is more rigid (Figure 17.114). After application of a DC offset at -1 V the DNA target gets denatured and repelled from the surface as the hydrogen bonds forming the DNA double strand are not strong enough (Figure 17.115). After the DC is turned off the rehybridisation occurs resulting again in the formation of a rigid structure(Figure 17.116).

The performed experiment is a proof of principle for this event. To ensure the specificity of the recorded signal a DC offset was applied to the nanowire after the immobilisation of the probe. The observed increase in resistance is attributed to the repulsion of the DNA probes from the surface. The DNA probes are flexible structures but the repulsion forces them to stand straight. After addition of the target DNA the resistance dropped as expected due to increased amount of negative charges in the nanowire vicinity. The applied DC offset results in the resistance increase to the level of the probe. The denaturation of the DNA requires some time thus the observed slow increase in the resistance. The resistance increase to the same level as after the probe immobilization indicates the denaturation of the DNA target, with only DNA probes remaining on the surface. When the DC offset was turned off the resistance gradually drops down to the previous value. It can be explained by rehybridisation of the previously denatured DNA.

We showed that it is possible to denature the target DNA by passing a DC voltage through the nanowire. Furthermore, we demonstrated the renewal of the sensor by denaturing only the target DNA without deactivating the biorecognition layer. This approach is easy and fast, however it needs to be optimized for a better control of the procedure.

17.5 Conclusions to Silicon Nanowires as BioFETs

In this chapter the work with silicon nanowires as DNA hybridisation sensors was presented. In most of the experiments the silicon nanowires fabricated in a fast and simple way were used. We have shown that they can be used as DNA hy-

bridisation sensors and we tested the detection limit to be 200 pM on one of the nanowires. As a proof of principle we demonstrated that the detection of chromosome translocation is possible on two independent SiNW chips. Furthermore, we tested the reusability of the sensors by applying a DC offset at -1 V to the nanowire to denature the target DNA. The obtained results are promising, but needs to be repeated to ensure reproducibility.

18. Faradaic Electrochemical Detection of DNA Hybridisation on Gold Electrodes

Electrochemical sensors are widely used in the biosensors field. They offer relatively fast response with a low cost equipment requirement. They are able to transform a chemical reaction or a recognition event into an electric signal. There are various electrochemical techniques that can be used for sensing of the biorecognition event such as potentiometry, amperometry or electrochemical impedance spectroscopy (EIS) (Park and Park, 2009).

Potentiometric sensors measure the potential of a solution between two electrodes. The potential is then translated to a concentration of one of the analytes present in the solution. The most common potentiometric sensor is a pH meter with ion selective electrodes. Amperometric sensors are used to measure the current resulting from an electrochemical reaction at the electrode surface, while keeping the potential constant. In this case the biorecognition element does not need to be electroactive itself but in presence of the analyte the reaction is initiated consuming or producing electroactive species. The most well known example of an amperometric sensor is a glucose blood concentration meter. It uses metallic electrodes with immobilized glucose oxidase (GOD). Glucose present in the blood sample is consumed by GOD to form gluconic acid. GOD uses oxygen for the reaction to proceed and depletion in oxygen concentration can be detected. Based on the measured oxygen concentration the glucose level in blood is given (Clark and Lyons, 1962).

Electrochemical impedance spectroscopy is a powerful technique that can measure the complex changes in the resistance of a system. Impedimetric sensors are very sensitive to the changes on the electrode surface, thus it is well suited for measuring the recognition events. They have high-sensitivity and can be completely label-free. These sensors are widely used in the biosensing field with applications ranging from antibody-antigen recognition (Guan et al., 2004), monitoring of cell growth and infection (Kiilerich-Pedersen et al., 2011), DNA hybridisation sensing (Park and Park, 2009). The main focus of this Chapter is on electrochemical impedance sensors so the theory behind technique will be thoroughly described in Section 18.1.

18.1 Theory

The electrochemical impedance spectroscopy is an expansion of a basic theory of electrical resistance of the system. The electrical system can resist the flow of

electric current and this ability is described by the Ohm's law.

$$I = \frac{E}{R} \tag{18.1}$$

where E = voltage, I = current, R = resistance

This equation is true only for an ideal resistor that is independent of the frequency of the signal, and follows Ohm's law at any voltage and current, and AC voltage and current are in phase. Such a simplification is not true for most of the electrical systems, as they contain more complex elements. To accommodate for these we use a more general term of impedance Z. The impedance Z is a complex electrical property consisting of a real part, the resistance R, and an imaginary part, the reactance X (Lingenfert et al., 2007). To measure electrochemical impedance the sinusoidal AC potential is applied to the electrochemical cell and the current is measured (Bonanni and del Valle, 2010). Electrochemical impedance is normally measured using a small excitation signal to ensure a pseudo-linear response. In this way the current response will be sinusoidal but shifted in phase.

The excitation signal as a function of time, has a form of

$$E_t = E_0 sin(\omega t) \tag{18.2}$$

where E_t is the potential at time t, E_0 is the amplitude of the signal, $\omega = 2\pi f$ is the radial frequency

The current response in such a system would be shifted in phase ϕ

$$I_t = I_0 sin(\omega t + \phi) \tag{18.3}$$

Thus a form of Ohm's law including the complex system would be

$$Z = \frac{E_0 sin(\omega t)}{I_0 sin(\omega t + \phi)} = Z_0 \frac{sin(\omega t)}{sin(\omega t + \phi)} \tag{18.4}$$

From this we can say that the system's impedance is characterized by two values Z_0 magnitude and ϕ phase shift (Bonanni and del Valle, 2010).

The impedance can also be presented as a complex number.

$$Z = Z_0(cos\phi + jsin\phi) \tag{18.5}$$

The EIS is normally measured at a range of frequencies. The absolute impedance ($|Z|$) or the phase shift of the system can be plotted versus the log of the frequencies range (Bode Plot). Alternatively, the real part of the impedance (Z') is

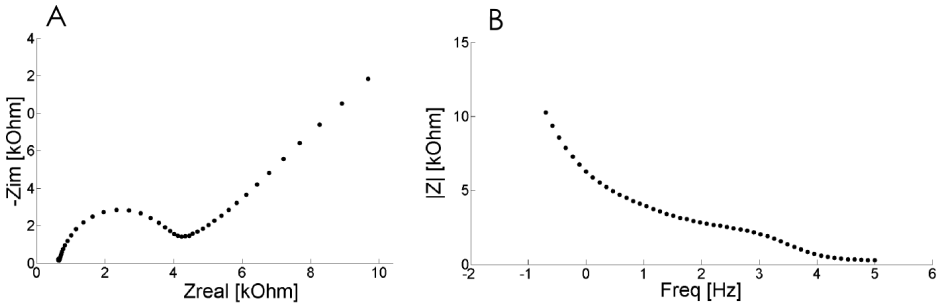

Figure 18.1: Typical EIS plots - a Nyquist plot on the left (A) and a Bode Modulus plot on the right (B).

plotted versus the imaginary part (-Z") in a form of a Nyquist plot (Bonanni and del Valle, 2010). The frequency information is hidden in the Nyquist plot with high frequencies on the left close to the origin and low frequencies on the right. The typical EIS plots are shown in Figure 18.1A and B, Nyquist and Bode Modulus plot respectively. For DNA hybridisation most commonly the Nyquist plot is used for the data representation.

The EIS data are often fitted to analogous equivalent electrical circuits for better understanding of the reaction. For most of the analyzed data it is enough to use the simple elements such as resistors, capacitors and inductors. The most common equivalent electrical circuit is a Randles circuit (Figure 18.2). It consists of a solution resistance (R_{Sol}) connected in series with the parallel combination of the constant phase element (CPE) and charge transfer resistance (R_{CT}) and Warburg (W) resistance (the two latter connected in series) (Daniels and Pourmand, 2007). For fitting data to equivalent circuits the solution resistance between the working electrode and counter/reference electrode needs to be considered. The R_{Sol} depends on the concentration of ions in the solution, temperature, and the electrode geometry (Daniels and Pourmand, 2007). For the microelectrodes the connections to the potentiostat often contribute to R_{Sol}. The resistance of the solution is connected in series as the signal goes through the electrolyte to reach the electrodes. To describe the behaviour of the coating on the electrodes the parallel combination of resistors and capacitors is used as they both contribute to the charge transfer reaction. A capacitor is formed when two conductive media such as electrode and electrolyte are separated by a non-conducting layer (Daniels and Pourmand, 2007). This is often the case when working with biosensors, as the electrode surface is covered by biomolecules. In the measurements there are often deviations from an ideal capacitor, which would be represented by a perfect semi-circle. To allow for more appropriate fitting of those imperfect semi-circles a constant phase element is used (Daniels and Pourmand, 2007). Many theories have been proposed to explain this non-ideal behaviour but none is universally accepted. Often, the capacitor element is exchanged for an empirical value α to omit the discussion

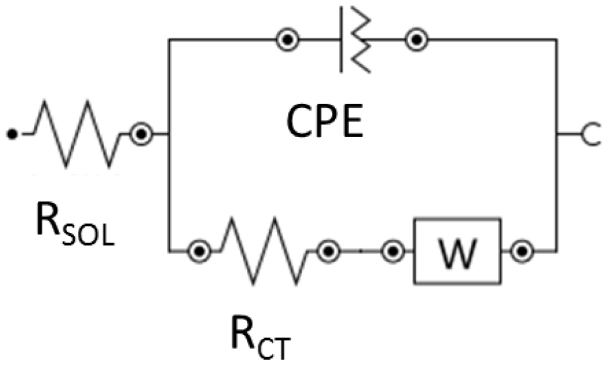

Figure 18.2: Randles circuit with a constant phase element.

on the physical basis of the observed behaviour. The R_{CT} occurs due to charge transfer from the electrons exchanged between the metal electrode and ions in the electrolyte. Once the surface of the electrode is blocked by biomolecules it changes the charge transfer resistance (Daniels and Pourmand, 2007). The Warburg resistance occurs due to diffusion of ions from and to the electrode surface. At high frequencies the ions do not move far thus the Warburg impedance at high f is small. Contrary, at low frequencies the ions diffuse further thus increasing the Warburg resistance (Daniels and Pourmand, 2007). The Warburg resistance is shown on a Nyquist plot as a straight diagonal line at 45 deg to the X axis in a low frequency region on the right. DNA hybridisation sensing is best described using the Randles circuit as a model. In case of faradaic measurements including a ferro/ferricyanide as a mediator it is most convenient to monitor changes in R_{CT} (Park and Park, 2009). For a non-faradaic measurements (no mediator) the changes in the double layer capacitance are most pronounced.

18.2 Chip Design and Fabrication

The chips used in these experiments were designed by Maria Dimaki for a European Project 'ExCell'. The chip is 22 x 22 mm composed of 12 individually addressable sets of electrodes. The electrodes' set consists of a round counter electrode (CE) (diameter 750 µm), two interdigitated electrodes (IDE) as a working electrode (WE) with a finger size and spacing of 10 µm, and a round reference electrode (RE) (diameter 50 µm) (see insert in Figure 18.3B). The chips are fabricated on a silicon wafer with gold electrodes and wiring that are passivated with silicon nitride to expose only the active area of the electrodes and the contact pads. The detailed fabrication procedure is presented in Appendix C. Briefly, the silicon wafers were passivated with 500-670 nm of silicon oxide. Afterwards the electrodes were structured by a negative photolithography step in AZ resist. Be-

fore the deposition of 10 nm of Titanium (Ti) and 150 nm of Gold (Au) the wafers were dipped in Buffered Hydrofluoric acid (BHF) to create 120 nm cavities for the metal. Following the lift-off, the chips were passivated with 500 nm of silicon nitride deposited using Plasma-Enhanced Chemical Vapor Deposition (PECVD). Subsequently, a second photolithography step was performed to create a pattern on the passivation layer. In the following etching process using RIE the exposed silicon nitride was etched away opening the active electrodes area and the contact pads. The resist was removed in an acetone sonication bath followed by MilliQ and Isopropanol wash. After dicing, the chips were ready for use in DNA hybridisation sensing experiments. For these experiments a custom made holder was micromilled in PMMA and a printed circuit board (PCB) was fabricated (Figure 18.3A). The picture of the entire wafer after completed fabrication process is shown in Figure 18.3B.

18.3 Electrodes Functionalization

The functionalization of a gold surface is often performed by self-assembly of thiol modified molecules. Before modification and the electrochemical measurements the chips were cleaned following a procedure described by Fischer and others (Fischer et al., 2009). Briefly, the chips were cleaned for 10 minutes in a mixture containing 25% H_2O_2 and 50 mM potassium hydroxide (KOH). After washing in MilliQ and drying, they were mounted in a measurement holder and a Linear Sweep Voltammetry (LSV) was performed in 50 mM KOH at 50 mV/s scan rate from -200 mV to -1200 mV. The cleaning performance was studied by cyclic voltammetry (CV) and electrochemical impedance spectroscopy measurements before and after each cleaning step in potassium ferro/ferricyanide 10 mM

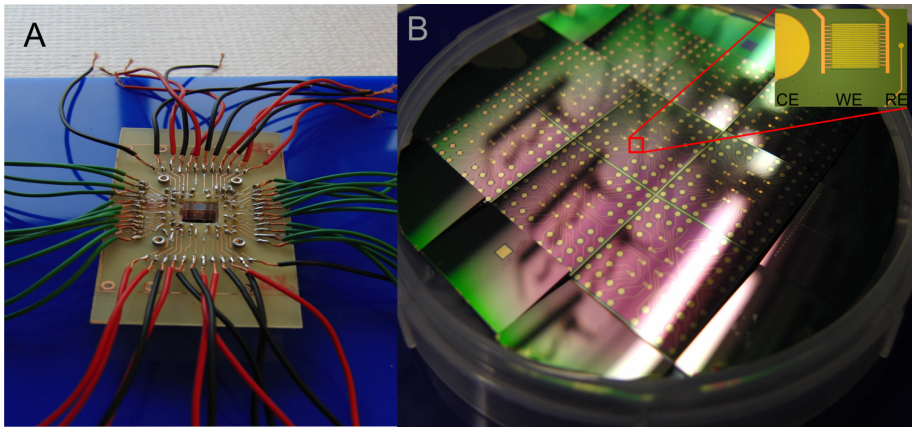

Figure 18.3: A) Single electrode chip inserted in a holder for interfacing with potentiostat, B) Electrodes chip on a wafer.

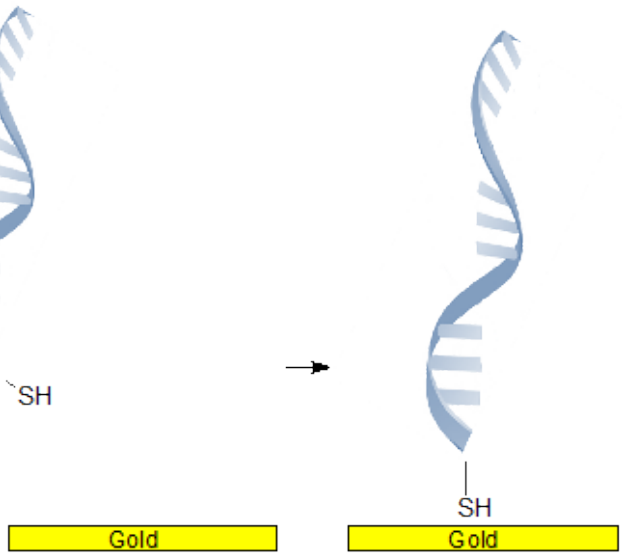

Figure 18.4: Functionalization of gold electrodes by self-assembly of thiolated DNA probes.

each in PBS. The EIS spectra was recorded from 1 MHz or 100 kHz to 200 mHz at amplitude of 10 mV vs open circuit potential. CVs were recorded at 100 mV/s scan rate from -0.5 to 0.5 V. All electrochemical procedures were performed with Autolab potentiostat PGSTAT302N (Metrohm, Utrecht, the Netherlands). After the chips' cleaning, they were modified by overnight incubation in a humidity chamber with a 1 µM thiol modified DNA probe in PBS (Figure 18.4). This was followed by washing in PBS. Subsequently a 1 µM non-complementary DNA solution in PBS was incubated for 15 minutes on the chip, followed by another washing step. After taking EIS measurements, a 1 µM complementary DNA solution in PBS was incubated for 15 minutes and washed. The DNA strands used in this project are listed in Table 18.1. For easier understanding of the matching probes with complementary DNA used in the experiments we created a colour coded scheme shown in Figure 18.5. For detection of the chromosome translocation the double hybridisation assay was used with two chips functionalized with probes matching the two chromosome sequences in a derivative chromosome. The target DNA captured on one chip was denatured at 95 °C and transferred to the second chip and incubated.

Table 18.1: DNA samples used in the project for detection of chromosome translocation. Der9 is complementary to probes 9.9 and 9.3; Der3 is complementary to probes 3.3 and 3.9. Nor9 is a normal chromosome 9 fragment complementary to probes 9.9 and 3.9. Nor3 is a normal chromosome 3 fragment complementary to probes 3.3 and 9.3.

Name	Sequence
Probe 9.9	sequence 5'-CCA ACA CCA ATT GTA TCC CG-C6-SH-3'
Probe 9.3	sequence 5'-SH-C6-TAA AAG CTA TTT TTA AAA GT-3'
Der9	5'-CGG GAT ACA ATT GGT GTT GGA CTT TTA AAA ATA GCT TTT A-3'
Nor9	5'-CGG GAT ACA ATT GGT GTT GGG TGT TTG TCA GGG AGG TTT T-3'
Probe 3.3	sequence 5'-TGT ACA TTT TCT TAT ATT CT-C6-SH-3'
Probe 3.9	sequence 5'-SH-C6-ACA ATT TAG AAA ACA GGA CA-3'
Der3	5'-AGA ATA TAA GAA AAT GTA CAT GTC CTG TTT TCT AAA TTG T-3'
Nor3	5'-AGA ATA TAA GAA AAT GTA CAT TAA CTT TTA AAA ATA GCT T-3'

18.4 Results and Discussion

18.4.1 Electrodes Cleaning

Initially, the cleaning procedure and the performance of the Excell electrodes as DNA hybridisation sensor were validated. The CV and EIS were recorded before and after each cleaning step and the results are shown in Figure 18.6. In both graphs there is an observed change in the signal at each step of the cleaning process. Initially the CV performed in ferro/ferricyanide does not have well resolved oxidation and reduction peaks. However, after each step the peaks get sharper and closer to each other. In case of the impedance spectra the results of a cleaning procedure are shown as a Nyquist plot. At the beginning the semi circle diameter is large with a diameter around 35 kOhm. After the first cleaning step the semi circle decreases with a final value of 5.5 kOhm after the second cleaning step.

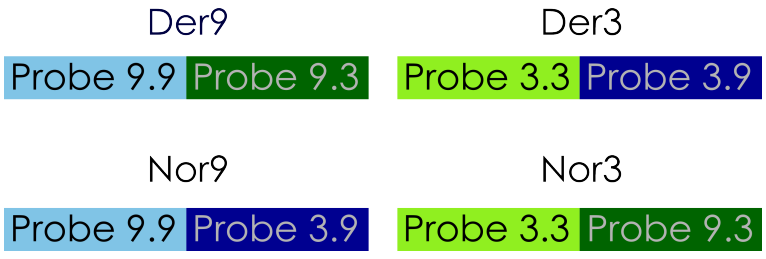

Figure 18.5: Schematics of DNA samples representing the derivative chromosome 9 (Der9), the derivative chromosome 3 (Der3), normal chromosome 9 (Nor9) and normal chromosome 3 (Nor3). The colors of the strands correspond to the colors in Table 18.1.

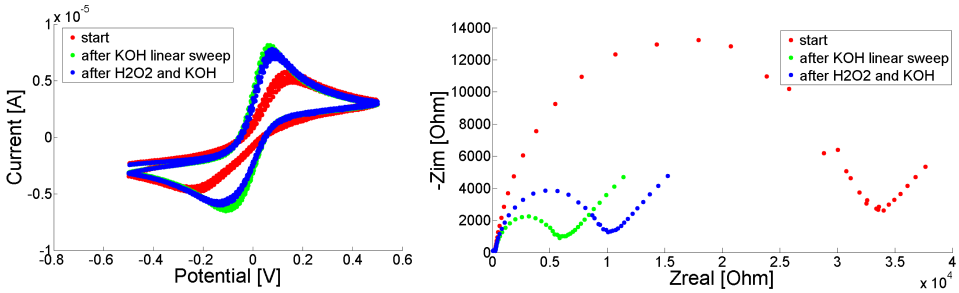

Figure 18.6: The monitoring of electrodes cleaning was done by CV (left) and EIS (right).

The quality of a gold surface can have a great influence on the performance of an electrochemical sensor. Both the CV and EIS response depend on the composition of the gold surface. The gold surface of the chips after being out of the clean room environment is subjected to various contaminants that may have an effect on the immobilization of thiol molecules. The cleaning removes any residues that may be present on the electrode surface. At the first step the gold electrode surface is oxidized, which is subsequently reduced by the potential sweep in KOH. The Figure 18.6 clearly shows that the cleaning is necessary to achieve the best performance of a gold surface. One of the measures of the gold cleanliness is to look at the semi circle diameter, which indicates the electron transfer resistance between the redox couple in the solution and the electrode surface. Thus, the cleaner the electrode, the easier is the electron transfer which is indicated by a smaller semi circle diameter. Another way of measuring the state of the electrode is by analysing the oxidation and reduction peaks in cyclic voltammetry. Ideally the peaks after the second cleaning step should be well refined and not too separated as shown in Figure 18.6 left. After a properly conducted cleaning procedure all the electrodes are in the same condition at the beginning of the sensing process. After cleaning, the EIS spectra were recorded on 12 electrodes. Initially all the electrodes gave rise to almost identical semi-circle diameter, which is shown in Figure 18.7.

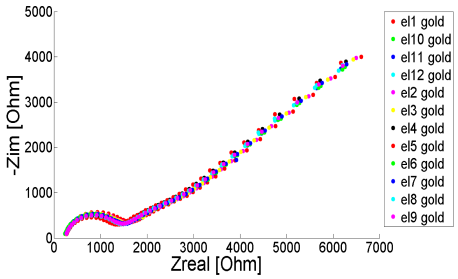

Figure 18.7: The reproducibility of all 12 electrodes on one chip represented as similar EIS spectra.

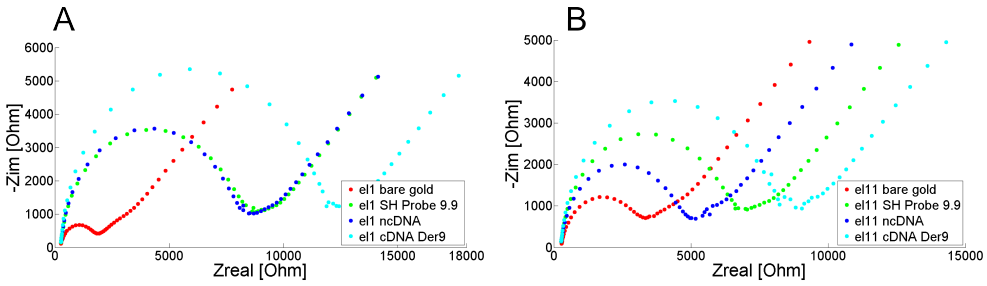

Figure 18.8: A typical Nyquist plot for a good (A) and bad (B) electrode representing each step of the DNA hybridisation sensing procedure. For a good electrode the semi circle diameter does not change significantly after incubation with non-complementary DNA (ncDNA).

18.4.2 DNA Hybridisation Sensing

After the electrodes were cleaned we started with the preparation of a DNA hybridisation sensor. The EIS was performed on all electrodes at each step of the procedure: *bare gold*, *DNA probe immobilization*, *control with a non-complementary DNA* and *incubation with a complementary DNA*. During the experiments there was always a fraction of the electrodes on a chip that performed better than the others. A typical Nyquist plot for a good electrode representing each step of the DNA hybridisation sensing procedure is shown in Figure 18.8A. The semi circle diameter increases after immobilization of the DNA probe. The incubation with a non-complementary DNA should not change the semi-circle diameter significantly. After the hybridisation with a complementary DNA strand the duplex is formed which causes an increase in the charge transfer resistance. Some of the tested electrodes behaved differently and a significant decrease in the semi-circle diameter was seen after incubation with a non-complementary DNA as shown in Figure 18.8B.

The immobilization of probes on the gold surface increased the R_{CT} for all tested electrodes. The R_{CT} values where obtained by fitting the obtained data to the equivalent circuit using a NOVA software from Autolab. The increase in R_{CT} values serves as an indication of a proper immobilization of thiolated DNA. Such a behaviour can be explained by the repulsion between the negatively charged DNA backbone and the redox label in the solution. After being covered with the probes the electrode surface is not easily accessible by the ions from the solution, which slows down the electron transfer. There was always an increase in R_{CT} observed on all electrodes as shown in Figure 18.9 representing the R_{CT} for each step normalized to the value of a bare gold (R_0). The data were normalized using the Equation (18.6).

$$\Delta R_{CT}X = \frac{R_{CT}X - R_0}{R_{CT}X} * 100\% \tag{18.6}$$

Figure 18.9: Relative change of charge transfer resistance after immobilization of the probe on the electrode surface. Error bars show standard deviation for the measurements of 24 electrodes on 2 chips.

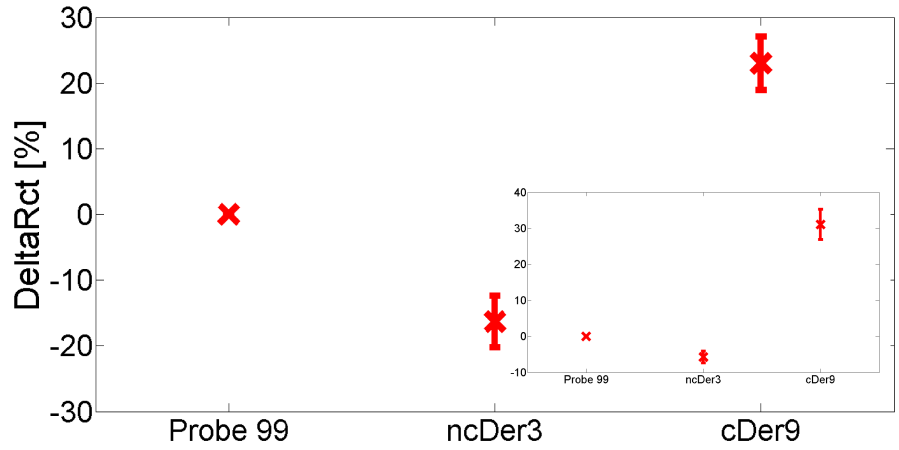

Figure 18.10: Relative change of charge transfer resistance for each step of biosensing procedure normalized to the probe value. Error bars show standard deviation for the measurements of 12 electrodes on 1 chip.

The relatively large standard deviation indicates the difference in the surface coverage. This difference arises from the overnight self-assembly process between the thiolated probes and gold surface that proceeds without any control.

The incubation with a non-complementary DNA followed by a washing step was not expected to change the semi-circle diameter significantly as the interaction is not specific. This was true for some electrodes as shown in Figure 18.8A. How-

ever, for some of the tested electrodes the R_{CT} was decreasing as is shown in Figure 18.8B. A possible explanation for such behaviour is the insufficient cleaning of the gold surface. The thiolated probes bind loosely to such a surface and can be displaced after several washing steps performed during the procedure. After incubation of the non-complementary DNA followed by washing, a fraction of the thiolated probes are removed exposing the underlying gold. This allows a better charge transfer between the solution and the electrode, which is shown by a decreased semi circle diameter. After the hybridisation with a complementary DNA strand the duplex is formed, which results in a double amount of negative charge on the electrode surface, which in turn increases the charge transfer resistance. This increase was observed on most of the electrodes due to the specific interactions between the probes and the target. This was also observed on the electrodes that performed worse after incubation with the non-complementary DNA. The DNA probes remaining on the electrode surface can still interact with the target DNA and thus the semi circle diameter increase is observed.

As explained earlier the tested electrodes can vary in the surface coverage of the thiolated probes. As a result some of the electrodes are covered more thoroughly by the probes as compared to others. However, for the sensor performance the most

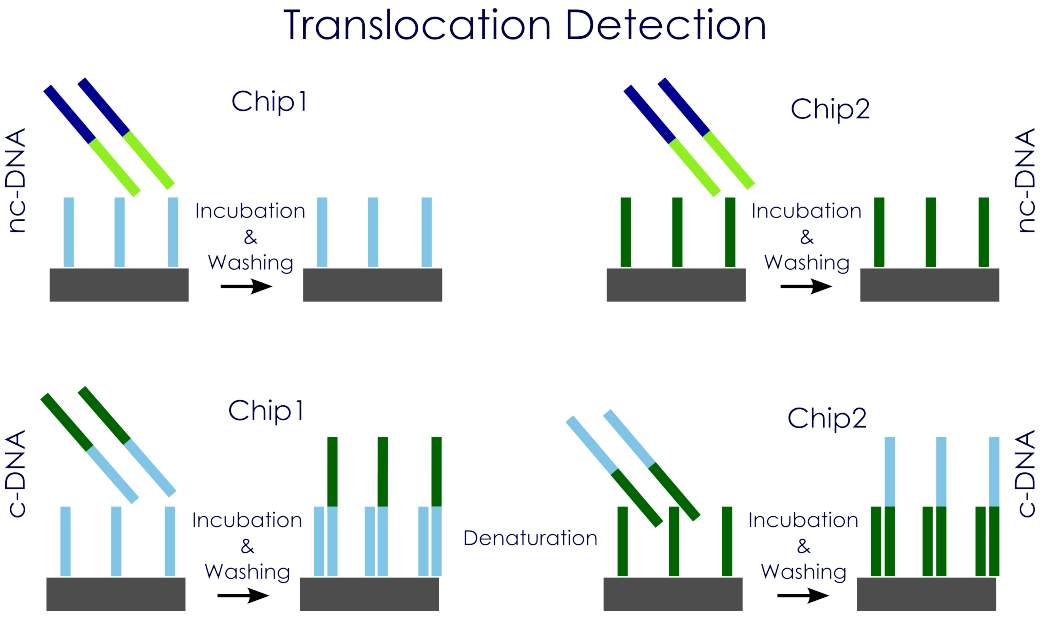

Figure 18.11: Schematic of a double hybridisation assay on Excell electrodes for translocation detection. Two chips were used with Chip1 covered with 9.9 probes and Chip2 with 9.3 probes. The first step was a control with a non-complementary strand that should not bind to the probes. After incubation with a DNA fragment complementary to the probes on Chip1, the captured fragment was released and incubated with the probes on Chip2. The colors correspond to the schematic shown in Figure 18.5.

important is the change in the charge transfer resistance between the probe and the complementary DNA. The result of charge transfer resistance analysis is shown in Figure 18.10. The graph represents the relative change of charge transfer resistance at each step normalized to the probe R_{CT} value (used as R_0 in Eq. (18.6)) for all 12 electrodes. Each data point is represented by an average difference of semi-circle diameters with error bars. For the sensor specificity the negative control was prepared by incubation of the electrodes with a non-complementary DNA. There is a decrease in the R_{CT} at this step which may indicate the removal of some probes from the electrode surface. After the sensor was incubated with a fully complementary DNA we observed an increase in the R_{CT} by 25 %. Due to hybridisation the electrode surface is covered with a double amount of negative charges, which cause a stronger repulsion of the ferro/ferricyanide ions in the solution. The plotted graph represents the data for all 12 electrodes, however in most of the experiments only a fraction of the electrodes worked well. The insert in Figure 18.10 represents the change in R_{CT} for the six selected electrodes that performed well in the experiment. In the case of these electrodes, the decrease in

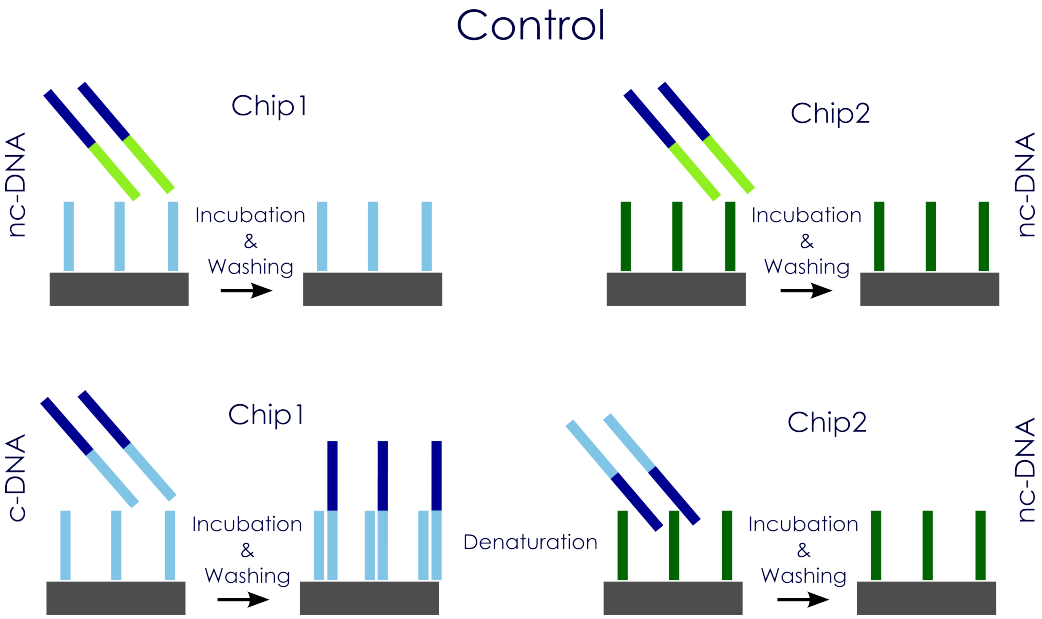

Figure 18.12: Schematic of a double hybridisation assay on Excell electrodes for the control experiment. Two chips were used with Chip1 covered with 9.9 probes and Chip2 with 9.3 probes. The first step was a control with a non-complementary strand that should not bind to the probes. After incubation with a DNA fragment complementary to the probes on Chip1, the captured fragment was released and incubated with the probes on Chip2. The hybridisation was done with a Nor9 fragment that was not complementary to probes 9.3 on Chip2 so no change in signal was expected. The colors correspond to the schematic shown in Figure 18.5.

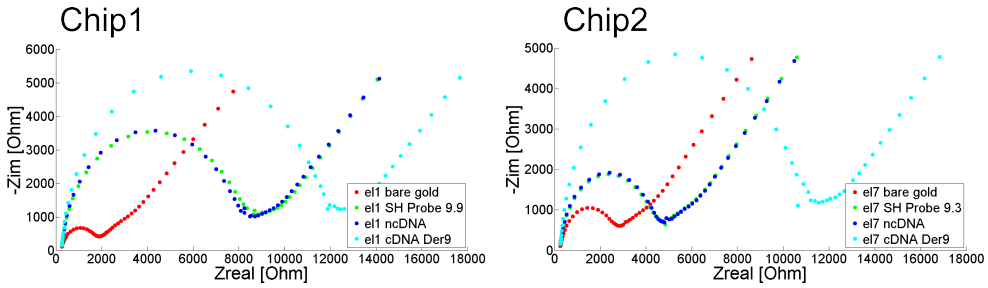

Figure 18.13: Chromosome Translocation Detection - Nyquist plot - EIS measurements on bare gold (red), Chip 1 SH-DNA 9.9 probe modified electrodes (green), Chip 2 SH-DNA 9.3 probe modified electrodes (green) after non-complementary DNA target hybridisation (dark blue) and after Der 9 complementary DNA hybridisation (light blue). The captured Der9 was denatured for 10 min at 95 °C and transferred manually from Chip1 to Chip2.

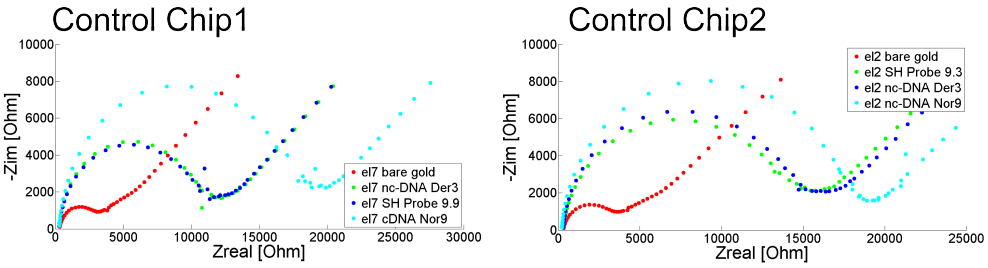

Figure 18.14: Control of chromosome translocation detection on Excell electrodes. EIS measurements on bare gold (red), Chip 1 SH-DNA 9.9 probe modified electrodes (green), Chip 2 SH-DNA 9.3 probe modified electrodes (green) after non-complementary DNA target hybridisation (dark blue) and after hybridisation of Normal 9 (Nor9) chromosome, which is a complementary DNA (light blue). The captured Nor9 was denatured for 10 min at 95 °C and transferred manually from Chip1 to Chip2. After incubation no change was expected as the DNA sequence of Nor9 is non-complementary to probe 9.3.

R_{CT} after incubation with the non-complementary DNA is less significant, while the increase after hybridisation with the complementary DNA is much more pronounced.

18.4.3 Translocation Detection

The concept of chromosome translocation detection is based on the fact that derivative chromosomes have sequence coming from two distinct chromosomes. As described in Part IV in the experiments we were using a synthetic oligonucleotide strand that acts as a 40 bp representative of the chromosome translocation. It contains a real sequence with 20 bp coming from chromosome 3 sequence and the other 20 bp from chromosome 9. As previously, we applied the double hybridisa-

tion assay on two independent electrodes' chips. The schematic of the detection principle is shown in Figure 18.12. Chip1 was covered with probes 9.9 targeting chromosome 9 sequence and Chip2 had probes 9.3 specific for chromosome 3. The experiments were done using Derivative 9 (Der9) sequence and as a control a Normal Chromosome 9 (Nor9) sequence. After the hybridisation on Chip1 the captured target DNA was released by heat denaturation and transferred to Chip2 for the second hybridisation step. For each step of the biosensor development we recorded the EIS spectra. For each chip a part of the procedure was a control with a non-complementary DNA (nc-DNA) strand to ensure the specificity of the biosensor. The experimental results on selected electrodes are shown in Figure 18.13 and Figure 18.14. As previously described the DNA hybridisation sensing worked as expected on both Chip1 and Chip2 in Figure 18.13. Immobilization of the probes induced an increase in R_{CT}, which remains almost unchanged after a control with the non-complementary DNA. Subsequent hybridisation with the complementary DNA caused a significant increase in the semi-circle diameter on Chip1. The target DNA was further released and transferred to Chip2. Again an increase in R_{CT} was observed, which was initially understood as a specific detection of the chromosome translocation.

We prepared a control experiment to ensure that the hybridisation event could be detected in a real patient sample. The hybridisation with a normal chromosome fragment was expected to occur only on Control Chip1. Control Chip2 was covered with the DNA probe 9.3, which is non-complementary to normal 9 chromosome. As previously, the DNA hybridisation sensing was satisfactory on Control Chip1. However, after heat denaturation of the captured DNA and its transfer to Control Chip2 a significant increase in the R_{CT} was seen. Such a behaviour was unexpected as no specific binding between the target and the probe was possible due to non-complementarity. This result can be explained by the instability of the self-assembled thiol layers at elevated temperatures (Herdt et al., 2006). During denaturation, the chips were treated for 10 minutes at 95 °C which could cause the release of the thiolated probes from the surface together with the bound target DNA. Transfer of such a solution to the other chip can result in reassembly of the thiols on the gold surface. As the gold surface is covered more tightly with the thiolated probes it repels the ferro/ferricyanide ions more effectively.

To minimize the risk of the thiols removal the denaturation conditions should be optimized. Alternatively, a second hybridisation should be performed on Chip1 using the probe 9.3 sequence but without the thiol modification as shown in Figure 18.15. After the second hybridisation another increase in the amount of negative charges on the surface would occur. This approach would be the most elegant and eliminate the requirement for heat denaturation. The presented results show the importance of a well planned procedure with the necessary controls thought through. Due to limited time the optimization of the denaturation conditions was not possible. The proposed alternative chromosome translocation detection was

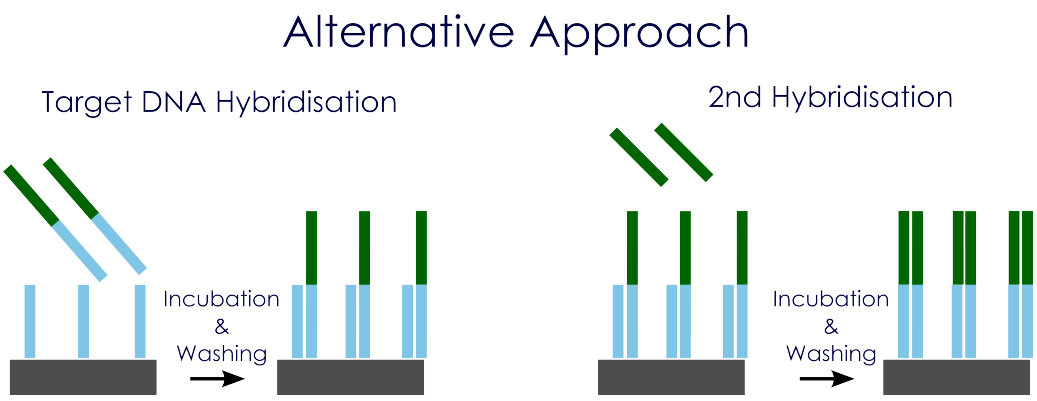

Figure 18.15: The alternative approach towards detection of chromosome translocation only involves one chip. After hybridisation of the DNA target containing translocation the flanking 20 bp is targeted by a matching probe. The measurement signal should change for each hybridisation step if the translocation is present. The colors correspond to the schematic shown in Figure 18.5.

initiated but could not be continued due to problems with the DNA hybridisation sensing.

18.5 Conclusions to Faradaic Electrochemical Detection Using Gold Electrodes

In this Chapter the use of gold electrodes for electrochemical detection of DNA hybridisation was described. We have fabricated a reliable electrodes' sensor that consists of 12 electrodes' sets with 3 electrode setup. The electrodes were thoroughly cleaned before use to ensure reproducible results on all 12 electrodes. The DNA hybridisation sensing procedure always involved incubation of the chip with immobilized probes with non-complementary DNA. Incorporating such a control in each measurement allows for determination of specificity of the obtained signal. Once we confirmed that the electrodes can be used for DNA hybridisation detection we proceeded towards the double hybridisation assay for chromosome translocation detection. We observed an increase in charge transfer resistance on both test chips, but a similar increase was observed on a control chip. We concluded that the denaturation procedure needs to be optimized to ensure the stability of the thiolated probes on the gold electrodes. A new approach towards detection of the translocation was proposed in which the heat denaturation step is omitted. The measurement uncertainties observed during the work with Excell electrodes are included in Appendix D.

19. Non-Faradaic Electrochemical Detection of DNA Hybridisation Using PEDOT Electrodes

This chapter is based on a work performed together with PhD student Johannes Daprá from Polymer Microsystems for Medical Diagnostics group at DTU Nanotech.

Polymers are thoroughly used as a substrate for microfluidic devices. However, their application as the electrode material is limited. Metal electrodes are used as standard material for electronic sensing units because they are well characterized, sensitive, specific and biocompatible towards various biological species. However, their high cost is often a limiting factor for their wide application. Conductive polymers such as polypyrrole (PPY) or poly(3,4-ethylenedioxythiophene) (PEDOT) can be used for covering the metallic electrodes to improve the ion selectivity or can be used directly as the electrodes' material (Balamurugan and Chen, 2007; Dapra et al., 2012; Kiilerich-Pedersen et al., 2011; Sasso et al., 2012). Over the years, their use has been proposed in many applications such as nanowire integration or biomedical sensors (Dapra et al., 2012). One of their advantages is the lower cost of the raw materials and typically inexpensive fabrication. Although they can be structured by standard cleanroom process they are often produced manually outside the cleanroom for reduced costs. However, one needs to remember that the cleanroom fabrication is done on a wafer scale with high reproducibility. When devices are fabricated manually their quality may vary from batch to batch. These limitations can be overlooked when working in laboratory settings for research purposes but once the device is entering the market some solutions for high scale production need to be employed.

In this part of the project PEDOT electrodes were used as sensors for non-faradaic electrochemical impedance spectroscopy measurements. The work included here is based on a manual fabrication of PEDOT electrodes by agarose stamping. The DNA hybridisation sensing is performed in a buffer solution without any mediator used. Such non-faradaic measurements represent a truly label-free sensor that can find its use in point-of-care field.

19.1 Chip Design and Fabrication

The purpose of this part of my work was to fabricate an inexpensive, easy to fabricate, disposable DNA hybridisation sensor. The chips were fabricated in 5 cm

diameter Topas® slides, which were prepared by injection moulding. The bottom disc was unstructured and used for electrodes fabrication, while the top disc consisted of 12 Luer connections, for interconnecting the chip to the peripheral equipment. The unstructured bottom disc was spin coated with a bilayer consisting of tosylate doped poly (3,4-ethylenedioxythiophene) (PEDOT:TsO) and the hydroxymethyl functionalized PEDOT-OH:TsO. A reactive mixture containing 107 mg (0.2 mmol) $Fe^{(III)}$tosylate, 6 µL (0.07 mmol) pyridine and 0.08 mmol of the monomer 3,4-ethylenedioxythiophene (EDOT) or ((2,3-dihydrothieno[3,4-*b*][1,4]dioxin-2-yl)methanol) (EDOT-OH), respectively in 280 µL *n*-butanol were thoroughly mixed, filtered through a 0.4 µm syringe filter and spun on the Topas® disc with 1000 rpm for 60 s. The polymerisation inhibitor pyridine was removed by evaporation on a 70 °C hotplate for ca. 5 minutes. A change in colour from yellow to blue/green indicates the formation of the conductive polymer. Excess reactants and by-products were removed by rinsing with de-ionised water; after drying the disc the second polymer layer was applied in the same way.

The microelectrode fabrication method was done by manual agarose stamping (Dapra et al., 2012; Hansen et al., 2007; Lind et al., 2012). It produces relatively reproducible chips with similar characteristics. During the stamping process the PEDOT layer spun on a Topas® substrate is exposed to hypochlorite solution, which dissolves the PEDOT layer. The agarose stamp was prepared by casting the 10 % (w/w) agarose/water gel over a silicon stamp with a 70 µm tall interdigitated wire pattern. Both wire width and spacing were 20 µm. The negative agarose stamp was then soaked in 1.5 % (w/v) sodium hypochlorite in water solution containing 0.1 % TritonX100 for 10 minutes, dried to remove the excess liquid and pressed together with the PEDOT covered Topas® disc. By applying a constant pressure for 1 minute the structures corresponding to cavities in the agarose stamp were formed. The PEDOT that was in direct contact with the agarose stamp was over-

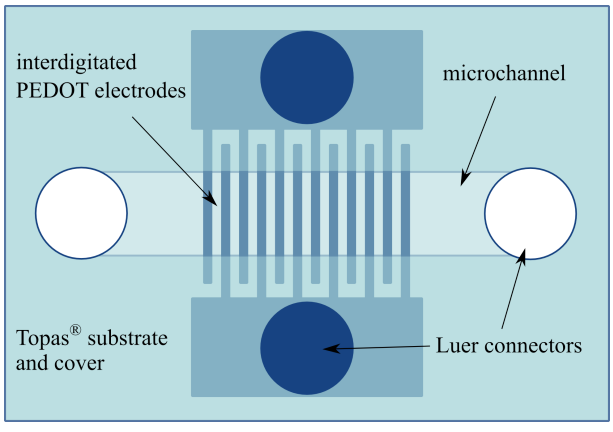

Figure 19.1: Schematic drawing of the assembled microfluidic chip with interdigitated PEDOT electrodes (blue). Measures are not to scale.

Table 19.1: DNA-sequences used in our experiments with their respective modifications or fluorescent labels. Mismatch bases are printed in red colour.

Name	Sequence
Probe	5' TCC ACT ATG GCC TCC ACC AT 3'–NH_2
cDNA	5' ATG GTG GAG GCC ATA GTG GA 3'–Cy3
Mismatch	5' ATG CTG GAT GCC GTA GTG GA 3'–FITC

oxidized by hypochlorite solution and removed by rinsing with MilliQ water. By performing the process manually some chips are over or underexposed and thus cannot be used for measurements. Conductivity was increased by re-doping the polymer by immersion in a 4 % (w/v) $Fe^{(III)}$tosylate/water solution.

The thus prepared Topas® disc is bonded with an injection moulded cover disc using a 150 µm thick sheet of transfer adhesive (ARcare 90106, Adhesive Research Ireland). Channels were cut into the transfer adhesive by laser ablation prior to assembly. All components were bonded with a force of 500 N at 75 °C for 5 minutes. A schematic drawing of the chip is shown in Figure 19.1.

19.2 Electrodes Functionalization

Functionalization of the electrodes was a two-step process. First, an ester was formed between the hydroxyl moiety of the polymer and one carboxylic acid group of succinic acid. Then, the amine-modified DNA probe was grafted onto the second acid group of succinic acid via an amide bond. The first reaction was carried out in 0.1 M MES buffer (2-(*N*-morpholino)ethanesulfonic acid) containing 50 mM 1-ethyl-3-(3-dimethylaminopropyl)carbodiimide (EDC) as coupling agent and 50 mM succinic anhydride. The reaction time was 30 minutes at ambient temperature. For the formation of the amide bond immobilised succinic acid was first activated using 50 mM EDC and 40 mM *N*-hydroxy succinimide (NHS) in MES buffer for 10–15 minutes. After rinsing with MES buffer 3'-amino-oligonucleotide (100 nM in MES) was added and incubated for 3 h. Hybridisation was done with 100 nM DNA in 2× SSC with 0.2 % Tween20 for 30 minutes at room temperature. We tested the specificity of the DNA probe by incubation with both fully complementary DNA strand and 3 base pair mismatch (Table 19.1). For the determination of the concentration dependence hybridisation buffer containing increasing concentrations of DNA was filled into the channels. After the impedance signal had stabilised, the next higher concentration was injected.

Both tested strands were labeled with a different fluorophore, which was used to asses the immobilisation specificity of the probe and to monitor possible unspecific binding of DNA to electrodes or substrate. Fluorescence of FITC and Cy3 labels was measured with a confocal laser scanning microscope (LSM 5 Pascal, Zeiss,

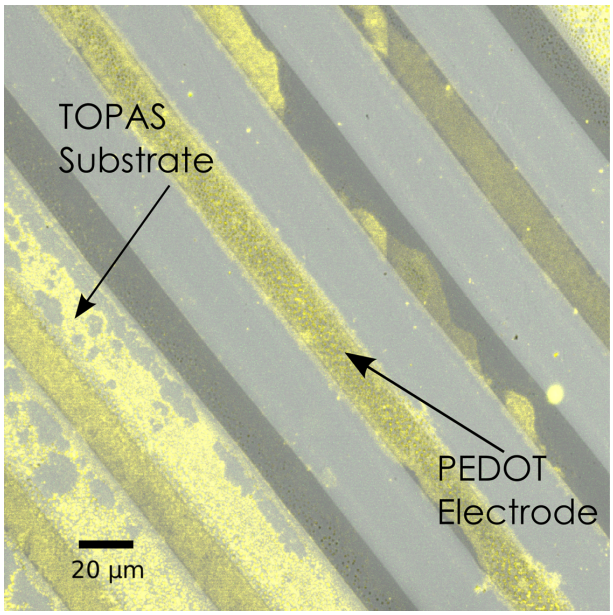

Figure 19.2: Fluorescence picture of conductive polymer electrodes with Cy3-labeled DNA bound to the immobilized probes. In the left corner the unspecific binding to Topas® substrate can be seen.

Germany) with Ar- (488 nm) or HeNe-laser (543 nm) excitation and a 505 nm or 560 nm low pass filter, respectively.

For electrochemical impedance spectroscopy two different instruments were used: A VersaSTAT 3 (Princeton Applied Research, USA) was used for single frequency scans at 501 mHz; all experiments involving only one concentration were carried out with this instrument. The measurement of the concentration dependence was done using a Zahner IM6 potentiostat (Zahner Elektrik, Germany). Wide spectrum sweeps in a frequency range from 100 kHz to 200 mHz (logarithmic scale with 10 points per decade for frequencies < 66 Hz and 4 points per decade for frequencies > 66 Hz) were recorded.

19.3 Results and Discussion

19.3.1 DNA Hybridisation Validation

The visualization of DNA hybridisation was done using the fluorescently labeled oligonucleotides and investigation with a confocal laser scanning microscope. The DNA probe had no label, however the complementary target was tagged with Cy3 to enable visualization. Fig 19.2 illustrates the successful immobilization of DNA on the electrodes. A small amount of undesirable unspecific binding to the

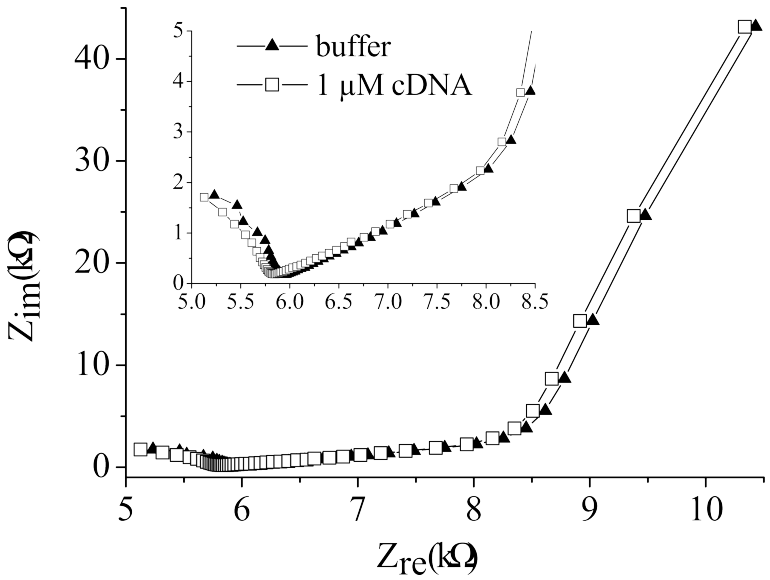

Figure 19.3: Nyquist plot of two impedance spectra before (triangles) and after (squares) injection of complementary DNA. The inset shows the high frequency part of the spectra in detail.

Topas® polymer surface is also visible. Control experiments using the mismatch strand or non-functionalized electrodes revealed that neither unspecific physisorption nor binding of the mismatch strand occurred to a significant degree (data not shown).

As can be seen in the lower left corner of the image, a small portion of fluorescent DNA was detected between the electrodes. This is most likely due to incomplete removal of over-oxidised PEDOT during the fabrication of the electrodes. As for now the fabrication of the electrodes is done manually with a visual inspection of resolved microelectrodes. To make sure that the remaining over-oxidized PEDOT is non conductive we check with a multimeter that there is no connection between the two electrodes. Even though this remainder of the polymer is non-conductive and should not disturb the measurements it can still be functionalized with the DNA probes. Hence, the sensitivity of the device might be diminished due to target DNA binding to insensitive surfaces. A solution for this problem would be to optimise the fabrication protocol.

19.3.2 DNA Hybridisation Sensing

In Figure 19.3 the Nyquist plot from a typical experiment is shown. A small change in the real part of the impedance is visible after addition of a complementary DNA strand. The signal is shifted to the lower values in the entire frequency range, while the imaginary part changed only slightly in the high frequency region (insert in

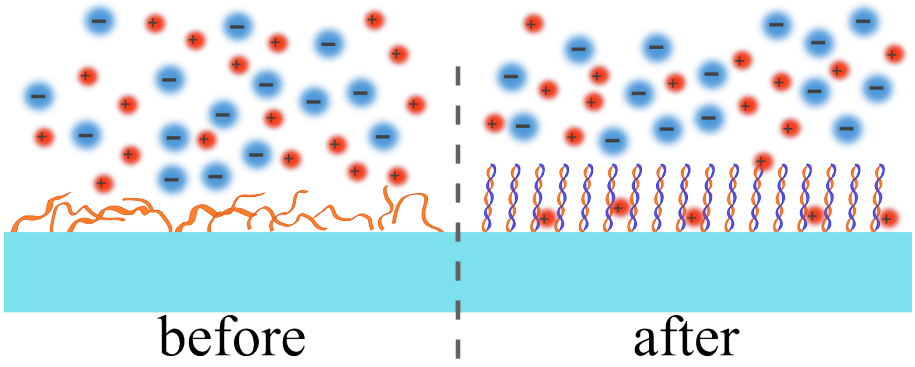

Figure 19.4: Schematic drawing of the possible surface model suggesting a reduced charge transfer resistance caused by conformational changes of the immobilised DNA due to hybridisation.

Fig 19.3).

In a number of studies involving sensing of DNA hybridisation using EIS a redox pair such as ferro/ferricyanide are added for detection (Ben-Yoav et al., 2012; Berdat et al., 2007; Wu et al., 2013; Wu and Yang, 2013). The same approach was applied in the previously described experiments with gold electrodes when such a mediator was used for better visualization of hybridisation. It is used for

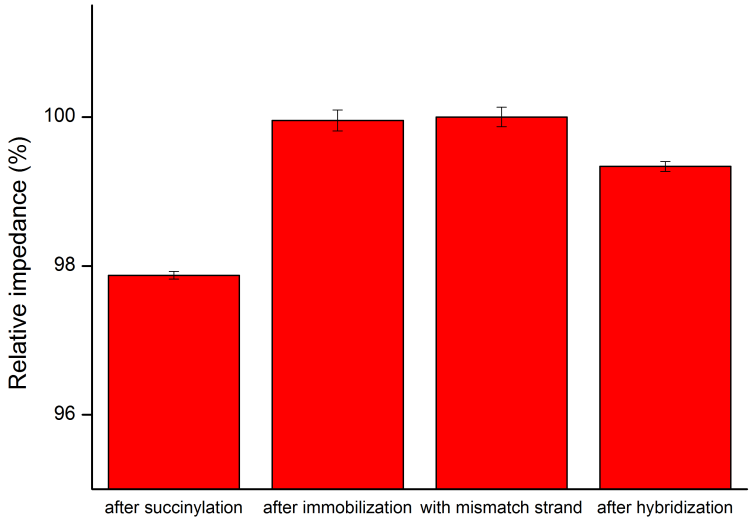

Figure 19.5: Comparison of impedance values measured at 501 mHz with succinylated electrodes, with immobilised DNA probe, after addition of mismatch strand and after hybridisation with complementary DNA. Error bars show standard deviation of 10 measurements performed at each concentration on the same chip.

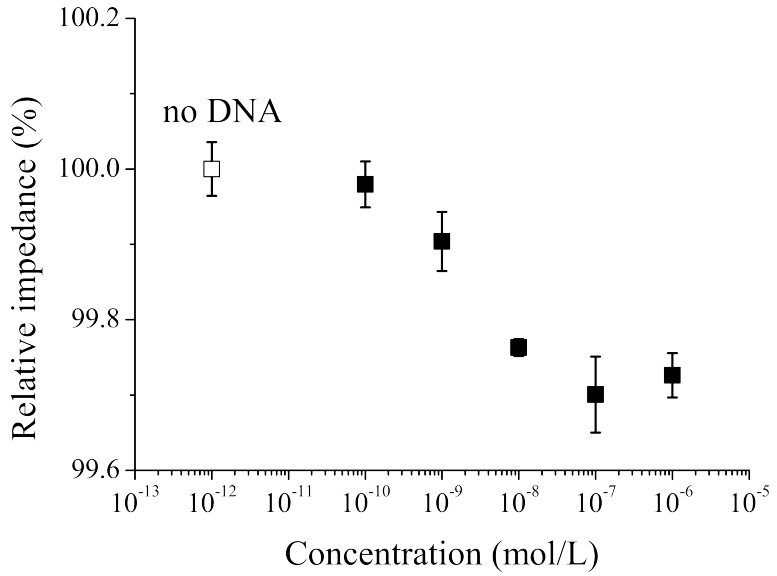

Figure 19.6: Impedance values measured at 356 mHz for a concentration series from 100 pM to 1 µM complementary DNA. The first value (squares) represents the impedance level before addition of DNA. Errorbars show standard deviation.

faradaic measurements as it enhances the signal. In those experiments it was found that DNA immobilization causes stronger repulsion of the negatively charged ferro/ferricyanide ions due to the anionic DNA on the surface, resulting in an increased charge transfer resistance. In an impedance spectrum – displayed as Nyquist plot – this leads to an increase of the diameter of the characteristic semi-circle. The semi-circle diameter increases further after addition of the complementary DNA strand. Contrary to this, in the experiments on PEDOT electrodes the impedance decreased after DNA hybridisation.

To understand these findings we suggest a model as illustrated in Fig. 19.4. After immobilization the single stranded DNA probes cover most of the electrode surface, thus reducing the area available for charge transfer. When the immobilised DNA hybridises with complementary strands α-helices are formed, which are more rigid and require less space therefore expose more of the electrode surface. It is reasonable to suppose that this effect could cause a reduction of the charge transfer resistance and might therefore lead to the decrease of the absolute impedance as observed in the spectra.

The model is also corroborated by the comparison of impedance measured before and after immobilisation of the DNA probe (see Fig. 19.5). Without the DNA probe the surface of the electrodes could interact with ions from the solution, thus the impedance was lower. The immobilisation of probes created an insulating layer, blocking the surface as described above. The addition of a mismatched

strand did not affect the signal significantly, while cDNA reduced it markedly. This proves the specificity of the biosensor.

19.3.3 Detection Limit

The detection limits of the sensor were assessed by recording impedance spectra continuously while increasing the DNA concentration in the channel after the signal stabilised. Starting at a concentration as low as 100 pM and increasing it logarithmically until 1 µM we were able to obtain the calibration curve presented in Fig. 19.6. The first concentration (100 pM) was already enough to cause a statistically significant (p=0.04) impedance decrease. Increasing the concentration lead to a fairly linear decrease of impedance in the logarithmic plot. The highest concentration tested (1 µM) did not result in a further signal decrease, so it can be assumed that the sensor was saturated at this point.

19.4 Conclusions to Non-Faradaic Electrochemical Detection Using PEDOT Electrodes

In this chapter an all-polymer biosensor for electrochemical detection of DNA hybridisation was described. The microelectrodes were fabricated manually in a conductive polymer PEDOT. The fabrication process was fast, easy and relatively reliable for fast prototyping. We tested the device for DNA hybridisation with a complementary DNA, which caused a decrease in an absolute impedance. In contrast, addition of a DNA strand with 3 bp mismatch did not cause any significant change in the impedance signal. Furthermore, the device detection limit was tested to be in the picomolar concentration range. As opposed to the previously described work with Excell electrodes, no electro-active additives were used to mediate detection and the microelectrodes were fabricated entirely in conductive polymer.

20. Conclusions Label-free Sensors

In this Part of the thesis the label-free sensing was shortly introduced. Three different platforms were used for detection of DNA hybridisation sensing. They were all based on electrical detection using various transducers such as silicon nanowires, metallic and conductive polymer electrodes. They are all simple to operate and use relatively inexpensive peripheral equipment that could be miniaturized in the future. The complete label-free approach was investigated on the silicon nanowires and PEDOT electrodes, while we used a mediator for experiments with metallic electrodes. The ideal approach would be to eliminate the need for the mediator, but it might compromise the reliability of the sensor. All sensors were used for successful detection of the hybridisation event. SiNW and gold electrodes were further tested for chromosome translocation detection. Although the change in the signal was observed it is important to perform all the necessary controls to ensure the specificity of the observed signal. During the course of the project several issues arose and if possible were addressed. However, the time frame and the problems with the fabrication were often a limiting factor. Among the tested sensors the results were the most reproducible in case of the metallic gold electrodes used for faradaic EIS measurements. Also, this type of sensor was the simplest to integrate with the centrifugal microfluidic system, which is the topic described in Part VI.

Bibliography

Andersen, K.B.; Castillo-Leon, J.; Bakmand, T.; Svendsen, W.E., *Alignment and Use of Self-Assembled Peptide Nanotubes as Dry-Etching Mask*, Japanese Journal of Applied Åhysics, **51**, 13-.1-13.5 (2012)

Balamurugan, A.; Chen, S.M., *Poly(3,4-ethylenedioxythiophene-co-(5-amino-2 naphthalenesulfonic acid)) (PEDOT-PANS) film modified glassy carbon electrode for selective detection of dopamine in the presence of ascorbic acid and uric acid*, Analytica Chimica Acta, **596**, 92-98 (2007)

Ben-Yoav, H.; Dykstra, P.H.; Bentley, W.E.; Ghodssi, R., *A microfluidics-based electrochemical biochip for label-free diffusion-restricted DNA hybridisation analysis*, Biosensors and Bioelectronics, **38**, 114-120 (2012)

Berdat, D.; Rodriguez, A.C.M.; Herrera, F.; Gijs, M.A.M., *Label-free detection of DNA with interdigitated micro-electrodes in a fluidic cell*, Lab on a Chip, **8**, 302-308 (2007)

Bonanni, A.; del Valle, M., *Use of nanomaterials for impedimetric DNA sensors: A review*, Analytica Chimica Acta, **678**, 7-17 (2010)

Chen, K.-I.; Lia, B.-R-; Chen, Y.-T., *Silicon nanowire field-effect transistor-based biosensors for biomedical diagnosis and cellular recording investigation*, Nanotoday, **6**, 131–154 (2011)

Chen, W.-Y.; Chen, H.-C.; Huang, C.-J.; Chan, H.W.-H.; Hu, W.-P., *Improved DNA detection by utilizing electrically neutral DNA probe in field-effect transistor measurements as evidenced by surface plasmon resonance imaging*, Biosensors and Bioelectronics, **41**, 795-801 (2013)

Clark, L.C.; Lyons, C., *Electrode systems for continuous monitoring in cardiovascular surgery*, Annals of the New York Academy of Sciences, **102**, 29-45 (1962)

Cosnier, S.; Mailley, P., *Recent advances in DNA sensors*, Analyst, **133**, 984-991 (2008)

Daniels, J.S.; Pourmand, N., *Label-Free Impedance Biosensors: Opportunities and Challenges*, Electroanalysis, **19**, 1239-1257 (2007)

Dapra, J.; Kiilerich-Pedersen, K.; Christiansen, N.O.; Poulsen, c.R.; Rozlosnik, N., *Chapter 5. in Nanomedicine in Diagnostics*, Edited by Rozlosnik, N., Science Publishers, ISBN 978-1-57808-738-9 (2012)

De, A.; van Nieuwkasteele, J.; Carlen, E.T.; van den Berg, A., *Integrated label-free silicon nanowire sensor arrays for (bio)chemical analysis*, Analyst, **138**, 3221-3229 (2013)

Drummond, T.G.; Hill, M.G.; Barton, J.K., *Electrochemical DNA sensors*, Nature Biotechnology, **21**, 1192-1199 (2003)

Fischer, L.M.; Tenje, M.; Heiskanen, A.R.; Masuda, N.; Castillo, J.; Bentien, A.; Emneus, J.; Jakobsen, M.H.; Boisen, A., *Gold cleaning methods for electrochemical detection applications*, Microelectronic Engineering, **86**, 1282-1285 (2009)

Gao, A.; Lu, N.; Dai, P.; Li, T.; Pei, H.; Gao, X.; Gong, Y.; Wang, Y.; Fan, C., *Silicon-nanowire-based CMOS-compatible field-effect trasistor nanosensor for ultrasensitive electrical detection of nucleic acids*, Nano Letters, **11**, 3974-3978 (2011)

Guan, J.-G.; Miao, Y.-Q.; Zhang, Q.-J., *Impedimetric Biosensors*, Journal of Bioscience and Bioengineering, **97**, 219-226 (2004)

Hahm,J.; Lieber, C,M., *Direct ultrasensitive electrical detection of DNA and DNA sequence variations using nanowire nanosensors*, Nano Letters, **4**, 51–54 (2004)

Hansen, T.S.; West, K.; Hassager, O.; Larsen, N.B., *Direct Fast Patterning of Conductive Polymers Using Agarose Stamping*, Advanced Materials, **19**, 3261-3265 (2007)

Herdt, A.R.; Drawz, S.M.; Kang, Y.; Taton, T.A., *DNA dissociation and degradation at gold nanoparticle surfaces*, Colloids and Surfaces B: Biointerfaces, **51**, 130-139 (2006)

Hunt, H.K.; Armani, A.M., *Label-free biological and chemical sensors*, Nanoscale, **2**, 1544-1559 (2010)

Kiilerich-Pedersen, K.; Poulsen, C.R.; Jain, T.; Rozlosnik, N., *Polymer based biosensor for rapid electrochemical detection of virus infection of human cells*, Biosensors and Bioelectronics, **28**, 386–392 (2011)

Larsen, M.B.; Andersen, K.B.; Svendsen, W.E.; Castillo-Leon, J., *Self-Assembled Peptide Nanotubes as an Etching Material for the Rapid Fabrication of Silicon Wires*, BioNanoScence, **1**, 31-37 (2011)

Li, Z.; Chen, Y.; Li, X.; Kamins, T.I.; Nauka, K.; Williams, R.S., *Sequence-specific label-free DNA sensors based on silicon nanowires*, Nano Letters, **4**, 245–247 (2004)

Lin, C.-H.; Hung, C.-H.; Hsiao, C.-Y.; Lin, H.-C.; Ko, F.-H.; Yang, Y.-S., *Polysilicon nanowire field-effect transistor for ultrasensitive and label-free detection of pathogenic avian influenza DNA*, Biosensors and Bioelectronics, **24**, 3019-3024 (2009)

Lind, J.U.; Acikgoz, C.; Daugaard, A.E.; Andresen, T.L.; Hvilsted, S.; Textor, M.; Larsen, N.B., *Micropatterning of Functional Conductive Polymers with Multiple Surface Chemistries in Register*, Langmuir, **28**, 6502-6511 (2012)

Lingerfelt, L.; Karlinsey, J.; Landers, J.; Guiseppi-Elie, A., *Impedimetric Detection for DNA Hybridization Within Microfluidic Biochips*, Methods in Molecular Biology, **385**, 103-120 (2007)

Mescher, M.; de Smet, L.C.P.M.; Sudholter, E.J.R.; Klootwijk, J.H., *Effect Transistors for Sensing Applications*, Journal of Nanoscience and Nanotechnology, **13**, 5649-5653 (2013)

Park, J.-Y.; Park, S.-M-, *DNA Hybridization sensors based on electrochemical impedance spectroscopy as a detection tool*, Sensors, **9**, 9513-9532 (2009)

Patolsky, F.; Zheng, G.; Hayden, O.; Lakadamyali, M.; Zhuang, X.; Lieber, C.M., *Electrical detection of single viruses*, Proceedings of the National Academy of Sciences of the United States of Americ, **101**, 14017–14022 (2004)

Sasso, L.; Vedarethinam, I.; Emneus, J.; Svendsen, W.E.; Castillo-Leon, J., *Self-assembled diphenylalanine nanowires for cellular studies and sensor applications*, Journal of Nanoscience and Nanotechnology, **12**, 3077-3083 (2012)

Shen, F.; Wang, J.; Xu, Z.; Wu, Y.; Chen, Q.; Li, X.; Jie, X.; Li, L.; Yao, M.; Guo, X.; Zhu, T., *Rapid Flu Diagnosis Using Silicon Nanowire Sensor*, Nano Letters, **12**, 3722-3730 (2012)

Teles, F.R.R.; Fonseca, L.P., *Trends in DNA biosensors*, Talanta, **77**, 606-623 (2008)

Wenga, G.; Jacques, E.; Sala, A.-C.; Rogel, R.; Pichon, L.; Geneste, F., *Step-gate polysilicon nanowires field effect transistor compatible with CMOS technology for label-free DNA biosensor*, Biosensors and Bioelectronics, **40**, 141-146 (2013)

Wu, N.-y.; Gao, W.; He, X.-l.; Chang, Z.; Xu, M.-t., *Direct electrochemical sensor for label-free DNA detection based on zero current potentiometry*, Biosensors and Bioelectronics, **39**, 210-214 (2013)

Wu, C.-C.; Yang, D.-Y., *A label-free impedimetric DNA sensing chip integrated with AC electroosmotic stirring*, Biosensors and Bioelectronics, **43**, 348-354 (2013)

Zhang, G.J.; Huang, M.J.; Luo, Z.H.; Tay, G.K.; Lim, E.J.; Liu, E.T.; Thomsen, J.S., *Highly sensitive and reversible silicon nanowire biosensor to study nuclear hormone receptor protein and response element DNA interactions*, Biosensors and Bioelectronics, **26**, 365–370 (2010)

Part VI

Integration of Lab-on-a-Disc with Label-free Sensing

21. Introduction

In this Part of the thesis a total integration of all the steps necessary for the novel detection of chromosome translocations is described. The centrifugal microfluidics system presented in Part IV was chosen for the final system. In the final system also the electrochemical sensor in the form of the gold electrodes described in Part V Chapter 18 was used. This work was partially performed by Sune Zoëga Andreasen during his Master's thesis project supervised by me in collaboration with Nanoprobes group at DTU Nanotech. This Part begins with a brief introduction and motivation for the total integrated system realization. Following, the setup considerations for the final version of the developed system are described. The experimental results from the testing of the setup are included afterwards. Finally, the results are discussed and summarized.

Lab-on-a-chip (LOC) devices are being continuously developed since the 1970s for miniaturization of various biological protocols. Although we experienced some impressive breakthroughs in the field, there is still a lack of available LOC devices on the market. Most of the bioanalyses are still performed in centralized facilities using expensive and bulky high-throughput equipment. The analysis process takes long time due to the need of transportation of the sample from the collection to the analysis point. Thus, LOC devices for point-of-care analysis would be beneficial to ensure shorter time and allow on site testing. From the point of commercialization and user-friendliness it is necessary to develop devices that are ready for use without the requirement of reassembling.

In the previous Parts the centrifugal microfluidics system and label-free sensors tested during the project were presented. They both were done as a development stage of an integrated device. Lab-on-a-disc platforms are advantageous in the liquid pumping mechanism (Gorkin et al., 2010; Madou and Kellogg, 1998). They allow fabrication of a complete device that does not require peripheral equipment for liquid propulsion. However, their main drawback is difficulty in integrating the electrical sensing. A major challenge is to enable electrical contact between a stationary peripheral equipment and a rotating disc. The incompatibility of the lab-on-a-disc platforms with wiring to the external equipment greatly limits their use for biosensing. So far, most of the examples of the sensors integrated on centrifugal microfluidic platforms are optical (Bosco et al., 2011; Chen et al., 2012; Navarro et al., 2013; Wang et al., 2013). As the electrical sensors are often the preferred choice due to their cost the main aim of this Part of the project was to build a setup for real-time measurements on a spinning disc.

22. Setup Considerations

Previous work presented in Part IV demonstrated the proof of concept of chromosome translocation detection on a centrifugal microfluidic platform. Based on those experiments the idea of the integration of a sensor into that platform has evolved. During integration, the design was based on this previously described lab-on-a-disc design with several channels consisting of two chambers on a disc. The metal electrodes used for electrochemical measurements described in Part V Chapter 18 were selected for the integration. One of the main tasks in developing the setup was to modify the electrodes design to fit the lab-on-a-disc design. As mentioned earlier the electrodes dimensions themselves were based on the gold electrodes used in label-free sensing part of the project.

The integration of electrical sensing on a rotating platform has been addressed in the past. The first example of such measurements was presented in 80s. (Cho et al., 1982). This work on detection of glucose presence in tested samples inspired the scientists working in lab-on-a-disc field. During the course of this project two recent articles on a similar topic have been published in Lab on a Chip journal (Abi-Samra et al., 2013; Kim et al., 2013). They describe work on electrical sensor integration on a spinning disc. However, the approach undertaken in this project targets a similar concept it differs from the others by the electrical connections used. The transfer of the electrical signal from the electrodes on a rotating disc to a stationary equipment is achieved by an electrical swivel, which characteristics are presented in the following section.

22.1 Electrical Swivel

Integration of electrical sensing on a spinning disc is intrinsically complex. During spinning any wires connected from the disc to a stationary equipment would get tangled and in the end break the connection. Different solutions to this problem were considered as the connection between the disc and the read out system (here a potentiostat) is the most crucial element of the setup. Three different solutions were proposed based on literature review:

1. Building a potentiostat system together with a signal generator and collector on the spinning platform.
2. Using non-contact slip rings that use inductive or capacitive principles.
3. Using direct contact slip rings also called swivels that allow for direct contact by a stationary brush pressing against a rotating metal ring.

All these solutions were considered in the initial stages of the project. The first one was regarded as the most elegant, but at the same time most complicated. It requires building active electronic components on the disc, which was not possible in the timescale of the project. The second option would allow for long lasting equipment with reliable readout. However, this method can only be applied to transferring digital and not analogue signals. The third solution is the simplest one, although it has a few disadvantages such as introduction of electrical noise. Moreover, in case of brushes used to create the connection there is a risk of a decay of a setup due to physical damage to the contact pads. In the timescale of the project the formation of a direct contact was the easiest so it was the selected one.

The choice of an electrical swivel was based on several criteria the setup needed to fulfil. For the electrochemical measurements most typically a three electrode setup is used, which allows for various techniques to be applied (Grieshaber et al., 2008). Thus, the electrical swivel needed to have at least three connections for working electrode, counter electrode and reference electrode. The setup was intended for measurements on a spinning disc platform, and so the maximum rotational speed was an important parameter for the choice of electrical swivel. The electrical swivel should be operational at spin speeds of 1000 RPM and higher. Furthermore, the electrochemical measurements on microelectrodes usually involve currents of the order of µA or lower thus the noise level from the swivel should be minimized.

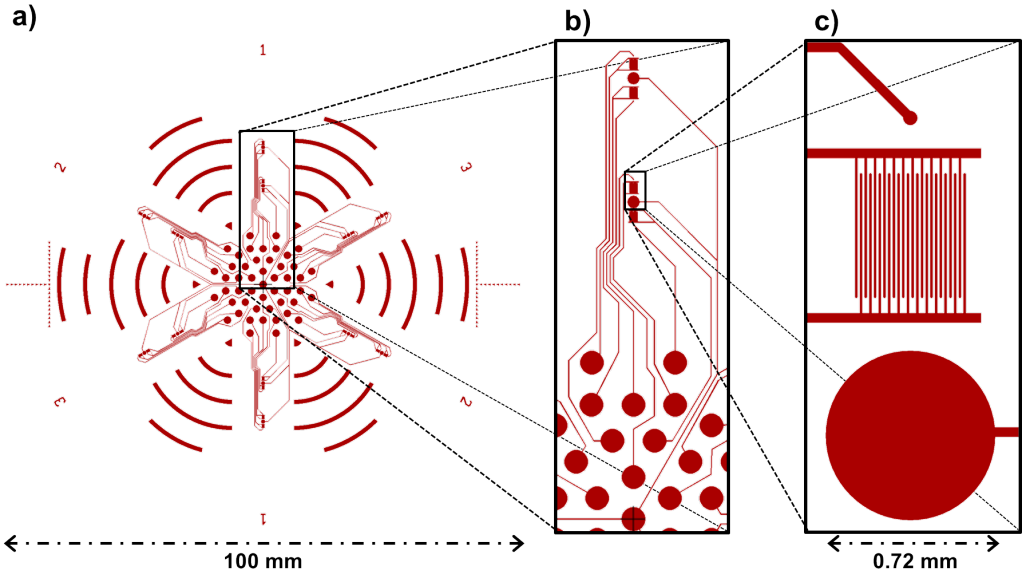

Figure 22.1: Design of electrodes on a disc with a zoom in to one of the channels. Each channel consists of two sets of electrodes containing one counter electrode, two working electrodes and two reference electrodes. *Courtesy of Sune Zoëga Andreasen.*

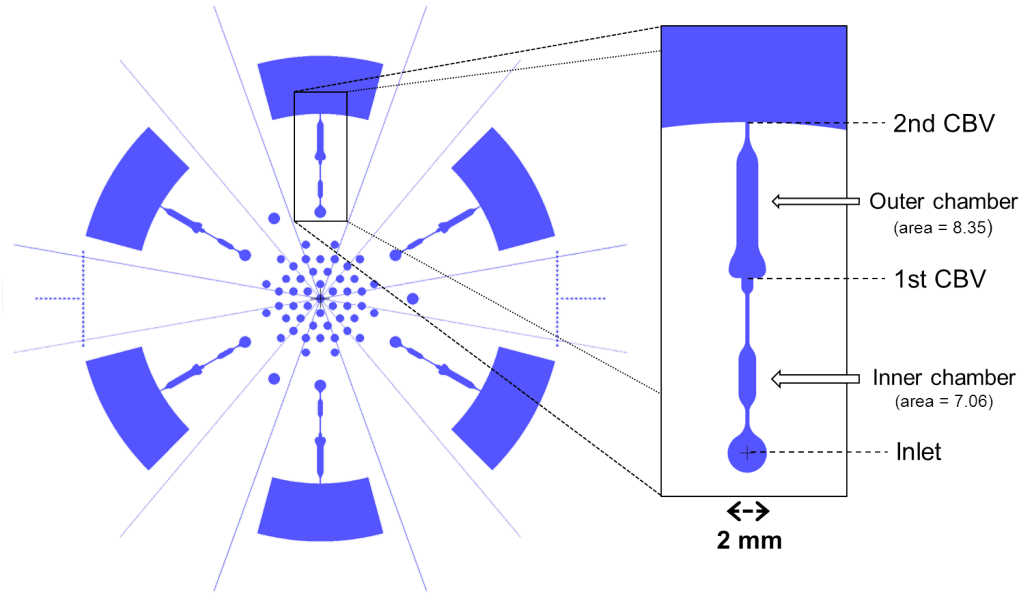

Figure 22.2: Design of microfluidics on a disc with a zoom in to one of the channels with all channel features marked. *Courtesy of Sune Zoëga Andreasen.*

After an initial search of such electrical swivels available on the market a brush-less swivel was selected. Its main advantage is the use of liquid mercury bound to the rotating and the stationary parts of the swivel that form the electrical contacts. The selected swivel Mercotac 430 was approved to a maximum of 1200 RPM spin rate and offered four noiseless connections.

22.2 Disc Design

The design of the disc was based on the previously used centrifugal microfluidics platform. However, the discs were previously micromachinned in PMMA while for this project the fabrication was done by standard cleanroom processes. It enabled better control of the fabrication and integration of the electrodes and the microfluidics with a proper alignment. The process of fabrication of the electrodes was identical as described in Appendix C without the initial step of the oxide growth as the fabrication is done on quartz wafers. Quartz wafers were selected to obtain transparent devices and for a process compatibility with cleanroom machines.

We started by planning the design of the electrodes disc to accommodate for the electrical connections to the electrodes. As in the previous design the channels were composed of two chambers for detection of the binding event. Thus, for

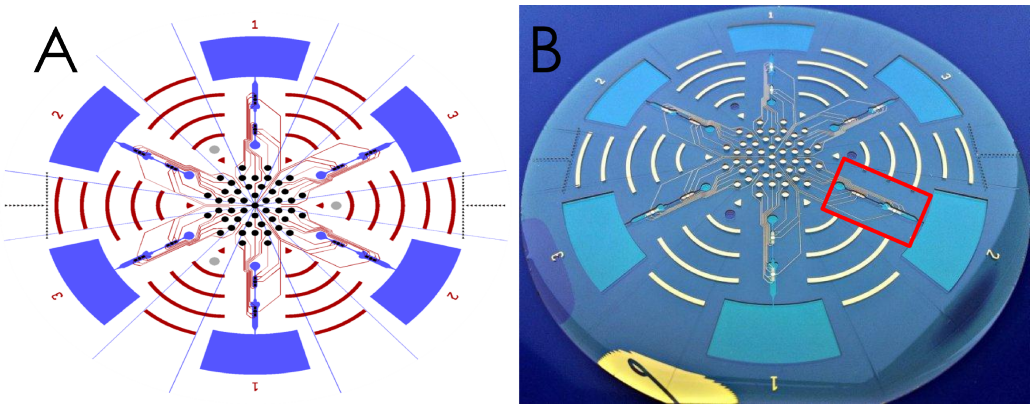

Figure 22.3: Final design of the electrodes on a disc - schematic(A) and the actual disc (B). The openings in SU-8 layer are marked with a red box. *Courtesy of Sune Zoëga Andreasen.*

the integration the electrodes needed to be placed in each chamber. During electrochemical measurements it is not unusual to destroy the electrodes by faulty connection of the wires. Thus, two working and two reference electrodes were positioned in each chamber with one common counter electrode. Having all these electrodes in one chamber required 5 different contact pads for each chamber. The design of a the electrodes for a single channel is shown in Figure 22.1. There is one large circular counter electrode in the middle of the chamber surrounded by two interdigitated WEs and two small circular REs. All the contact pads are placed in the middle of the disc to connect them to the electrical swivel. The swivel contains only four connections so the measurements can be performed on a single electrode set at a time. Ideally the swivel would have more connections to allow for simultaneous measurements on the electrodes in both chambers. However, a multichannel potentiostat would also be required for simultaneous measurements and for this project it was sufficient to measure on one of the electrodes at a time.

Due to limited space for placement of the contact pads in the middle of the disc the design consists of 6 channels with 3 different designs. In each design the position of the two capillary burst valves was kept the same with varied width to optimize the burst frequencies. The microfluidics was fabricated in SU-8 to ensure proper alignment of the chambers over the electrodes. An example of a design of the SU-8 layer is shown in Figure 22.2. In the figure all 6 channels have the same width and valve position. The final disc design and picture of a wafer after fabrication are shown in Figure 22.3. In the SU-8 layer the openings over the electrodes and the contact pads can be seen (red box).

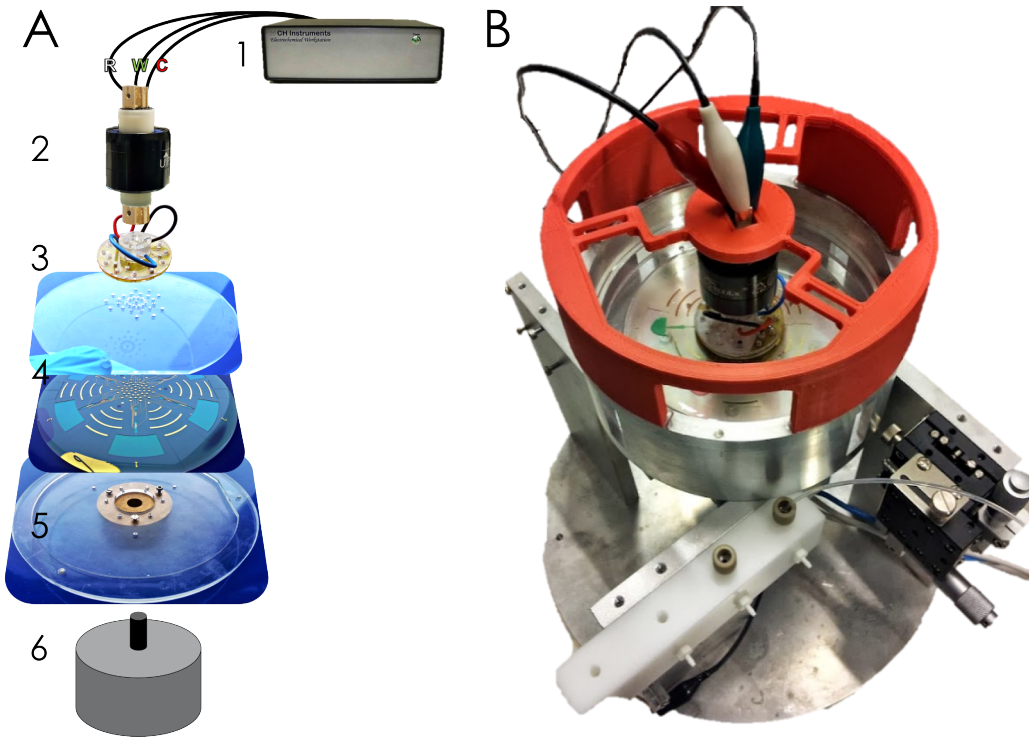

Figure 22.4: (A) An exploded view of the final setup used for measurements on a spinning disc that consisted of an electrical swivel (2) connected to the potentiostat (1). The swivel was placed in a custom made holder (3) for contacting to the electrodes on the disc below (4). To ensure the stability of the setup it was assembled on a bottom holder (5) and mounted to the rotating stage (6). For better connections to the potentiostat a red top holder was fabricated by 3D printing (B). *Courtesy of Sune Zoëga Andreasen.*

23. Results and Discussion

23.1 Final Setup

The final setup is shown in Figure 22.4A. It consists of the electrical swivel (2) connected to the potentiostat (1). A custom made socket (3) for placement of the swivel directly above the contact pads of the disc with the electrodes and microfluidics (4). A bottom holder (5) for mounting of the entire setup on a rotating platform (6). In the end the red top holder was added to the setup to ensure stable and reliable contact (Figure 22.4B).

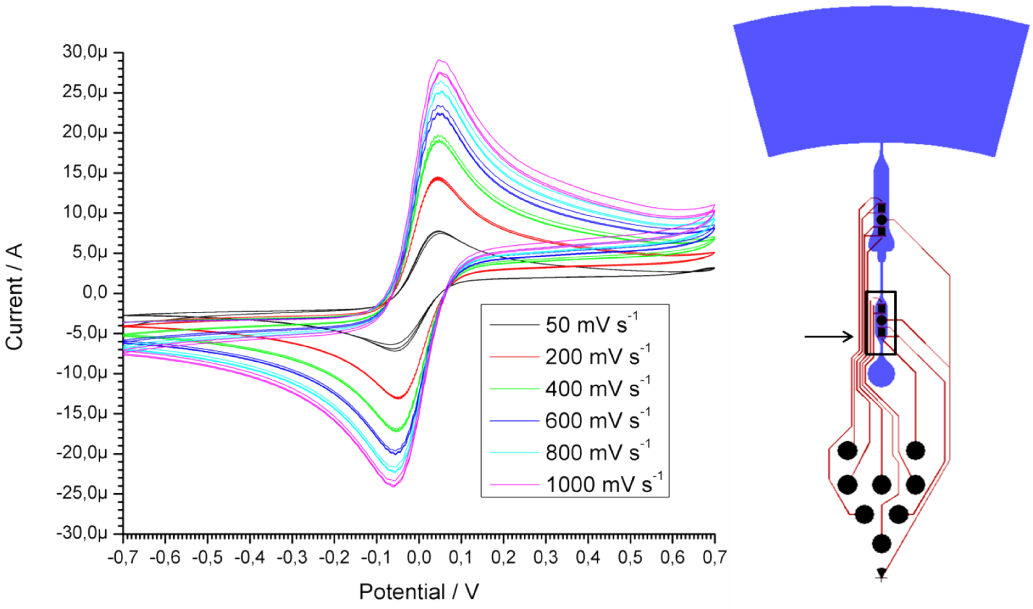

Figure 23.1: Overlay of series of CVs at different scan rates (left) with a scheme of the electrodes position (right). *Courtesy of Sune Zoëga Andreasen.*

23.2 Electrodes Characterization

The electrodes were first characterized in static conditions to ensure their good performance. This is a typical procedure performed on any setup used for electrochemical measurements. The electrodes were cleaned as described in Part V Chapter 18 according to the method in (Fischer et al., 2009). The cleaning procedure ensures that all electrodes are initially almost identical. The characterization of the electrodes involved cyclic voltammetry measurements in 10 mM ferro/ferricyanide solution in PBS from -0.7 to 0.7 V at different scan rates from 50 to 1000 mV/s^{-1}. The measurements were performed using CH Instruments CHI660c potentiostat. The results of the experiments with overlay of CV graphs for each scan rate tested is shown in Figure 23.1.

These measurements were performed to characterize the electrodes for better understanding of their behaviour. During the measurements different scan rates were applied to determine the system's reversibility. In the recorded voltammograms the peak current was increasing with increasing scan rate. However, the oxidation peak current was slightly larger than the reduction peak current. For an ideal reversible system the ratio should be 1:1. As the peak position remained constant for each tested scan rate we concluded that the system is quasi-reversible and diffusion-controlled (Bard and Faulkner, 2001).

For measurements performed on the outer electrode set a 50 Hz noise was obtained (data not shown). It probably arises from the connection wires between the electrodes and contact pads. On the electrodes' scheme in Figure 23.1 a lot of parallel wires connecting the outer electrodes and contact pads can be seen. These wires are placed close to each other which can results in higher noise level. This issue was dealt with by undersampling the measurements, which solved the problem of 50 Hz noise but can also change the signal. However, as the measurements were qualitative and the same undersampling was performed for each tested scan rate we concluded that the measurements were conducted properly.

23.3 Stationary vs. Rotating System

Based on the previous characterization of the electrodes a test during spinning was conducted. After the electrodes cleaning the disc was assembled and aligned at a rotating stage. Subsequently, the ferro/ferricyanide solution at 10 mM in PBS

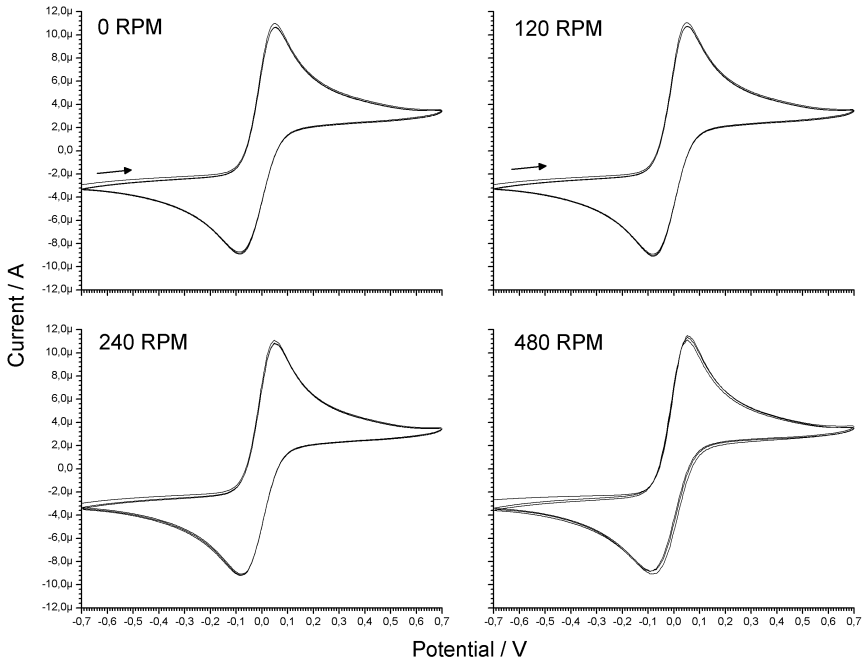

Figure 23.2: Series of cyclic voltammetry measurements performed on a stationary (0 RPM) and rotating system (120, 240 and 480 RPM). *Courtesy of Sune Zoëga Andreasen*

was added and the top holder was mounted together with the electrical swivel. The potentiostat was connected and the electrical connections were confirmed by doing a test measurement with the disc at rest followed by disc spinning and further measurements. In Figure 23.2 a series of CVs obtained at different spin rates from 0 up to 480 RPM are shown. All four graphs show similar behaviour with almost identical current peak amplitude and position. Only at 480 RPM a slightly more noisy signal was observed. The obtained peak positions and currents were comparable to the measurements done with a stationary setup.

After these first successful experiments we concluded that the setup can be used for measurements at spin rates up to 480 RPM without any significant change to the obtained signal. By applying a simple electrochemical technique we showed that it is possible to achieve reliable contact between a stationary potentiostat and a rotating disc. The low noise introduced at a spin rate of 480 RPM is most likely a mechanical noise arising from a misalignment of the disc from the center of rotation.

23.4 Detection of Analytes

After the successful results using cyclic voltammetry we proceeded towards using amperometry as a detection method. This is a commonly used technique at which the potential is kept constant and the current variations during electrochemical reaction are recorded (Grieshaber et al., 2008). If the potential is applied above or below the threshold for oxidation and reduction respectively, the electrolyte in the vicinity of the electrode will be oxidized or reduced and due to the exchange of the electrons the current will flow. This technique is very sensitive to changes in the liquid properties both at the interface and in the bulk. Any perturbations in the solution will be immediately recorded.

Here, the amperometric measurements were performed in a solution of 10 mM ferricyanide in PBS. By applying a negative potential of -100 mV the reduction of ferricyanide to ferrocyanide was achieved. During this experiment the current becomes more negative but for the ease of interpretation it is plotted as an absolute current value. In Figure 23.3 the effect of starting and stopping the disc rotation was investigated. Before spinning the disc at various spin rates the disc was at rest. The initiation of the spinning (lasting 50-100s) is marked as green lines and the termination of spinning as red lines. In the graph it can be seen that the current increases during spinning. However, the increase was not proportional to the spin rate. The highest current increase was observed for a disc spinning at 0.5 Hz while the lowest increase was shown for 3 Hz. A similar experiment was conducted using MilliQ water instead of ferro/ferricyanide solution in PBS. It was performed to determine whether the spinning induces some mechanical noise to the measurements. The results are shown in Figure 23.4. The spinning is indicated

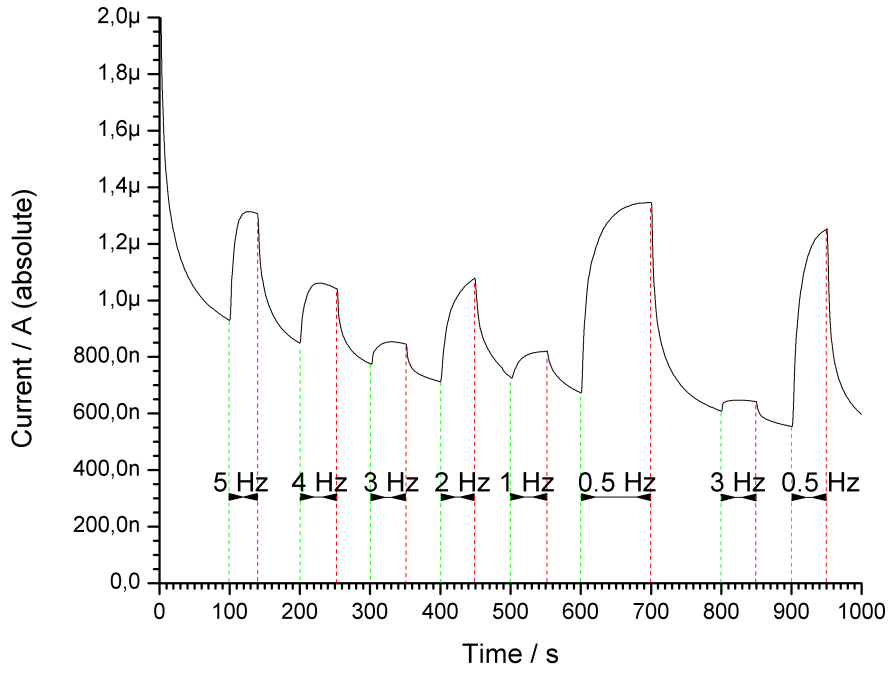

Figure 23.3: Amperometric measurements on a disc rotating at different spin rates. Green lines indicate the spinning initiation and red lines show the spinning termination. *Courtesy of Sune Zoëga Andreasen.*

by the dashed lines. The measured current is very low at a level of nA. There is no significant change observed when disc is spinning thus we concluded that the current increase observed in Figure 23.3 is not mechanical.

The increase in signal in Figure 23.3 during spinning occurs most likely due to the induced convection. While the disc is at rest, there is no mixing of the solution in the channels, but once the disc is spun the mixing is introduced. The mixing disturbs the diffusion layer that is formed by ions in the solution on the electrodes and thus changes the signal. The most surprising was the lack of correlation between the spin rate and the current increase. It was expected that the current would increase with an increasing spin rate. However, the highest current increase was observed for the spin rate of 0.5 Hz (30 RPM). The non-linear correlation between the current increase and the spin rate can be related to the used stepper motor in a rotating stage. In principle it moves in discrete steps, which is a series of very short pulses. Those pulses can be different for different spin rates, which in turn can induce a different mixing pattern. Previous studies have shown the electrochemical signal enhancement by application of a low frequency

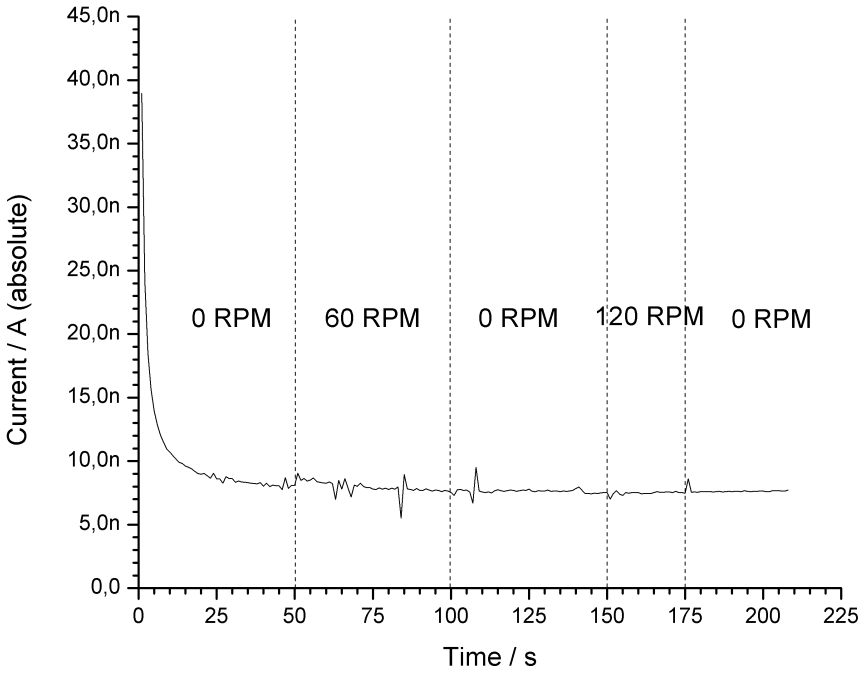

Figure 23.4: Amperometric measurements performed in MilliQ water on a disc rotating at different spin rates. Dashed lines indicate the periods of disc resting and spinning. No significant change in current is induced by increasing the spin rate. *Courtesy of Sune Zoëga Andreasen.*

sound (Mikkelsen and Schrøder, 1999).

To test whether the behaviour is reversible we performed a series of measurements with a spinning disc and a disc at rest. The applied spin rate was always 30 RPM but for one experiment the disc was initially spinning, while for the other the measurements started with the disc at rest. The results of the increase in current due to spinning are shown in Figure 23.5. It can be seen that the change in the current is predictable regardless of the initial state of the disc. The current increase is always by around 100 % and can be used as beneficial signal enhancement in the sensing experiments.

However, for future experiments it is important to characterize the behaviour further. Moreover, choosing the right spin rates for opening the valves in series is crucial to measure a specific current change due to the binding events. It is possible to plan the experiments with a reference system measured simultaneously to enable differential measurements of the obtained signal. For such a reference system a solution without the targeted analyte should be used to determine whether

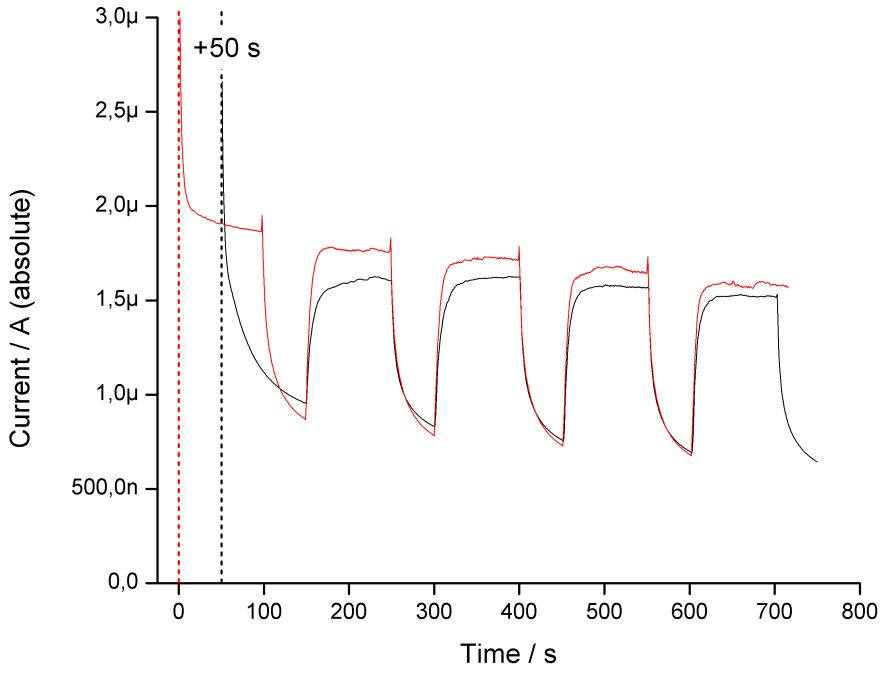

Figure 23.5: Amperometric measurements on a series of spinning and stopping the disc initially rotating (red line) and static (black line) at 30 RPM. *Courtesy of Sune Zoëga Andreasen.*

a signal increase is specific for the binding event. Moreover, the system should be characterized also for other electrochemical techniques such as EIS to determine if such measurements while spinning are also possible with this common technique. In the future, all experimental parameters need to be adjusted for each specific detection to get more reliable results and good control of the reaction.

24. Conclusions

The main goal of this part of the project was to integrate a label-free electrical sensor with a centrifugal microfluidics platform to enable electrical measurements

during spinning. We developed a system using a commercially available electrical swivel with a custom made plug. The microelectrodes were designed to fit a microfluidic disc developed previously and to accommodate for the electrical connections to the swivel. The design of the electrodes was based on the previously described and tested gold electrodes, which performed exceptionally well in the DNA hybridisation detection. By designing a custom made plug for the electrical swivel we achieved a reliable contact between the microfabricated electrodes and potentiostat. The system proved to be useful in electrochemical measurements, which were used for testing its performance as well as for optimization. We showed that the cyclic voltammetry measurements are not significantly affected by the rotation at the same time proving the concept of sensing during spinning. Performing amperometric measurement needs to be well controlled as the spin rate induces mixing of the solution, which signifiantly changes the signal. Further experiments using impedance spectroscopy are planned to perform the actual detection of DNA hybridisation using the setup.

Bibliography

Abi-Samra, K.; Kim, T.-Y.; ark, D.-k.; Kim, N.; Kim, J.; Kim, H.; Cho, Y.-K.; Madou, M., *Electrochemical velocimetry on centrifugal microfluidic platforms*, Lab on a Chip, **13**, 3253-3260 (2013)

Bard, A.J.; Faulkner, L.R., *Electrochemical methods: fundamental and applications*, Wiley, ISBN 978-0-471-04372-0 (2001)

Bosco, F.G.; Hwu, E.-T.; Chen, C.-H.; Keller, S.; Bache, M.; Jakobsen, M.H.; Hwang, I.-S.; Boisen, A., *High throughput label-free platform for statistical biomolecular sensing*, Lab on a Chip, **11**, 2411-2416 (2011)

Chen, Q.L.; Cheung, K.L.; Kong, S.K.; Zhou, J.Q.; Kwan, Y.W.; Wong, C.K.; Ho, H.P., *An integrated lab-on-a-disc for automated cell-based allergen screening bioassays*, Talanta, **97**, 48-54 (2012)

Cho, H.K.; Lee, Y.H.; Couch, R.A.; Jagadeesh, J.M.; Olson, C.L., *Development of a multi channel electrochemical analyzer*, Clinical Chemistry, **28**, 1956-1961 (1982)

Fischer, L.M.; Tenje, M.; Heiskanen, A.R.; Masuda, N.; Castillo, J.; Bentien, A.; Emneus, J.; Jakobsen, M.H.; Boisen, A., *Gold cleaning methods for electrochemical detection applications*, Microelectronic Engineering, **86**, 1282-1285 (2009)

Grieshaber, D.; MacKenzie, R.; Voeroes, J.; Reimhult, E., *Electrochemical biosensors - Sensor principles and architectures*, Sensors, **8**, 1400-1458 (2008)

Gorkin, R.; Park, J.; Siegrist, J.; Amasia, M.; Lee, B.S.; Park, J.-M.; Kim, J.; Kim, H.; Madou, M.; Cho, Y.-K., *Centrifugal microfluidics for biomedical applications*, Lab on a Chip, **10**, 1758-1773 (2010)

Kim, T.-H.; Abi-Samra, K.; Sunkara, V.; Park, D.-K.; Amasia, M.; Kim, N.; Kim, J.; Kim, H.; Madou, M.; Cho, Y.-K., *Flow-enhanced electrochemical immunosensors on centrifugal microfluidic platforms*, Lab on a Chip, **13**, 3747-3754 (2013)

Madou, M.J.; Kellogg, G.J., *LabCD: a centrifuge-based microfluidic platform for diagnostics*, Proceedings of Systems and Technologies for Clinical Diagnostics and Drug Discovery, **3259**, 80-93 (1998)

Mikkelsen, Ø.; Schrøder, K.H., *Sensitivity Enhancements in Stripping Voltammetry from Exposure to Low Frequency Sound*, Electroanalysis, **11**, 401-405 (1999)

Navarro, P.; Morai, S.; Gabaldon, J.A.; Perez, A.J.; Puchades, R.; Maquieira, A., *Arrays on disc for screening and quantification of pollutants*, Analytica Chimica Acta, **784**, 59-64 (2013)

Wang, G.; Ho, H.-P.; Chen, Q.; Yang, A.K.-L-; Kwok, H.-C.; Wu, S.-Y.; Kong, S.-K.; Kwan, Y.-W.; Zhang, X., *A lab-in-a-droplet bioassay strategy for centrifugal microfluidics with density difference pumping, power to disc and bidirectional flow control*, Lab on a Chip, **13**, 3698-3706 (2013)

Part VII

Conclusions and Outlook

25. Summary of Results

The overall aim of the project was to develop microsystems for cytogenetics. In this thesis I have presented various approaches that led to achieving the goal. Here I will conclude on my work focusing on the most interesting findings.

25.1 Chromosome Total Analysis System

A microfluidic device for cytogenetics was developed and described in Part III. We aimed at fabrication of an all-polymer device that would allow for reliable chromosome spreading. The current methods of preparation of the chromosome spreads rely on various environmental factors such as humidity, temperature and rate of the solution evaporation. Normally, the spreading process is adjusted based on these factors. Thus, for an untrained person it is extremely difficult to prepare usable spreads. We have addressed the need for a more controlled preparation of the chromosome spreads by developing a semi-closed polymer device. The device was fabricated in Topas® in two layers featuring a microfluidic chamber with perforation holes from the top. The bottom substrate was modified by plasma treatment coupled with photografting of hydrophilic monomers. It resulted in a long lasting hydrophilic surface as tested over a period of 3 weeks. The device was tested for chromosome spreading to be used in further cytogenetic analysis. We tested the spreading on various samples as a control and showed that chromosome spreads were properly formed on both control glass slide and the modified Topas®. In a semi-closed device the evaporation of the fixative is the main factor affecting the spreads. To ensure that it is only the drying rate that influences the spreading two devices with glass and modified Topas® bottom were used. The usability of the obtained spreads was further checked using FISH. It showed that even though the spreads were formed in both semi-closed devices, the metaphase spreads formed on a modified Topas® did not show any hybridisation signals. Further improvements towards achieving usable spreads need to be performed. The optimization of the Topas® modification procedure should lead to better spreading on the surface with less condensed chromosomes. Furthermore, the denaturation conditions in FISH protocol could be adjusted to account for the difference in thermal conductivity of glass and Topas®.

25.2 NanoKaryotyping on Lab-on-a-Disc

An alternative approach towards detection of the chromosome translocations was described in Part IV of the project. It was based on the surface immobilized DNA probes targeting the derivative chromosomes. As the derivative chromosomes are characterized by a sequence coming from two different chromosomes involved in the translocation a double hybridisation assay was proposed. The assay was realized on a lab-on-a-disc platform developed for the translocation detection. Lab-on-a-disc devices are operated by rotating stage with a centrifugal force used for liquid propulsion. The device was designed to accommodate two hybridisation chambers that were used for sequential hybridisation. The chambers were designed to operate separately with a valve stopping the liquid just before the second chamber. Simple valves operating on a principle of an increased surface tension at a wide opening of the channel were used. Such capillary burst valves do not require additional surface treatment and are solely based on the physical parameters of the channels. The probes targeting the two sequences of derivative chromosome were immobilized in designated chambers. After the first recognition measured by fluorescence microscopy the captured DNA fragment was heat denatured and transferred to the second hybridisation chamber by spinning the disc. All required controls were performed to ensure the specificity of the binding between the designed probe targeting the translocation between chromosome 3 and chromosome 9. The findings of this part of the project were published in a research paper 'Centrifugally driven microfluidic disc for detection of chromosomal translocation' in Lab on a Chip journal. This project was carried out in collaboration with NanoProbes group at DTU Nanotech and was the basis of Anna Line Brøgger's Master thesis.

25.3 Label-free Sensing

In Part V three different electrical sensors were applied for detection of DNA hybridisation. The main goal of this part of the project was to develop a reliable sensor for double DNA hybridisation to integrate in the microfluidic platform. The first tested sensor was based on silicon nanowires in which the changes in the current through the nanowire are measured and correlated to the sensing event. The nanowire sensors are very sensitive towards the surrounding charged particles and thus are well suitable for detection of DNA hybridisation. The silicon nanowires used in this project were fabricated using a novel method utilizing diphenylalanine peptides as etching masks. The nanowires fabricated in this way are smaller, however their size distribution is relatively large and should be controlled for a more reliable sensor. The nanowires were successfully applied for DNA hybridisation sensing and were also tested for chromosome translocation detection in a double hybridisation assay. We demonstrated their usability in the sensing ex-

periments, however the functionalization process needs to be optimized to enable reproducibility.

Another sensor tested for DNA hybridisation was based on metallic electrodes fabricated by standard cleanroom processes. These electrodes were applied for faradaic electrochemical impedance spectroscopy measurements. A commonly used negatively charged redox mediator ferro/ferricyanide was used in the experiments. It is well suited for DNA hybridisation sensing as it is strongly repelled by the negatively charged DNA backbone during the measurements. The parameter used for sensing is a charge transfer resistance, which is the exchange of electrons between the metal electrode and the redox mediator in the solution. After immobilization of DNA probes the access of ferro/ferricyanide ions to the electrode surface is blocked, which is even more pronounced after the successful DNA hybridisation between the probes and the complementary DNA. In the experiments 12 electrodes present on the chip were always tested, however only a fraction of the electrodes was behaving as expected. A thorough analysis of the sensing was done and the sensor was also applied for chromosome translocation detection. After performing a control experiment, with a normal DNA fragment only matching one set of probes, it was noticed that the heat denaturation is probably disturbing the DNA probes layer. The denaturation was performed at 95 °C, which is enough for the self-assembled thiolated DNA to be removed from the surface. We concluded that the heat denaturation should be optimized or avoided entirely.

The last tested electrical sensor was based on conductive polymer electrodes as transducers. They were used for non-faradaic measurements of EIS for DNA hybridisation sensing. Conductive polymer are becoming more popular for sensors applications with a main advantage of reduced costs of production. The electrodes in this project were structured by manual agarose stamping, which is a fast method of prototyping of PEDOT electrodes. The electrodes were used for impedance measurements without a mediator present in the solution. In this way a truly label-free sensor was developed without the need for additional solutions. The sensor was able to distinguish between a fully complementary DNA strand and a 3 bp mismatch strand used as a control. The detection limit was determined to be 100 pM of the complementary DNA measured in 1xSSC buffer with surfactant. The double hybridisation assay was never tested on PEDOT electrodes as they are extremely sensitive to temperature changes and thus heat denaturation was not possible.

25.4 Integration

Most recently the work leading to integration of an electrical sensor on a lab-on-a-disc platform was initiated. The project aimed at the development of the measurement system to perform the detection on a rotating disc platform. The

problem of connecting a stationary equipment with a spinning disc was solved by application of electrical swivel. The electrodes disc and microfluidics were fabricated using standard cleanroom techniques and were used for electrochemical detection. The preliminary results are very promising and in the future can allow for real-time sensing on a spinning disc. Up until now the setup has been tested with standard electrochemical techniques such as cyclic voltammetry and amperometry. Even though no actual sensing was performed, we have shown that the oxidation and reduction signals in the CV are not affected significantly by the increasing spinning rate. However, the amperometric measurements showed an increase in current during the rotation, which means that a signal enhancement is possible with convective mixing induced by the spinning. A better characterization of this behaviour is required for the setup application as a sensing platform. This project was carried out in collaboration with NanoProbes group at DTU Nanotech and was the basis of Sune Zoëga Andreasen's Master thesis.

26. Conclusions and Future Work

The work presented in this thesis aimed at the development of microsystems for cytogenetics. At the beginning of the project a literature review was performed to determine the size of the field. At that time very few scientific groups were working in the field of chromosome analysis using microdevices. The main research focus was always at miniaturization of the existing assays to minimize the amount of reagents used. Furthermore, the development of devices for cytogenetics had also an advantage of reduced risk of errors introduced in the analysis during the manual handling. New approaches towards detection of chromosome translocations are rarely proposed. The growing field of DNA biosensors that enables detection of the presence of a specific sequence in the sample should be used for the benefit of the cytogenetics analyses. The microarrays are gaining more popularity in the cytogenetics field, thus by organizing arrays of probes in a specific manner they could be used for detection of chromosome translocations.

We have demonstrated a prototype of such a device, which was based on a centrifugal microfluidics platform. Further development of the device would allow for multiplexed detection of various chromosome translocations. The presented device was limited by the availability of the DNA probes to demonstrate the chromosome translocation detection. The project would greatly benefit from collaboration with one of the microarray manufacturers, that could prepare the microarray in the format of centrifugal microfluidics. Such a multiplexing of the translocation

detection would be by far better than any of the currently used detection methods and could find its way to routine use in cytogenetics. The device in its current form has other limitations. Namely, the manual washing of the unbound DNA after hybridisation followed by careful channels drying for the capillary burst valves to function properly. Incorporating the chambers with a washing buffer on a disc designed to keep the valves dry would enable easier operation.

Further work needs to be devoted towards better understanding of the nature of label-free sensing of DNA hybridisation. The presented electrical sensors are sensitive enough for this application but their reliability is questionable. This issue is mostly attributed to the prepared biorecognition layer. Its further optimization is necessary for better understanding of the sensing event. Some more systematic work with various concentrations and compositions of the biorecognition layer would be beneficial for the reproducibility. Blocking of the remaining sensor active areas should be carried out to minimize the unspecific binding. Moreover, the sensors need to be tested with real samples such as PCR amplified DNA or total extracted DNA. These samples contain a lot of other biomolecules that may interfere with the binding and the sensing. It is crucial for the POC devices to be able to operate with non-purified patient's samples.

The combination of centrifugal microfluidics with label-free sensing presents a lot of advantages over fluorescent detection. It is amenable for miniaturization, requires a minimum of additional periphery equipment and can be powered by batteries. So far electrochemical measurements while spinning were only performed on a standard electrochemical solution, but I imagine that the setup could easily be transformed into a biosensor for real-time DNA hybridization detection. Further setup development towards fabrication of a custom-made potentiostat and data recording system will be undertaken. This step is necessary for the successful application of lab-on-a-disc as a POC device.

Application of microtechnologies in cytogenetics offer a vast variety of opportunities. It can result in much faster and reliable analysis at a lower cost. However, it needs time to be universally accepted as was initially the case with microarrays. They are now a trusted analysis method and are used routinely in most of cytogenetic laboratories. Further development of the devices by application of micro- and nanotechnologies is inevitable and may lead to new diagnostic methods.

Part VIII

Appendices

A. List of Publications

Journal Articles

1. Brøgger, A.; **Kwasny, D.**; Bosco, F.; Tumer, Z.; Boisen, A. and Svendsen, W.E., 'Centrifugally driven microfluidic system for detection of chromosomal translocation', Lab on a Chip, **12**, issue 22, 4628-4634 (2012)

2. **Kwasny, D.**; Vedarethinam, I.; Shah, P.; Dimaki, M.; Silahtaroglu, A.; Tumer, Z. and Svendsen, W.E., 'Advanced microtechnologies for detection of chromosome abnormalities by fluorescent in situ hybridization', Biomedical Microdevices, **14**, issue 3, 453-460 (2012)

3. **Kwasny, D.**; Kiilerich-Pedersen, K.; Moresco, J.L.; Dimaki, M.; Rozlosnik, N. and Svendsen, W.E., 'Microfluidic device to study cell transmigration under physiological shear stress conditions', Biomedical Microdevices, **13**, issue 5, 899-907 (2011)

4. Shah, P.; Vedarethinam, I.; **Kwasny, D.**; Andresen, L.; Skov, S.; Silahtaroglu, A.; Tumer, Z.; Dimaki, M. and Svendsen, W.E., 'FISHprep: A novel integrated device for metaphase FISH sample preparation', Micromachines, **2**, issue 2 , 116 (2011)

5. Shah, P.; Vedarethinam, I.; **Kwasny, D.**; Andresen, L.; Dimaki, M.; Skov, S. and Svendsen, W.E., 'Microfluidic bioreactors for culture of non-adherent cells', Sensors and Actuators B:Chemical, **156**, issue 2, 1002-1008 (2011)

Book Chapters and Books

1. **Kwasny, D.**; Vedarethinam, I.; Shah, P.; Dimaki, M. and Svendsen, W.E., 'Microtechnologies Enable Cytogenetics in Recent Trends in Cytogenetic Studies - Methodologies and Applications', Book Chapter, ISBN 978-953-51-0178-9, editor Padma Tirunilai, InTech Publisher, 2012

2. Okkels, F. and **Kwasny, D.**, 'Bioprocessing in microreactors', Book Chapter in a book 'Microreactors in Preparative Chemistry', Wiley Publisher 2012

Conference Contributions

1. Andreasen, S.Z.; Brøgger, A.L.; **Kwasny, D.**; Bosco, F.; Boisen, A.; Svendsen, W.E., 'Real-time electrochemical detection on a spinning disc platform', Gordon Research Conference, Barga, Tuscany, Italy, June 2013, poster presentation
2. Frederiksen, G.; **Kwasny, D.**; Pfreundt, A.; Svendsen, W.E.; Berg-Sorensen, K., 'Mimicking Sugar Translocation in Plants in a Microfludic Chip', Gordon Research Conference, Barga, Tuscany, Italy, June 2013, poster presentation
3. **Kwasny, D.**; Dapra, J.; Brøgger, A.L.; Bosco, F.; Tumer, Z.; Dimaki, M.; Boisen, A.; Rozlosnik, N. and Svendsen, W.E., 'DNA hybridization sensors for cytogenetic analysis', Analytix Congress 2013, Suzhou, China, March 2013, oral presentation
4. **Kwasny, D.**; Andersen, K.B.; Frohling, K.B.; Silahtaroglu, A.; Tumer, Z.; Castillo-Leon, J. and Svendsen, W.E., 'Label Free Chromosome Translocation Detection with Silicon nanowires', IEEE EMBS Micro- and Nanotechnology in Medicine, December 2012, poster presentation
5. Svendsen, W.E.; Kirkegaard, J.; Ajine, M.A.; Hermann, H.P.; **Kwasny, D.**; Iuliano, F.; Pastorekova, S.; Harlow, K.; Skov, J. and Rodriguez-Trujillo, R., 'Micro device for multiple disease diagnostic and monitoring', IEEE EMBS Micro- and Nanotechnology in Medicine, Ka'anapali, Hawaii, December 2012, poster presentation
6. **Kwasny, D.**; Vedarethinam, I.; Shah, P.; Dimaki, M.; Silahtaroglu, A.; Tumer, Z. and Svendsen W.E., 'Advanced microtechnologies for cytogenetic analysis',NanoBioPL conference, Warsaw, Poland, 2012, oral presentation
7. Hermann, H.P.; Rodriguez-Trujillo, R.; **Kwasny, D.**; Iuliano, F.; Pastorekova, S.; Dimaki, M. and Svendsen, W.E., 'On-chip cell viability studies using label-free impedance detection', WAM Nano 2012 Conference, Barcelona, Spain, 2012, poster presentation
8. Frohling, K.B.; **Kwasny, D.**; Andersen, K.B.; Castillo-Leon, J. and Svendsen, W.E., 'Rapid Fabrication of Silicon Nanowires Using Self-Assembled Diphenylalanine Peptide Nanostructures', WAM Nano 2012 Conference, Barcelona, Spain, 2012, poster presentation
9. Brøgger, A.L.; **Kwasny, D.**; Bosco, F.G.; Silahtaroglu, A.; Tumer, Z.; Boisen, A. and Svendsen, W.E., 'Microfluidic system with capillary burst valves for detection of chromosomal translocations', WAM Nano 2012 Conference, Barcelona, Spain, 2012, poster presentation
10. **Kwasny, D.**; Vedarethinam, I.; Mednova, O.; Almdal, K. and Svendsen, W.E., 'All-Polymer Microfluidic Device for Metaphase FISH on Chip', Lab

on a Chip European Congress, Edinburgh, Scotland, 2012, poster presentation

11. Dapra, J.; **Kwasny, D.**; Svendsen, W.E. and Rozlosnik, N., 'All-polymer chip for electrochemical detection of DNA hybridization', 2nd NanoToday conference, Hawaii, 2011, poster presentation

12. **Kwasny, D.**; Kiilerich-Pedersen, K.; Moresco, J.L.; Dimaki, M.; Rozlosnik, N. and Svendsen, W.E., 'Microfluidic device as a novel cell transmigration assay', NanoBioTech Conference, Montreux, Switzerland, 2011, poster and short oral presentation

13. **Kwasny, D.**; Bertelsen, B.; Dimaki, M.; Silahtaroglu, A.; Tumer, Z. and Svendsen, W.E., 'Microsystem for label-free detection of chromosomal translocations', 8th European Cytogenetics Conference, Porto, Portugal, 2011, poster presentation

14. **Kwasny, D.**; Bertelsen, B.; Dimaki, M.; Silahtaroglu, A.; Tumer, Z. and Svendsen, W.E., 'Microsystem for label-free detection of chromosomal translocations', Wilhelm Johannsen Symposium, Copenhagen, Denmark, March 2011, poster presentation

15. **Kwasny, D.**; Dimaki, M.; Tumer, Z. and Svendsen, W.E., 'Nano-Karyotyping. Application of microsystems and nanotechnology in the cytogenetic diagnosis of hematological malignancies', DTU Symposium for Biotech Research, Kgs. Lyngby, Denmark, 2010, poster presentation

16. **Kwasny, D.**; Dimaki, M.; Tumer, Z. and Svendsen, W.E., 'Nano-Karyotyping. Application of microsystems and nanotechnology in the cytogenetic diagnosis of hematological malignancies', PhD Nano 2010, Goteborg, Sweden, October 2010, poster and oral presentation

B. Nanowire Fabrication Process

Process flow title				Revision
Peptide Poly Silicon Nanowires				**1.0**
DTU Nanotech Department of Micro- and Nanotechnology	Contact email karsten.andersen@nanotech.dtu.dk		Contact person Karsten B. Andersen	Contact phone 31164864
	Labmanager group NaBIS	Batch name PepPolySionQua	Date of creation 19-Dec-12	Date of revision 19-Dec-12

Objective

Batch name: Peptide Poly Silicon Nanowires

The objective with this process flow is to fabricate poly silicon nanowire devices utilizing peptide nanotubes (PNTs) formed in water from the dipeptide diphenylalanine as a masking material

The diphenylalanine peptide nanotubes have been approved as an allowed material in the clean room. And it has been approved to be used in all the processes and machines that it is introduced to in this process flow by the safety comity and the machine responsible.

The PNTs is formed from a small dipeptide consisting of two phenylalanine amino acids. The formed peptide nanotubes are non toxic and dissolve rapidly in all liquids including water. However it has been proven able to mask dry etching procedures in the reactive ion etch machines.

Substrates

Substrate	Orient.	Size	Doping/type	Polish	thickness	Box	Purpose	#	Sample ID
Silicon	<100>	4”	n (Phos.)	DSP	350±25µm		Substrate	4	SI 1-4

Figures

Figure	Caption	Step	Figure (Side and top view)
1	After Poly Si Deposition	2.2	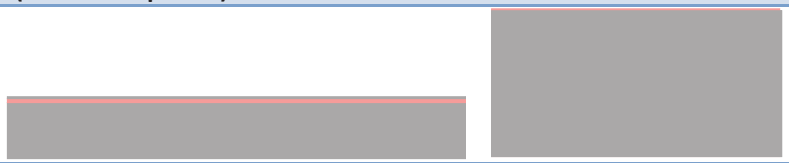
2	After lithography	3.8	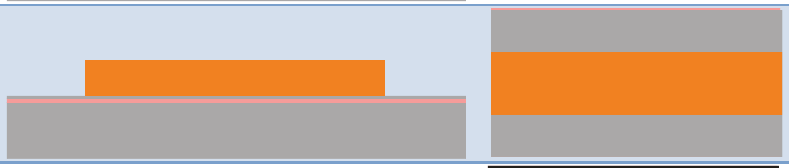
3	After Aluminum deposition	4.1	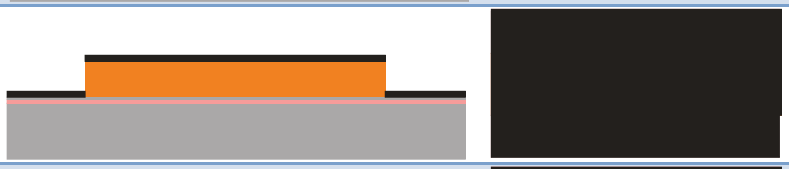
4	After lift off	4.2	
5	After Peptide positioning	5.1	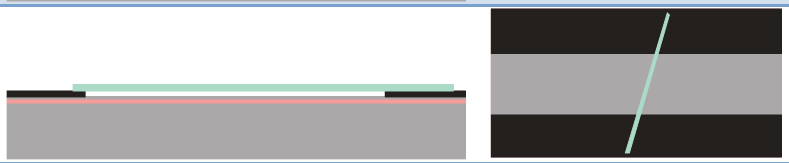
6	After Poly si etch and water dip	5.4	
7	After photolithography	6.7	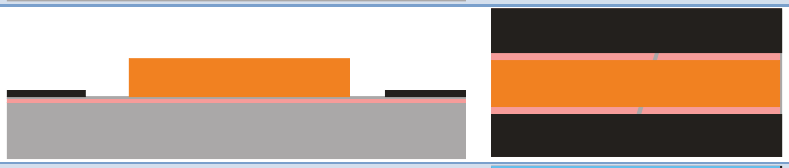
8	After TiO2 deposition	7.1	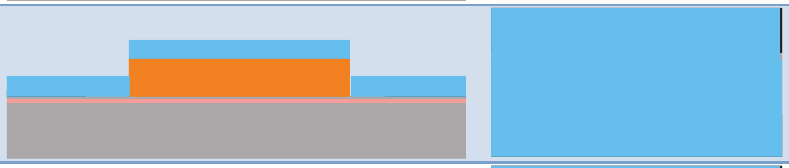
9	After lift off	7.2	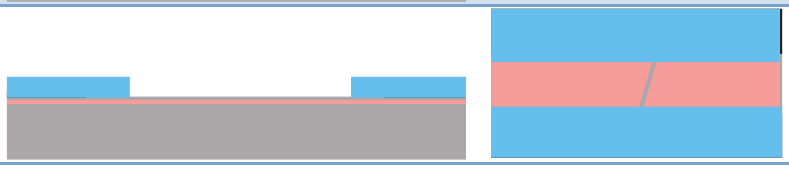

Comments: Color Legend

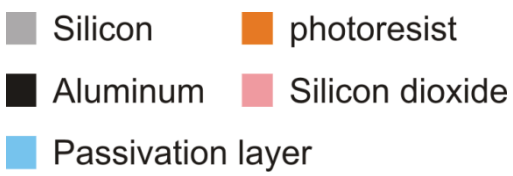

Step	Heading	Equipment	Procedure	Comments
1	**Preparation**			SI 1-4
1.1	Wafer selection	Wafer box	Take the wafers from the storage and put them in a wafer box.	Note the wafer IDs in the batch traveler.
1.2	Oxide growth	Drive In furnace	Process	To grow 500 nm SiO_2, remember to include test wafers
2	**Poly Silicon deposition**			SI 1-4
2.1	RCA cleaning	RCA Bench		Note that procedure must be performed right before polysilicon deposition. Remember to include test wafer with oxygen for polydeposition. If performed immediately after oxide growth cleaning can be skipped
2.2	Poly Silicon deposition	LPCVD Poly-Si (B4)	Place a test wafer in the center of the boat and place device wafers equally distributed on each side of the test wafer (wafer with oxide). Finally fill up with dummy wafers for n-type poly. Wafers in every other slot Recipe: Poly620PX, time: 5min Target thickness: 55±5nm	Measure poly silicon thickness on the filmtech and note the result in the furnace log. Remember to leave the test wafer in the designated box after investigation
3	**Lithography – 1.5µm standard**			SI 1-4
3.1	Surface treatment	HMDS oven	Load wafers in oven for ~30 mins Recipe: program 4	Note time in logbook, can be replaced by 15 s. HF dip
3.2	Clean spinner	SSE spinner	Clean spinner nozzle and run the dummy wafers Recipe: 1.5 4inch	1-3 dummies Note time in logbook
3.3	Coat wafers	SSE spinner	Coat the device wafers 1.5 µm AZ5214e Novolac resist Softbake on hotplate Recipe: 1.5 4inch (Temp: 90°C, time:60 sec)	Resist thickness not checked Note time in logbook
3.4	Exposure	Aligner-6inch	Align to flat. Hard contact Recipe: first print neg. process Exposure time: 1.7 sec Mask: Electrodes	Note time in logbook
3.5	Reverse bake	Manual Hot plate	Temp: 110 °C Time: 100 sec	Placed in the old yellow room
3.6	Flood exposure	Aligner-6inch	Recipe: Flood exposure Exposure time: 15 sec Mask: none	Note time in logbook
3.7	Transport of wafers	transport box	Load wafers into the Black or blue transport box	To avoid unwanted exposure from the white light

3.8	Develop	Developer bench	Develop in 351B for 60±10 sec	Note time in logbook
3.9	Rinse/dry	Wet bench/ Spin dryer	Rinse in DI water for 5 min (300±30 sec). Spin dry	
3.10	Inspection	Optical microscope	Check pattern and alignment marks	
4	**Aluminum deposition**			SI 1-4
4.1	Aluminum deposition	Alcatel	Metal: Al Thickness: 25 nm	Note time in logbook
4.2	Lift-off	Remover 1165 lift off	Ultrasound on for 30 min	
4.3	Rinse/dry	Wet bench/ Spin dryer	Rinse in DI water for 5 min (300±30 sec). Spin dry	
4.4	Inspection	Optical microscope	Check for completeness	
4.5	Inspection	Dektak	Measure heights and widths	Note on measurement sheet
5	**Nanowire Definition with Peptides**			SI 1-4
5.1	Spin casting peptides	Portable spinner	4000 rpm for 15 s. Spin dry	Specific process will be demonstrated by Karsten
5.2	Inspection	Optical microscope	Check for alignment and density	Rinse in water if not succesfull and redo step 5.1
5.3	Poly Silicon Etching	RIE 2	Recipe: oh_polya Time: ~30s.	Use endpoint detection to determine when the silicon layer has been removed
5.4	Removal of peptides	Dedicated petridish	Place in water in dedicated petridish for ~1h	
5.5	Verify peptide removal	Optical microscope	Check removal for peptides	Most easily seen at the border of the electrodes
6	**Lithography – 1.5µm standard**			SI 1-4
6.1	Surface treatment	HMDS oven	Load wafers in oven for ~30 mins Recipe: program 4	Note time in logbook
6.2	Clean spinner	SSE spinner	Clean spinner nozzle and run the dummy wafers Recipe: 1.5 4inch	1-3 dummies Note time in logbook
6.3	Coat wafers	SSE spinner	Coat the device wafers 1.5 µm AZ5214e Novolac resist Softbake on hotplate Recipe: 1.5 4inch (Temp: 90°C, time:60 sec)	Resist thickness not checked Note time in logbook
6.4	Exposure	Aligner-6inch	Align to flat. Hard contact Recipe: 1.5 µm positive resist Exposure time: 3 sec Mask: Passivation	Note time in logbook
6.5	Transport of wafers	transport box	Load wafers into the Black or blue transport box	To avoid unwanted exposure from the white light
6.6	Develop	Developer bench	Develop in 351B for 60±10 sec	Note time in logbook
6.7	Rinse/dry	Wet bench/ Spin dryer	Rinse in DI water for 5 min (300±30 sec). Spin dry	
6.8	Inspection	Optical microscope	Check pattern and alignment marks	

7 SiO2 Deposition				SI 1-4
7.1	SiO2 deposition	Ion FAB	Recipe: TiO2 Acceptance Time: 30 min Thickness: 100 nm	Note time in logbook
7.2	Lift-off	Dedicated petridish	In single wafer ultrasound bath for petridish Time: 15 min	Can be performed in parallel with SiO2 deposition on following wafer
7.3	Rinse/dry	Fumehood	Flush with DI water and Spin dry on single wafer dryer	
7.4	Inspection	Optical microscope	Check for Complete lift off	
7.5	Inspection	Dektak	Measure heights and widths	Note on measurement sheet

C. Gold Electrodes Fabrication Process

EXCELL ELECTRODES: FABRICATION PROCESS

1. One-sided silicon wafer a. 670 nm of thermal oxide	Phosphor drive-in, wet growth 1050 C, 01:35	
2. Photolithography a. HMDS oven b. Spin 1.5 µm resist c. Exposure Mask "Electrodes" d. Develop	KS Aligner, negative process, 1st exposure 3.5 s (1.7s in 6' aligner), reverse bake 100 s @ 120 °C, flood exposure 30 s, development 70 s	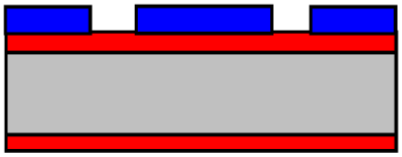
3. Wet etch	BHF etch, 1min 40 s (expected 117-133 nm etching)	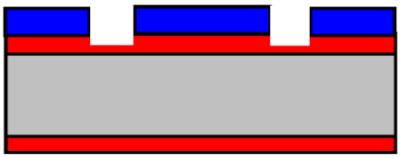
4. Metal deposition	Wordentec, 100 Å Ti + 1500 Å Au (or 100A Cr + 1500A Au)	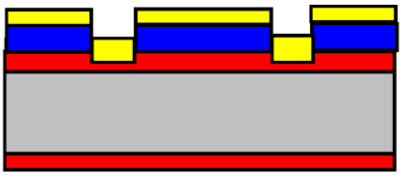
5. Lift-off	Acetone with ultrasound	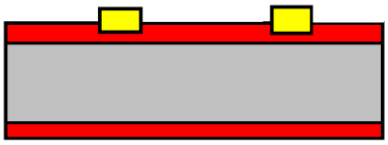
6. Nitride deposition	PECVD3, recipe MFSiNLS, 42 min. Deposition of 500 nm of nitride	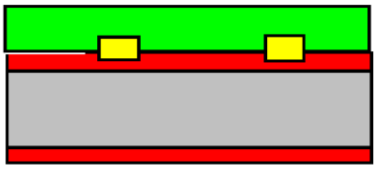
7. Photolithography a. HMDS oven b. Spin 1.5 µm resist c. Exposure Mask "Electrodes" d. Develop	KS Aligner, negative process, 1st exposure 3.5 s, reverse bake 100 s @ 120 °C, flood exposure 30 s, development 70 s	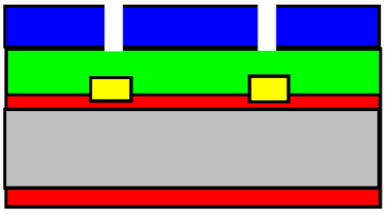
8. Nitride etch	RIE2, recipe OH_PolyA, 7 min. (but the opening of the metal pads needs to be checked if not open than needs more time in the RIE)	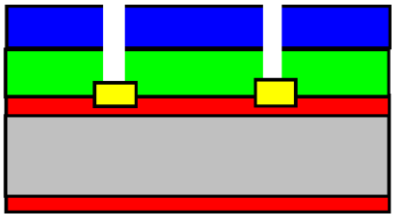
9. Resist removal	Acetone bath with sonication	

D. Measurement Uncertainties with Gold Electrodes

During performing the electrochemical impedance spectroscopy measurements we noticed that the measurement setup was behaving differently depending on the conditions. One of the most remarkable differences was observed after introduction of the ferro/ferricyanide solution. Often, just after introduction of the solution the semi circle diameter of the Nyquist plot was larger as compared to the semi circle measured 30 minutes after. The results are shown in Figure D.1A. Such behaviour was observed on the first 6 electrodes on the chip. For some chips the opposite behaviour was observed. We carried out a thorough investigation of the changes in the semi circle diameter over the period of 2 hours. The results of the investigation are presented in Figure D.1B. In this case the electrodes were probably being passivated with some molecules present in the solution. Also, some noticeable differences in the electrodes performance at later stages of the DNA hybridisation sensing were observed. These changes were attributed to faulty electrodes fabrication and was only seen on the chips that have a relatively large semi circle diameter from the beginning. For any further experiments the measurements were timed and all started 30 minutes after introduction of the ferro/ferricyanide solution.

One of the steps in the double hybridisation assay was the heat denaturation of the target DNA. As we noticed that the denaturation at 95 °C probably removes the thiolated probes from the surface we aimed at optimization of the heat treatment. One of the first measurements performed during the optimization was heating of a bare chip on a hot plate at 50 °C for 10 minutes. The reason for the experiment was to determine that no changes in the electrodes resistance are induced during heating. However, the measurements showed a great increase in the semi circle diameter after heating at 50 °C for 10 minutes as shown in Figure D.2B. Furthermore, the oxidation and reduction peaks in cyclic voltammetry changed due to heating (Figure D.2A). The peak potentials are shifted so that they are more separated and also the peak current is lowered. This behaviour was unexpected as the gold resistance should not vary greatly due to heating at 50 °C. Based on these results the heating of the chips was omitted and a different approach towards detection of the translocation was proposed as described in Part VII 26.

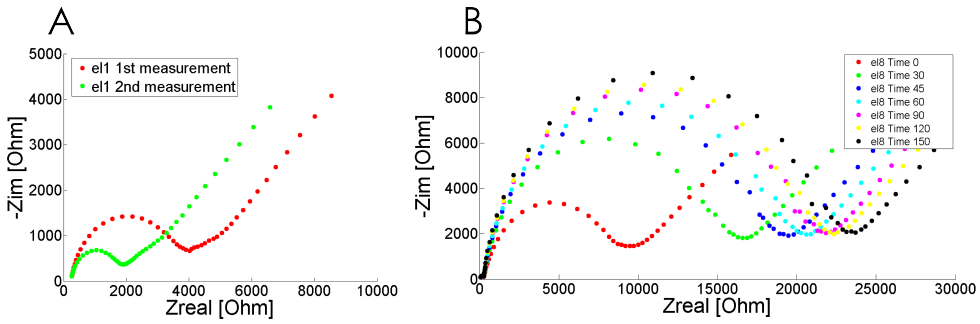

Figure D.1: Changes in the Nyquist plot over time. For some electrodes the semi circle diameter was decreasing over time (A), while for others there was an increase in the diameter observed within 2 hr (B).

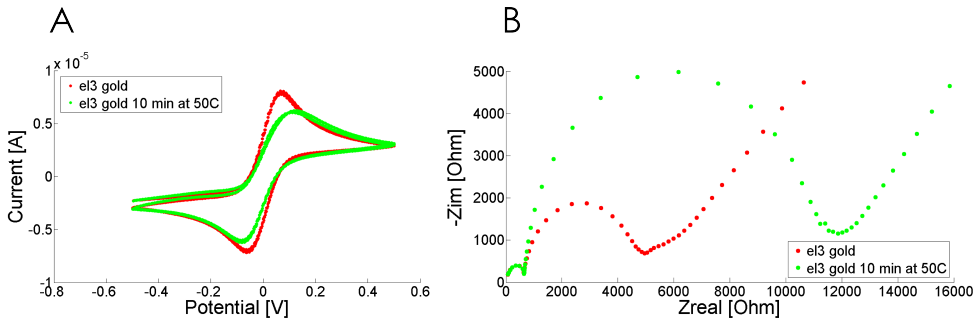

Figure D.2: Changes in the Nyquist plot after heating